CENTER FOR ADVANCED RESEARCH IN FINANCE

CARF Working Paper

CARF-F-526

Price Stability of Cryptocurrencies as a Medium of Exchange

Tatsuru Kikuchi
Faculty of Economics, The University of Tokyo

Toranosuke Onishi
Tokio Marine & Nichido Fire Insurance Co., Ltd.

Kenichi Ueda
Faculty of Economics, The University of Tokyo

November, 2021

CARF is presently supported by Nomura Holdings, Inc., Sumitomo Mitsui Banking Corporation, The Dai-ichi Life Insurance Company, Limited, The Norinchukin Bank, MUFG Bank, Ltd. and Ernst & Young ShinNihon LLC. This financial support enables us to issue CARF Working Papers.

Price Stability of Cryptocurrencies as a Medium of Exchange

Tatsuru Kikuchi[1], Toranosuke Onishi[2], and Kenichi Ueda[1]

[1] *Faculty of Economics, The University of Tokyo*

[2] *Tokio Marine & Nichido Fire Insurance Co., Ltd.*

(November, 2021)

Abstract

We present positive evidence of price stability of cryptocurrencies as a medium of exchange. For the sample years from 2016 to 2020, the prices of major cryptocurrencies are found to be stable, relative to major financial assets. Specifically, after filtering out the less-than-one-month cycles, we investigate the daily returns in US dollars of the major cryptocurrencies (*i.e.*, Bitcoin, Ethereum, and Ripple) as well as their comparators (*i.e.*, major legal tenders, the Euro and Japanese yen, and the major stock indexes, S&P 500 and MSCI World Index). We examine the stability of the filtered daily returns using three different measures. First, the Pearson correlations increased in later years in our sample. Second, based on the dynamic time-warping method that allows lags and leads in relations, the similarities in the daily returns of cryptocurrencies with their comparators have been present even since 2016. Third, we check whether the cumulative sum of errors to predict cryptocurrency prices, assuming stable relations with comparators' daily returns, does not exceeds the bounds implied by

the Black-Scholes model. This test, in other words, does not reject the efficient market hypothesis.

1 Introduction

A key question on cryptocurrencies is whether they can be used as money, a medium of exchange. Many argue they cannot. It is said to be primarily because they are not backed by any valuable goods and because their price movements are too volatile to use as money.

This paper presents positive evidence of price stability of cryptocurrencies as a medium of exchange. For this purpose, we examine price stability after filtering out the high frequency components. For example, the Euro or Japanese yen are known to be quite volatile against the US dollar but still they are used in the daily lives by people in the Euro area countries or in Japan because the high-frequency exchange rate volatility does not matter much for daily real-goods transactions, as long as their average values are stable against the US dollar.

Specifically, we apply the frequency-filtering technique developed by Müller and Watson (2018), abbreviated as the MW filter hereafter, to the daily returns of major cryptocurrencies, legal tenders, and stock indexes. We essentially get rid of the less-than-one-month (*i.e.*, 20 business days) movements in their daily returns. Then, we compare the stability in the filtered daily returns of cryptocurrencies against those of legal tenders and stock indexes. For cryptocurrencies, we pick the three major ones, that is, Bitcoin (BTC), Ethereum (ETH), and Ripple (XRP). For major legal tenders to compare, we pick the Euro (EUR) and Japanese yen (JPY), and we pick the S&P 500 (S&P500) and MSCI World Index (MSCI) for the major stock indexes. All values are defined in terms of US dollars. The daily data are taken from the beginning of 2016 to the end of 2020.

To see the stability of these prices based on the MW-filtered daily returns, we use three different measures. The first one is the Pearson correlation as is also used by Müller and Watson (2018) in a different context. We find that the MW filter makes cryptocurrency

returns closer to the other financial asset returns. Moreover, the correlations in daily returns between cryptocurrencies and other assets increased in later years in our sample.

The second one is a measure based on the dynamic time warping (DTW) algorithm. In general, DTW is a method that calculates an optimal match between two time series data. For the Pearson correlation, we compare, for example, BTC returns with S&P 500 returns in each same day. However, in DTW, the data sequences are *warped* non-linearly in the time dimension to see a similar pattern allowing for lags and leads. DTW is a widely applied algorithm in non-economic fields, such as speech pattern recognition, though some studies have already used DTW in economics, for example, Augustyński and Laskoś-Grabowski (2018), Franses and Wiemann (2020), and Sidi (2020). Based on the DTW-based similarity measure, we find that the similarity in daily returns of cryptocurrencies with other assets has been present even since 2016, the beginning of our sample, and not much has changed throughout our sample period. Note that the MW filtering also does the job by removing erratic ups and downs in the similarity over the years for some pairs of cryptocurrencies and other assets.

The third one is the cumulative sum (CUSUM) test, a test of the structural stability under the efficient market hypothesis. It is simply a two-sample Kolmogorov-Smirnov test in statistics. It was first developed based on the recursive residuals by Brown, Durbin, and Evans (1975), and the method was refined using the OLS residuals by Ploberger and Krämer (1992). Some discussions on the boundaries were made by Zeileis (2004)[1]. The CUSUM test is essentially based on the Black-Scholes model with the assumption of stable relationships with other financial assets. In economics literature, for example, the stability of money-demand models has been examined by the CUSUM test (see Stock and Watson (1996), Piehl, Cooper, Braga, and Kennedy (2003) and Elliott and Müller (2006)).

We find that cryptocurrency daily returns, based on the whole sample period, do pass

[1]R package was also developed by Zeileis, Leisch, Hornik, and Kleiber (2002).

the CUSUM test after the MW filtering, though they do not pass before the MW filtering. As for the other assets (EUR, JPY, S&P500, and MSCI), all of them essentially pass the test either before or after the MW filtering. In other words, cryptocurrency price movements have been enjoying stable relations with other major assets over the whole sample period, from 2016 to 2020. We also conduct the CUSUM tests for later years only, that is, samples starting from 2017, 2018, or 2019. BTC starting 2018, and JPY starting 2018 do not pass the test before the MW filtering. However, after the MW filtering, only ETH starting 2018 fails the test.

There have been a few studies that examined the price stability of cryptocurrencies, such as Vejačka (2014). A typical finding is a high price volatility of cryptocurrency compared with traditional financial assets. Some similarity between Bitcoin and gold has been discussed in Dyhrberg (2016). A more comprehensive study has been done in Sovbetov (2018), who analyzed the underlying factors that influence prices of cryptocurrencies, stocks, and gold in both the short- and long-term. Also, Kim, Kim, and Kim (2020) show a somewhat stable relationship across prices of Bitcoin, gold, and S&P 500 based on a GARCH model. Moreover, Shams (2019) shows that cryptocurrency prices co-move a lot, perhaps based on SNS-based demand effects. Most of these existing studies, however, methodologically requires some sort of stationarity or parametric stability, for which Müller and Watson (2018) renounce for key economic and financial time series data and instead advocate to use nonparametric or semi-parametric models, such as the Pearson correlation after the MW filtering. Note that DTW is also nonparametric, and the CUSUM test is the test for a stable relationship itself, not taking it as given.

A few studies on cryptocurrency price movements have shown that the high frequency movements may be contaminated by inefficient market forces. This is also a key reason to get rid of such high frequency components of price movements. For example, Aoyagi and Hattori (2018) find that a technical cost issue (*i.e.*, hash rate) matters for determining the daily raw returns of Bitcoin. Moreover, Li, Shin, and Wang (2020) show that pump-and-

dump schemes have been prevalent in cryptocurrency markets. Such a scheme is an illegal act in the US stock market as it is backed by a small group of people who buy up a target cryptocurrency up to a target price level and then sell it, all under close coordination, to obtain huge profits.

A fact that a cryptocurrency is not backed by real assets cannot be used as a reason to dismiss a cryptocurrency's role as a medium of exchange. The theory-of-money literature has shown the existence of a fiat money that is not backed by any real assets. Indeed, money has a role when financial contracts are not completely enforceable due to costs (especially for small transactions), and such an environment is often considered as trading with strangers for whom contract enforcement is difficult (Bewley (1979), Townsend (1980), and Kiyotaki and Wright (1989)). Moreover, intrinsically valueless money has a value only when people think it is accepted by other people, who think it is accepted by yet other people, who think... (repeated infinitely). This means that money is in essence a *bubble* and has to be *common knowledge* (Chwe (1999)). Given these formal theoretical definitions in economics, cryptocurrencies (or sea shells in old times) are legitimate candidates of money. What has remained is an empirical question as to whether an acceptance by the people is stable or not.

The rest of the paper is organized as follows. In Section 2, we give a detailed description of the data for the cryptocurrencies and other financial assets. In Section 3, we perform a standard spectrum analysis to see the frequency distributions. Section 4 gives a brief explanation of the MW filter. In Section 5, we show the Pearson correlation before and after the MW filtering. Section 6 explains the DTW method and results. In Section 7, we discuss the structural stability based on the CUSUM test. Section 8 concludes.

2 Data

We use daily time series data from January 1, 2016, to December 31, 2020, for three major cryptocurrencies, Bitcoin (BTC), Ethereum (ETH), and Ripple (XRP). Those data are ob-

tained through the API provided by the Cryptocompare (`https://min-api.cryptocompare.com/`). We evaluate the stability of cryptocurrency values compared with the other financial data, such as S&P500, gold, MSCI World Index (MSCI), Japanese Yen (JPY), and the Euro (EUR). While the historical data of gold prices and the MSCI World Index are obtained from Investing.com (`https://investing.com/`), the historical data of S&P500 is obtained from Yahoo finance (`https://finance.yahoo.com/`), and the historical data of JPY and EUR are obtained from the API provided by Cryptocompare (`https://min-api.cryptocompare.com/`).

The prices of the cryptocurrencies and other financial assets are all defined in US dollars. We let P_t denote the price of a financial asset at time t and P_{t-1} the price of the asset at time $t-1$, and r_t the (logarithmic) returns of the asset at t by

$$r_t = \log \frac{P_t}{P_{t-1}} \times 365 \, . \tag{2.1}$$

The descriptive statistics of the daily returns of cryptoprices and the key financial assets for the whole sample period are described in Table 1[2]. Figure 1 shows the 50-day moving averages of the daily returns of the cryptocurrencies and other financial assets.

3 Short-Run and Long-Run Movements

The short-run and long-run price stability appear a bit differently in the return data. The daily movements of cryptocurrencies are in general very large, relative to the traditional financial assets. This means that when we make a Fourier transformation from the time domain to the frequency domain, it is expected to see a large amount of high-frequency component in their spectrum.

[2]The skewness measures symmetricity of the distribution. The kurtosis tells us whether the data is heavy-tailed or light-tailed, relative to a normal distribution. Both skewness and kurtosis of normal distribution are equal to 0.

A power spectrum analysis is a useful tool to see the frequency distribution of some financial assets data. Let us consider the daily return of asset data r_t of length $T = n\,\Delta t = 1.258\times 10^5$, where $n = 1258$ is the number of daily data and $\Delta t = 100$ is taken as the sampling interval, and the frequency is defined by $f = 1/T = 1/(n\,\Delta t) = 7.949 \times 10^{-6}$. Then, the discretized frequency and the discretized time are given by $f_k = k/(n\,\Delta t)$ $(k = 1, \cdots, n)$ and $t_j = j\,\Delta t$ $(j = 1, \cdots, n)$, respectively. With this setup, the discrete Fourier transformation (DFT) of the return of asset data r_j is defined by

$$Q_k = \sum_{j=1}^{n} r_j \exp(-i\,2\pi j\,k/n)\ , \tag{3.2}$$

where $i = \sqrt{-1}$ is the imaginary unit. The discretization of time with the sampling period Δt implies a limitation of frequency f to the band $f \in [-\frac{1}{2\,\Delta t},\ \frac{1}{2\,\Delta t}]$ as frequencies outside the range are folded inside by the finite sampling (see, for example, Hamming (2012)). This boundary frequency is called the Nyquist frequency, $f_{\rm NQ} = 1/(2\,\Delta t)$.

The power spectrum density $I_{\rm PSD}(f_k)$ for the return of asset data r_t is then calculated by

$$I_{\rm PSD}(f_k) = \frac{2\,\Delta t^2}{n} Q_k\,Q_k^*\ , \tag{3.3}$$

where $*$ stands for the complex conjugate. In practice, we use the Fast Fourier Transformation (FFT) to calculate the Fourier transformation of the return of asset data, and take the sampling period as $\Delta t = 100$, hence, the Nyquist frequency is $f_{\rm NQ} = 0.005$.

The power spectrum density for the returns of cryptocurrencies and key financial assets are shown in Figures 2, 3, 4, 5, 6, 7, 8, and 9. These figures typically show that returns of cryptocurrencies and key financial assets vary intensively with frequency. In the frequency region higher than $f_{\rm NQ} = 0.005$, the noises seem dominant over the structurally important signals. On the other hand, the structural signals are quite clear in the frequency region lower than $f_{\rm NQ} = 0.005$ (*i.e.*, 5×10^{-3}).

4 Frequency Filtering

Now we know that the short-run movements of cryptocurrencies are somewhat strange, we focus on the rest by filtering out the short-run movements. A proper way of using a high-frequency filtering method for noisy non-stationary data has been proposed in Müller and Watson (2018), who use an orthogonal projection of time series data $y_j (j = 1, \cdots, n)$ onto the space spanned by the cosine function based on low-frequency periodic vectors. Their approach is an extension of the discrete cosine transformation (DCT) for the time series y_j,

$$\begin{aligned} \hat{y}_1 &= \sqrt{\frac{1}{n}} \sum_{j=1}^{n} y_j \ , \\ \hat{y}_k &= \sqrt{\frac{2}{n}} \sum_{j=1}^{n} \cos\left[(j-1) \left(k - \frac{1}{n} \right) \frac{\pi}{n} \right] y_j \ , \ \text{for } k = 2, \cdots, n \ . \end{aligned} \tag{4.4}$$

The long-run projection of Müller-Watson is made by using the following transformation, truncating the approximation with $q < n$,

$$\begin{aligned} \hat{y}_1 &= \sqrt{\frac{1}{n}} \sum_{j=1}^{q} y_j \ , \\ \hat{y}_k &= \sqrt{\frac{2}{n}} \sum_{j=1}^{q} \cos\left[(j-1) \left(k - \frac{1}{2} \right) \frac{\pi}{n} \right] y_j \ , \ \text{for } k = 2, \cdots, q \ . \end{aligned} \tag{4.5}$$

Here, up to the frequency that is represented by parameter q are extracted. More specifically, $\hat{y}_q$ is the data that is filtered to extract only frequencies lower than $\hat{f} = 1/\hat{T} = q/(2n)$ or $\hat{T} = 2n/q$ period. We use the following condition to decide the value of parameter q.

$$q = \left[\frac{n}{10} \right] + 3 \ , \tag{4.6}$$

where $\left[\frac{n}{10} \right]$ is the integer part of $\frac{n}{10}$. For example, in the case of BTC, we set these parameters as $n = 1420$ $(i.e., q = 145)$, $\hat{T} = 19$, $\hat{f} = 0.0526$. This roughly means that we take out short-run cycles occurring for less than 20 business days, which is essentially one month in

the calendar[3].

In other words, the MW filtering smooths the higher frequency movements in more than one month (20 business days) as shown in the power spectrum density in Figures 2, 3, 4, 5, 6, 7, 8, and 9. Note that the MW filtering also somewhat smooths the low frequencies.

5 Similarity to the Major Financial Assets: The Müller-Watson (2018) Approach

Recall that our objective in this study is to see the stability of prices or returns of cryptocurrencies relative to key financial assets. The time series similarity could be measured by the degree of comovements across two or more variables. How to evaluate comovements is discussed extensively in Müller and Watson (2018). They renounce the cointegtation approach and instead propose to use the Pearson correlation after filtering out high-frequency movements in the data.

Recall that the Pearson correlation is defined for two time series of data x_t and y_t as

$$P(x_t, y_t) = \frac{\text{cov}\,(x_t, y_t)}{\sigma_x\ \sigma_y} = \frac{\mathbb{E}\left[(x_t - \mu_x)\,(y_t - \mu_y)\right]}{\sigma_x\ \sigma_y}\ . \tag{5.7}$$

In order to show the importance of the Müller-Watson filtering, we show the correlation matrices for both before and after filtering. The correlations before the Müller-Watson filtering are shown in Tables 2, 3, 4, 5, and 6 for 2016, 2017, 2018, 2019, and 2020, respectively. The correlations after the Müller-Watson filtering are shown in Tables 7, 8, 9, 10, and 11 for 2016, 2017, 2018, 2019, and 2020, respectively.

The correlation matrices indicate the long-run stability of cryptocurrencies relative to the major financial assets. More specifically, we find three patterns. First, the correlations

[3]In the literature, a similar method of high-frequency filtering has been proposed and named as the separating information maximum likelihood (SIML) method in Kunitomo and Sato (2013). We use an R script provided by Sato, for whom we are grateful.

between the returns of cryptocurrencies and key financial assets becomes more significant after the Müller-Watson filtering for each year. Second, the returns of cryptocurrencies and key financial assets become more and more correlated to each other in later years. Third, the correlations among cryptocurrencies are getting stronger over time.

6 Dynamic Time Warping

Next, we investigate the similarities of cryptocurrency returns to key financial asset returns by looking at the Dynamic Time Warping (DTW). This is often used in pattern recognition, as developed by Itakura (1975) and Sakoe and Chiba (1978) (for a review, see Müller (2007)), which allows leads and lags of data sequences over time when measuring the similarity.

A set of time series, which are the returns of assets in our case, $x = \{x_t\} = (x_1, \cdots, x_n)$ and $y = \{y_t\} = (y_1, \cdots, y_m)$, can be expressed in terms of the warping path, $\Lambda = (w_1, \cdots, w_K)$. The warping path is a contiguous set of matrix elements that define a mapping between x_t and y_t. A typical element w_ℓ is represented by (i, j), that selects x_i from x and y_j from y.

Formally, the DTW distance between two given sequences, x and y, can be calculated by

$$D(x, y) = \min_{\Lambda^*} \sum_{(i,j)\in\Lambda^*} d(x_i, y_j) \ , \tag{6.8}$$

where Λ^* is the warping path that minimizes the cumulative distance of all mapped point-pairs on the path. Although the element distance function $d(x_i, y_j)$ could take one of several forms, normally and here, it is given by the Euclidean distance, that is,

$$d(x_i, y_j) = \sqrt{(x_i - y_j)^2} \ . \tag{6.9}$$

The best warping path Λ^* is found using a dynamic programming approach to align two sequences. Going through all possible paths is combinatorially explosive, as pointed out by Berndt and Clifford (1994), hence, the possible warping paths need to be restricted. When

we apply the DTW method to two economic data series, we think it natural to constrain the possible warping paths by following three conditions.

The first constraint is the boundary condition. This requires the warping path to start and finish in diagonally opposite corner cells (*i.e.*, the starting date and the ending date of the sample) of the warping path matrix,

$$w_1 = (1,1) \text{ and } w_K = (n,m) \; . \tag{6.10}$$

The second constraint is the continuity condition. This constraint limits the path transitions to adjacent points in time,

$$w_\ell - w_{\ell-1} \in \{(1,0) \, , (0,1) \, , (1,1)\} \; . \tag{6.11}$$

The third constraint is the monotonicity condition. This constraint preserves the time-order of points.

$$\text{If } w_\ell = (i,j) \text{ and } w_{\ell+1} = (i',j') \; , \text{ then } i \leq i' \text{ and } j \leq j' \; . \tag{6.12}$$

In practice, the DTW distance is calculate in a recursive way. First, we construct two subsequences $\tilde{x}_i = (x_1, \cdots, x_i)$ for $i = 1, \cdots, n$ and $\tilde{y}_j = (y_1, \cdots, y_j)$ for $j = 1, \cdots, m$ from an assumed optimal path sequence. Then, we define the cost function for each subsequence as

$$\gamma(i,j) = D(\tilde{x}_i, \tilde{y}_j) \text{ for } i = 1, \cdots, n \text{ and } j = 1, \cdots, m \; . \tag{6.13}$$

The cost function $\gamma(i,j)$ specifies the total cost of an assumed optimal warping path starting from $w_1 = (1,1)$ and ending at $w_\ell = (i,j)$.

Second, we find the cost function $\gamma(i,j)$ in the recursive way. Namely, it is computed iteratively using a nested loop according to the following formula,

$$\hat{\gamma}(i,j) = d(x_i, y_j) + \min\{\gamma(i-1,j), \, \gamma(i,j-1), \, \gamma(i-1,j-1)\} \; , \tag{6.14}$$

and

$$\hat{\gamma}(i,j) = \gamma(i,j) \; , \tag{6.15}$$

where $i = 1, \cdots, n$ and $j = 1, \cdots, m$, with appropriate initial values[4]. Once the cost function is found, it is the DTW distance, $D(x, y) = \gamma(n, m)$, and the optimal warping path Λ^* is identified. For example, the paired data (*i.e.*, the DTW optimal warping path Λ^*) between BTC and GOLD in 2020 is shown in Figure 10.

Note that the Pearson correlation always compares the same period data (x_t, y_t). For the DTW distance, the periods to compare are related (x_i, y_j), though i and j are not necessary the same time t. For example, if $x = \{x_t\}$ and $y = \{y_t\}$ follow the simple sine and cosine functions, respectively, in the time dimension, then they are orthogonal, and thus their Pearson correlation is zero. However, they look the same when one of their phases is shifted by π, thus, their DTW distance is 0, which means their shapes are exactly the same.

It is useful to normalize the DTW distance relative to some base value. Let us use the maximum of the DTW distance between a pair of key financial assets (*i.e.*, JPY, EUR, GOLD, S&P500, and MSCI), $D_{\max}$, as the base value for all other DTW distances. That is, we normalize the DTW distance as follows,

$$\bar{D}(x, y) = \frac{D(x, y)}{D_{\max}} \, . \tag{6.16}$$

We show the normalized DTW distance $\bar{D}(x, y)$ before the Müller-Watson filtering in Tables 12, 13, 14, 15, and 16 for each sample year. The corresponding results after the Müller-Watson filtering are shown in Tables 17, 18, 19, 20, and 21.

There are several salient features which appear in these Tables. First, the strengthening trend in similarities among returns of cryptocurrencies and key financial assets seem less clear than in the Pearson correlations (Tables 2 and 3). Before the MW filtering, they, especially BTC, seem to behave similarly even in 2016, that is the initial period of our sample. These similarities dwindled in 2017 until 2019. In 2020, it recovered especially for BTC. However, after the MW filtering, similarities are less fluctuating and relatively stable, especially for BTC, in almost all the sample years.

[4]The python code is available upon request.

Second, frequency filtering does make some differences. For example, Table 13 shows quite a different movement only in XRP in 2017 compared with the other assets. This result also seems to be supported in Figure 1. In particular, it is shown in Figure 1 that the returns of XRP dramatically rises in 2017. However, after the MW filtering, the returns of XRP behave in a similar way, as shown in Table 18. The following year, 2018, also show almost the same case for the returns of XRP before the MW filtering (see Table 14) and after the frequency filtering (see Table 19). This is interesting as there was the well-known 2018 cryptocurrency crash (also known as the great crypto crash). Note, however, that even after the MW filtering, XRP seems to move somewhat differently compared to other assets in 2020.

7 Stability from the Viewpoint of the Black-Scholes Model

Under a simple, efficient market hypothesis, can we assume the price stability of cryptocurrencies? Since the traditional financial asset returns can be considered as more or less following the Brownian motion, we test whether the cryptocurrency returns also follows a simple form of the Black-Scholes formula under stable relationships with key financial asset returns.

Following Elliott and Müller (2006), we consider the tests of the null hypothesis of a stable coefficient $\bar{\beta}$ in

$$z_t = \mathbf{X}_t^T \bar{\beta} + \mathbf{Z}_t^T \bar{\gamma} + \bar{\epsilon}_t \tag{7.17}$$

against the alternative of variable coefficient β_t in

$$z_t = \mathbf{X}_t^T \beta_t + \mathbf{Z}_t^T \gamma + \epsilon_t \ . \tag{7.18}$$

The null hypothesis of stable $\bar{\beta}$ is rejected, if the cumulative sum (CUSUM) of residual

with constant $\bar{\beta}$ exceed the limit that is consistent with the Brownian bridge (see, Appendix A).

First, we consider the structural stability based on the OLS-CUSUM test by using all the data. Here, $\bar{\beta}$ is obtained once by OLS. As is clearly explained in Krämer, Ploberger and Schlüter (1991), the sum of the OLS residual always starts from 0 and ends with 0. In between, it has some bounds.

Second, we also employ the recursive CUSUM (Rec-CUSUM) test, which can be useful to monitor price stability every day. Here, the residuals are obtained as one-step ahead forecast errors. In other words, $\bar{\beta}$ is obtained using historical data at each date. The null hypothesis of the structural stability depends on the choice of the sampling periods. We divide our data into four sets of data samples as follows: (i) all the data; (ii) a sample data from 2017 to 2020; (iii) a sample data from 2018 to 2020; and (iv) a sample data from 2019 to 2020. We then proceed with the Rec-CUSUM test for each sample set.

We consider two types of boundaries for the CUSUM tests[5]. We use the following two types of boundaries for the OLS-CUSUM test. One is a constant in time and another is proportional to the standard deviation function of the corresponding theoretical process, as proposed in Zeileis (2004),

$$b(t) = \nu \tag{7.19}$$

$$b(t) = 2\nu\sqrt{t(1-t)} \tag{7.20}$$

for the OLS-CUSUM path. We take $\nu = 1.358$ at the 95% confidence interval.

When we apply the Rec-CUSUM test, we consider the following two types of boundaries

[5]The crucial difference between the Rec-CUSUM test and the OLS-CUSUM test is in the limiting process. In the former case, the limiting process is the Wiener process (Brownian motion), but in the latter case, the limiting process is the Brownian bridge.

as proposed in Brown, Durbin, and Evans (1975) and Zeileis (2004),

$$b(t) = \lambda\,(2\,t-1) \tag{7.21}$$

$$b(t) = 2\nu\,\sqrt{t} \tag{7.22}$$

with λ takes the value $\lambda = 0.948$ at the 95% confidence interval[6].

Note that there is no need to change conditions in the test of the structural stability even if we apply frequency filtering. This is known as pattern recovery in Mehrizi and Chenouri (2020) and Mehrizi and Chenouri (2021). Similar studies can be found, for example, in Kim, Koh, Boyd, and Gorinevsky (2009) and Phillips and Jin (2021).

We perform the test of this structural stability, based on the following regression for the daily returns of each cryptocurrency or key financial asset on the returns of other financial assets. For example, for Bitcoin,

$$\begin{aligned} \texttt{BTC}_\texttt{t} &= \bar{\beta}_0 + \texttt{BTC}_{\texttt{t}-1}\,\bar{\beta}_1 + \texttt{JPY}_{\texttt{t}-1}\,\bar{\beta}_2 + \texttt{EUR}_{\texttt{t}-1}\,\bar{\beta}_3 + \texttt{GOLD}_{\texttt{t}-1}\,\bar{\beta}_4 + \texttt{S\&P500}_{\texttt{t}-1}\,\bar{\beta}_5 \\ &+ \texttt{MSCI}_{\texttt{t}-1}\,\bar{\beta}_7 + \bar{\epsilon}_\texttt{t}\ , \end{aligned} \tag{7.23}$$

where the symbolic notations stand for the daily returns, for example, $\texttt{BTC}_\texttt{t}$ for the BTC daily return at time t.

First, we show the results of the OLS-CUSUM test for both before and after the MW filtering is applied. Figures 11, 12, 13, 14, 15, 16, 17 and 18 illustrate the results, that is, whether the daily returns exceed the boundary consistent with the Black-Scholes formula under the assumption of a stable relationship with other financial assets before the Müller-Watson filtering.

[6]There are several constructions of the boundaries of the stochastic process. In the monitoring context, a nearly linear boundary was considered in Chu, Stinchcombe and White (1996) and Leisch, Hornik, and Kuan (2000), which is written as follows:

$$b(t) = \left[t(t-1)\left(a^2 + \ln\left(\frac{t}{t-1}\right)\right)\right]^{1/2}\ ,$$

where a only depends on the confidence level α.

Based on the OLS-CUSUM test, there are two findings from the structural stability tests. We find that before the MW filtering, only ETH and XRP apparently exceed the boundaries of the Brownian bridge. Moreover, BTC almost reaches the boundaries of the Brownian bridge as well.

However, this is not the case after the MW filtering. Also, all the other assets do not exceed the boundaries either, before or after the MW filtering (see Figures 19, 20, 21, 22, 23, 24, 25 and 26). In other words, cryptocurrencies are stable enough within the boundaries of the Brownian bridge after the MW filtering is applied, as is the case for the key financial assets.

Second, we conduct the Rec-CUSUM test. Figures 27, 31, 35, 39, 43, 47, 51 and 55 illustrate the results using all the data, that is, whether the daily returns exceed the boundary consistent with the Black-Scholes formula before the MW filtering.

Similar to the OLS-CUSUM test, we find that before the MW filtering, only ETH (and perhaps GOLD) exceeds the boundaries of the Brownian motion in the Rec-CUSUM test when we use all the data from 2016 to 2020.

However, once again, this is not the case after the MW filtering. All assets (perhaps except for GOLD) do not exceed the boundaries of the Brownian motion after the MW filtering (see Figures 59, 63, 67, 71, 75, 79, 83 and 87). Once again, these results show that cryptocurrencies are stable enough within the boundaries of the Brownian motion after the MW filtering is applied, as is the case for the key financial assets.

In addition to that, we also conduct the Rec-CUSUM tests using the latter parts of data before the MW filtering, that is, (i) a sample data from 2017 to 2020; (ii) a sample data from 2018 to 2020; and (iii) a sample data from 2019 to 2020. The results before the MW filtering can be seen in Figures 28, 29, and 30 for BTC, Figures 32, 33, and 34 for ETH, Figures 36, 37, and 38 for XRP, Figures 40, 41, and 42 for JPY, Figures 44, 45, and 46 for EUR, Figures 48, 49, and 50 for GOLD, Figures 52, 53, and 54 for S&P500, and Figures 56, 57, and 58 for MSCI.

For the sample data from 2018 to 2020, BTC and JPY before the MW filtering exceed the boundaries of the Brownian motion. For other subsample years, all the return movements are within the boundaries.

However, the results change in the Rec-CUSUM tests after the MW filtering (see Figures 60, 61, and 62 for BTC, Figures 64, 65, and 66 for ETH, Figures 68, 69, and 70 for XRP, Figures 72, 73, and 74 for JPY, Figures 76, 77, and 78 for EUR, Figures 80, 81, and 82 for GOLD, Figures 84, 85, and 86 for S&P500, and Figures 88, 89, and 90 for MSCI). Even for the sample data from 2018 to 2020, all the assets, except for ETH, after the MW filtering do not exceed the boundaries of the Brownian motion.

In summary, we confirm that the returns on cryptocurrencies after the MW filtering are essentially stable enough within the boundaries of the Brownian bridge or the Brownian motion, as is the case for the key financial assets.

8 Conclusion

A key question on cryptocurrencies is whether they can be used as money, a medium of exchange. Many argue they cannot. A major reason is that their price movements are too volatile to use as money.

We have presented positive evidences of price stability of cryptocurrencies. We focus on the daily returns after filtering out the high frequency components, which are contaminated by technical forces. Also, for the daily transaction uses, people do not seem to care about the high frequency movements of money, say, the Euro or Japanese yen against the US dollar.

Specifically, we apply the filter developed by Müller and Watson (2018) to the daily return data of major cryptocurrencies (*i.e.*, Bitcoin (BTC), Ethereum (ETH), and Ripple (XRP)) as well as their comparators (*i.e.*, major legal tenders, the Euro (EUR) and Japanese yen (JPY), and major stock indexes, the S&P 500 and the MSCI World Index (MSCI)). By doing so, we essentially get rid of the less-than-one-month cycles of their price movements.

We then investigate the stability of the filtered daily returns using three different measures. First, we find that the Pearson correlations in the daily returns between cryptocurrencies and other assets increased in latter years in our sample from the beginning of 2016 to the end of 2020. Second, however, based on the DTW method that allow lags and leads, we find that the similarity in the daily returns of cryptocurrencies with other assets has been present even since 2016, the beginning of our sample, and not much changed throughout our sample period. Third, we test the stability of the relationships between daily returns of cryptocurrencies and those of their comparators by checking if the cumulative sum of errors, under the assumption of stable coefficients on comparators' daily returns, does not exceeds the statistical bounds. This CUSUM test is based on the efficient market hypothesis and the results assure the market efficiency and structural price stability of cryptocurrencies, as is also the case for other major financial assets.

In summary, interestingly, for the years from 2016 to 2020, the prices of major cryptocurrencies are found to be stable. This conclusion is not well shown without filtering out the high frequency movements or without conducting deeper investigations than simple correlations. Still, apparently, an empirical question remains if such stability can be continued for the foreseeable future.

Acknowledgement

The views expressed in this paper are those of the authors and should not be attributed to the Tokio Marine & Nichido Fire Insurance Co., Ltd., or any institutions that the authors have been affiliated with. This work is supported by the Digital Economy Project at the University of Tokyo, funded by the Silicon Valley Community Foundation. We would like to thank these organizations. We are grateful for the helpful comments from participants of The University Blockchain Research Initiative (UBRI) Conference, hosted (online) by the University of London, the Digital Currency and Finance Workshop, hosted (online) by the

University of Tokyo, and the Blockchain in Kyoto 2021 Conference, hosted (online) by the Kyoto University.

Appendix

A CUSUM Test

Let $\{z_t\}$, for $t = 1, \cdots, n$, be the observed time series and we write it as.

$$z_t = \mu_t + \epsilon_t \ , \tag{A.24}$$

where $\mu_t = \mathbf{X}_t^T \beta_t$ is a trend component in the linear regression model and ϵ_t is the *i.i.d.* disturbances, which are assumed to be stationary and ergodic with the following condition:

$$\mathbb{E}\left[\epsilon_t\right] = 0 \text{ and } \mathbb{V}\left[\epsilon_t\right] = \sigma^2 \ . \tag{A.25}$$

In the standard linear regression model, the coefficients β_t is estimated as $\hat{\beta}_t$ by using the ordinary least squares (OLS) method. Then, the OLS residual $\hat{\epsilon}_t$, can be also estimated with

$$\mathbb{E}[\hat{\epsilon}_t] = 0 \text{ and } \mathbb{V}[\hat{\epsilon}_t] = \hat{\sigma}^2 \ . \tag{A.26}$$

The key is to evaluate the fluctuations of the cumulative sum (CUSUM) of residuals. The null hypothesis is that $\hat{\sigma}^2$ is not explosive. See discussion by Brown, Durbin, and Evans (1975).

It is useful to define a continuous time stochastic process (sometimes known as the empirical fluctuation process) of the sum of residuals as

$$W_n(\tau) = \frac{1}{\hat{\sigma}\sqrt{n}} \sum_{i=1}^{n} \mathbf{1}_{\{\tau \leq t\}} \hat{\epsilon}_i \ . \tag{A.27}$$

In the recursive CUSUM (Rec-CUSUM) test, the residual $\hat{\epsilon}_t$ is essentially the one-step-ahead forecast error and given by

$$\hat{\epsilon}_t = \frac{z_t - \mathbf{X}_t^T \hat{\beta}_{t-1}}{\sqrt{1 + \mathbf{X}_t^T \left(\sum_{i=1}^{t-1} \mathbf{X}_i \mathbf{X}_i^T\right)^{-1} \mathbf{X}_t}} \ . \tag{A.28}$$

Here, $\hat{\beta}_{t-1}$ is estimated by the OLS using the data up to the previous period $t-1$. In this case, the limiting process becomes the Brownian motion (*i.e.*, Wiener process).

In fact, according to the functional central limit theorem or the Donsker's theorem, $W_n(\tau)$ converges to the Wiener process $W(\tau)$:

$$W(\tau) = \lim_{n\to\infty} \|W_n(\tau)\| \ , \ \text{for } 0 \le \tau \le 1 \ , \tag{A.29}$$

where the convergence means the weak convergence of the associated probability measures. The Wiener process (*i.e.*, the Brownian motion) has the following properties:

$$\mathbb{E}\left[W(\tau)\right] = 0 \text{ and } \mathbb{V}\left[W(\tau)\right] = \tau \ . \tag{A.30}$$

Based on this property, the Rec-CUSUM test bounds are obtained.

In the case of the OLS-CUSUM tests, $\hat{\beta}$ based on all samples is used instead of $\hat{\beta}_{t-1}$. As the OLS residuals are correlated to each other and their sum is zero by definition, the limiting process of the OLS-CUSUM is no longer a Brownian motion. Instead, the limiting process is known to become a Brownian bridge:

$$B(\tau) = W(\tau) - \tau\, W(1) \ , \ \text{for } 0 \le \tau \le 1 \ . \tag{A.31}$$

An alternative representation of the Brownian bridge is given by the stochastic differential equation,

$$dB(\tau) = dW(\tau) - \frac{B(\tau)}{1-\tau} d\tau \ , \ \text{for } 0 \le \tau \le 1 \ , \tag{A.32}$$

whose solution is given by

$$B(\tau) = \int_0^\tau \frac{1-\tau}{1-t}\, dW(t) \ , \ \text{for } 0 \le \tau \le 1 \ . \tag{A.33}$$

The Brownian bridge has the following properties:

$$\mathbb{E}\left[B(\tau)\right] = 0 \text{ and } \mathbb{V}\left[B(\tau)\right] = \tau(1-\tau) \ . \tag{A.34}$$

Here, the OLS-CUSUM test uses the following quantity:

$$M_n(\tau) = \max_{0 \le s \le \tau} \|W_n(s)\| \ . \tag{A.35}$$

The distribution $M_n(\tau)$ converges to the Kolmogorov distribution (or the Markov process) as follows:

$$M(\tau) = \lim_{n \to \infty} \|M_n(\tau)\| \ , \tag{A.36}$$

then, it satisfies

$$M(\tau) = \sup_{0 \le \tau \le 1} \|B(\tau)\| \ . \tag{A.37}$$

In general, the cumulative distribution function of the Kolmogorov distribution $M(\tau)$ is given by

$$\mathbb{P}\left(M(\tau) \le x\right) = 1 - 2\sum_{k=1}^{\infty} (-1)^{k-1} \exp(-2k^2x^2) \ . \tag{A.38}$$

The goodness-of-fit test or the Kolmogorov–Smirnov test can be constructed by using the critical values of the Kolmogorov distribution,

$$\mathbb{P}\left(\sup_{0 \le \tau \le 1} \|B(\tau)\| \le b(\tau)\right) = 1 - \alpha \ , \tag{A.39}$$

where $1 - \alpha$ represents the confidence interval.

References

Müller, U. K. and Watson, M. W. (2018). *"Long-Run Covariability,"* Econometrica, 86(3): 775–804.

Augustyński, I. and Laskoś-Grabowski, P. (2018). *"Clustering Macroeconomic Time Series,"* Ekonometria, 22(2): 74–88.

Franses, P. H. and Wiemann, T. (2020). *"Intertemporal Similarity of Economic Time Series: An Application of Dynamic Time Warping,"* Computational Economics, 56(1): 59–75.

Sidi, L. (2020). *"Improving S&P Sock Prediction with Time Series Stock Similarity."* (arXiv preprint arXiv:2002.05784.)

Brown, R. L., Durbin, J., and Evans, J. M. (1975). *"Techniques for Testing the Constancy of Regression Relationships Over Time,"* Journal of the Royal Statistical Society: Series B (Methodological), 37(2): 149–63.

Ploberger, W. and Krämer, W. (1992). *"The CUSUM Test with OLS Residuals,"* Econometrica: Journal of the Econometric Society, pp. 271–85.

Zeileis, A. (2004). *"Alternative Boundaries for CUSUM Tests,"* Statistical Papers, 45(1): 123–31.

Zeileis, A., Leisch, F., Hornik, K., and Kleiber, C. (2002). *"Strucchange: An R Package for Testing for Structural Change in Linear Regression Models,"* Journal of Statistical Software, 7(1): 1–38.

Stock, J. H. and Watson, M. W. (1996). *"Evidence on Structural Instability in Macroeconomic Time Series Relations,"* Journal of Business & Economic Statistics, 14(1): 11–30.

Piehl, A. M., Cooper, S. J., Braga, A. A., and Kennedy, D. M. (2003). *"Testing for Structural Breaks in the Evaluation of Programs,"* Review of Economics and Statistics, 85(3): 550–58.

Elliott, G. and Müller, U. K. (2006). *"Efficient Tests for General Persistent Time Variation in Regression Coefficients,"* The Review of Economic Studies, 73(4): 907–40.

Vejačka, M. (2014). *"Basic Aspects of Cryptocurrencies,"* Journal of Economy, Business and Financing, 2(2): 75–83.

Dyhrberg, A. H. (2016). *"Bitcoin, Gold and the Dollar—A GARCH Volatility Analysis,"* Finance Research Letters 16: 85–92.

Sovbetov, Y. (2018). *"Factors Influencing Cryptocurrency Prices: Evidence from Bitcoin, Ethereum, Dash, Litcoin, and Monero,"* Journal of Economics and Financial Analysis, 2(2): 1–27.

Kim, J. M., Kim, S. T., and Kim, S. (2020). *"On the Relationship of Cryptocurrency Price with US Stock and Gold Price using Copula Models,"* Mathematics, 8(11): 1859.

Shams, A. (2019). *"What Drives the Covariation of Cryptocurrency Returns,"* in Association of Financial Economists & American Economic Association Beyond Bitcoin Paper Session Conference.

Aoyagi, J. and Hattori, T. (2018). *"The Empirical Analysis of Bitcoin Market in the General Equilibrium Framework."* (Available at SSRN 3433833.)

Li, T., Shin, D., and Wang, B. (2020). *"Cryptocurrency Pump-and-Dump Schemes."* (Available at SSRN 3267041.)

Bewley, T. (1979). *"The Optimum Quantity of Money,"* (No. 383). Discussion Paper No. 383 (Evanston, IL: Northwestern University, Kellogg School of Management, Center for Mathematical Studies in Economics and Management Science).

Townsend, R. M. (1980). *"Models of Money with Spatially Separated Agents,"* Models of Monetary Economies, pp. 265–303.

Kiyotaki, N. and Wright, R. (1989). *"On Money as a Medium of Exchange,"* Journal of Political Economy, 97(4): 927–54.

Chwe, M. S. Y. (1999). *"The Reeded Edge and the Phillips Curve: Money Neutrality, Common Knowledge, and Subjective Beliefs,"* Journal of Economic Theory, 87(1): 49–71.

Hamming, R. (2012). Numerical Methods for Scientists and Engineers (Courier Corporation).

Kunitomo, N. and Sato, S. (2013). *"Separating Information Maximum Likelihood Estimation of the Integrated Volatility and Covariance with Micro-Market Noise,"* The North American Journal of Economics and Finance, 26: 282–309.

Itakura, F. (1975). *"Minimum Prediction Residual Principle Applied to Speech Recognition,"* IEEE Transactions on Acoustics, Speech, and Signal Processing, 23(1): 67–72.

Sakoe, H. and Chiba, S. (1978). *"Dynamic Programming Algorithm Optimization for Spoken Word Recognition,"* IEEE Transactions on Acoustics, Speech, and Signal Processing, 26(1): 43–9.

Müller, M. (2007). *"Dynamic Time Warping,"* Information Retrieval for Music and Motion, pp. 69–84.

Berndt, D. J. and Clifford, J. (1994). *"Using Dynamic Time Warping to Find Patterns in Time Series,"* KDD Workshop, 10(6): 359–70.

Krämer, W., Ploberger, W., and Schlüter, I. (1991). *"Recursive vs. OLS Residuals in the CUSUM Test,"* in Economic Structural Change, pp. 35–47 (Springer, Berlin, Heidelberg).

Mehrizi, R. V. and Chenouri, S. (2020). *"Detection of Change Points in Piecewise Polynomial Signals Using Trend Filtering."* (arXiv preprint arXiv:2009.08573.)

———. (2021). *"Valid Post-Detection Inference for Change Points Identified Using Trend Filtering."* (arXiv preprint arXiv:2104.12022.)

Kim, S. J., Koh, K., Boyd, S., and Gorinevsky, D. (2009). *"$\ell 1$ Trend Filtering,"* SIAM Review, 51(2): 339–60.

Phillips, P. C. and Jin, S. (2021). *"Business Cycles, Trend Elimination, and the HP Filter,"* International Economic Review. (Available at https://doi.org/10/1111/iere.12494.)

Chu, C. S. J., Stinchcombe, M., and White, H. (1996). *"Monitoring Structural Change,"* Econometrica: Journal of the Econometric Society, pp. 1045–65.

Leisch, F., Hornik, K., and Kuan, C. M. (2000). *"Monitoring Structural Changes with the Generalized Fluctuation Test,"* Econometric Theory, 16(6): 835–54.

Figure 1: 50 days moving average returns (annualized, %) of cryptocurrencies and key financial assets

(a) 50 days moving average returns (annualized, %) of cryptocurrencies (BTC, ETH, and XRP)

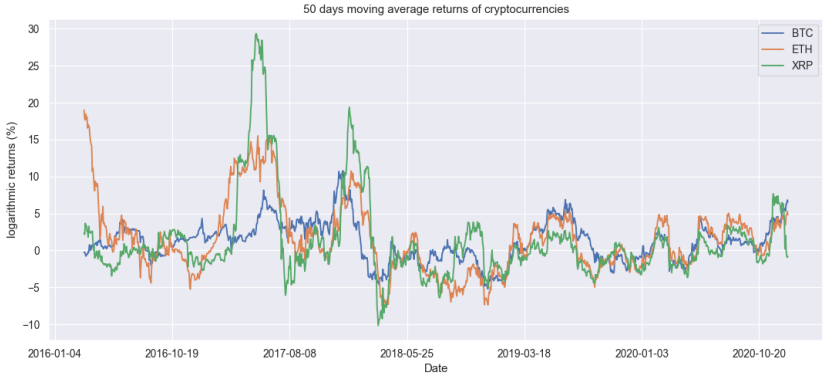

(b) 50 days moving average returns (annualized, %) of JPY, EUR, and GOLD

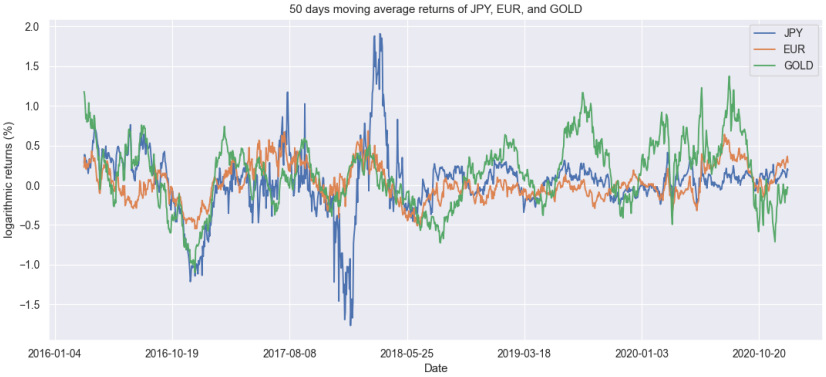

(c) 50 days moving average returns (annualized, %) of S&P500 and MSCI

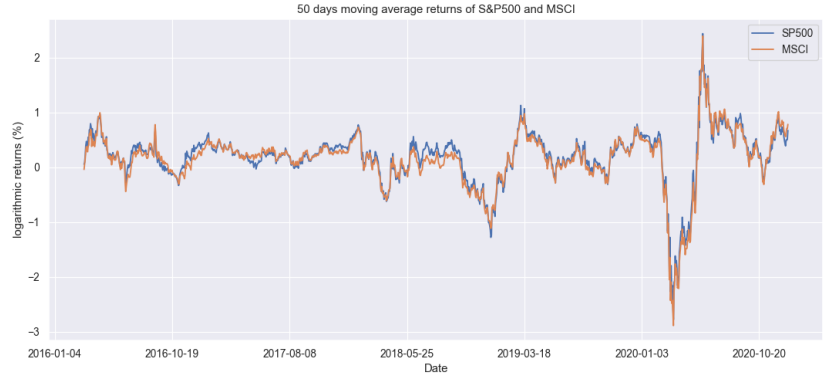

Figure 2: The power spectrum density (PSD) of BTC

(a) The power spectrum density (PSD) of BTC (before the Müller-Watson filtering)

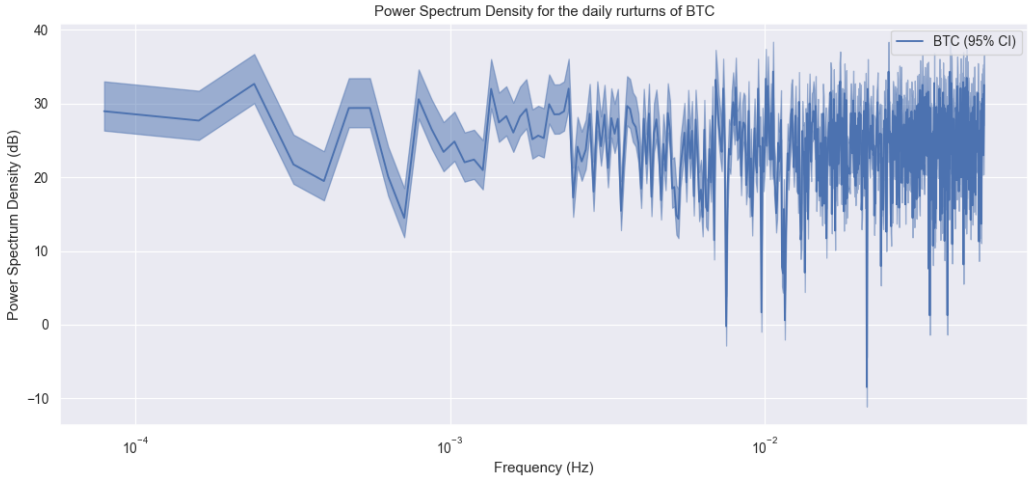

(b) The power spectrum density (PSD) of BTC (after the Müller-Watson filtering)

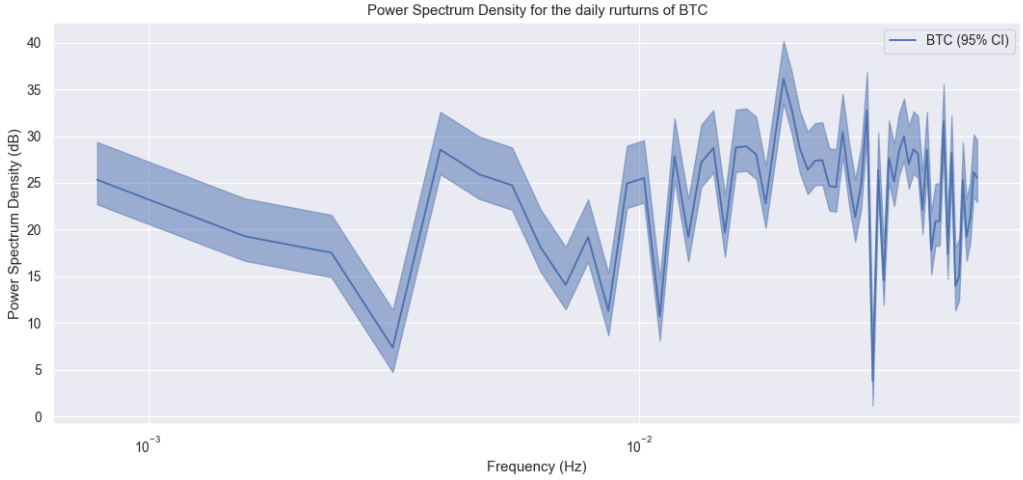

Figure 3: The power spectrum density (PSD) of ETH

(a) The power spectrum density (PSD) of ETH (before the Müller-Watson filtering)

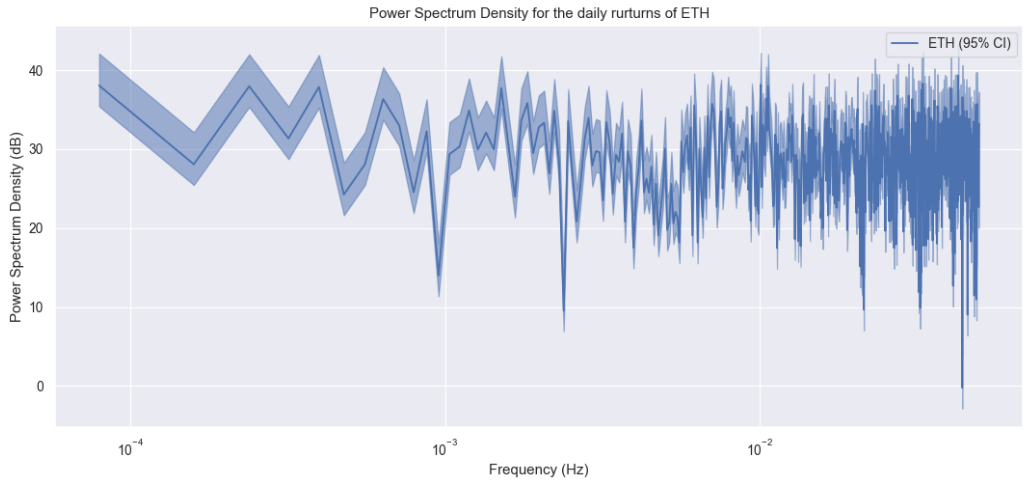

(b) The power spectrum density (PSD) of ETH (after the Müller-Watson filtering)

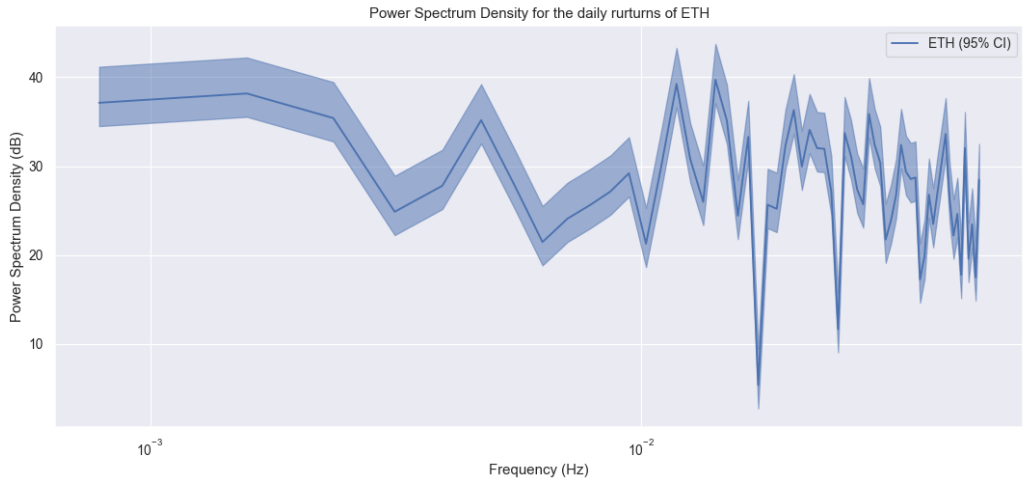

Figure 4: The power spectrum density (PSD) of XRP

(a) The power spectrum density (PSD) of XRP (before the Müller-Watson filtering)

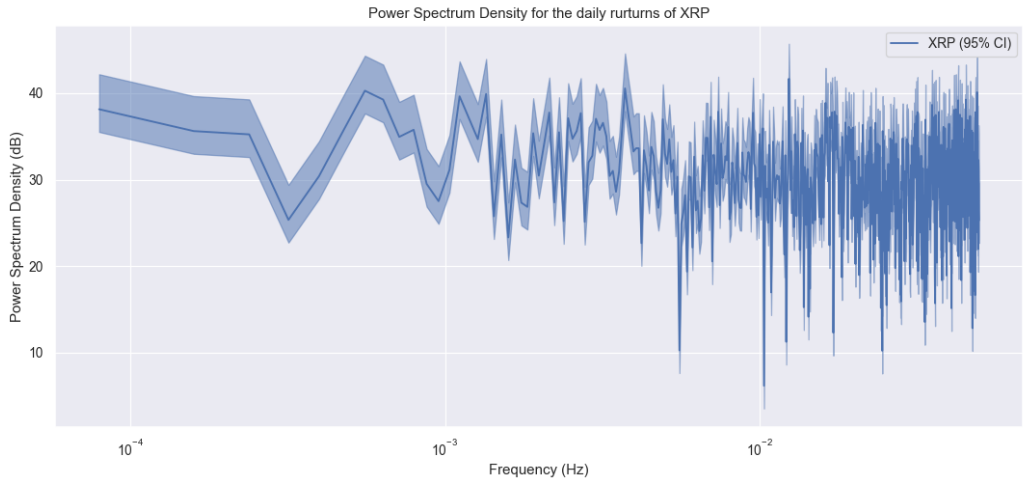

(b) The power spectrum density (PSD) of XRP (after the Müller-Watson filtering)

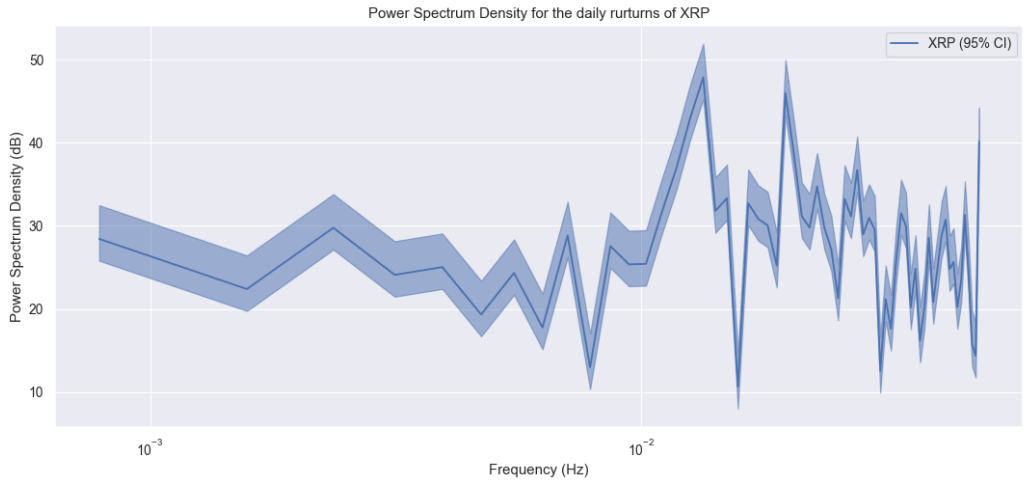

Figure 5: The power spectrum density (PSD) of JPY

(a) The power spectrum density (PSD) of JPY (before the Müller-Watson filtering)

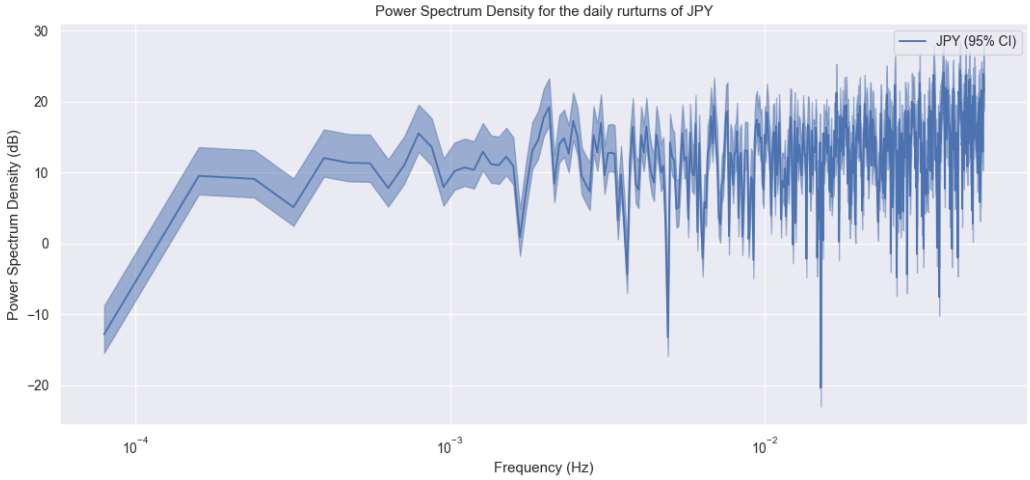

(b) The power spectrum density (PSD) of JPY (after the Müller-Watson filtering)

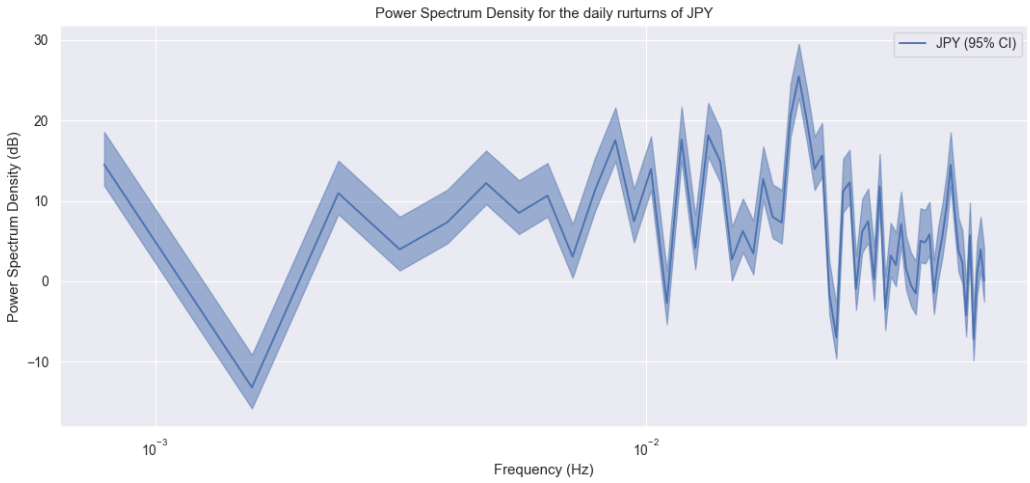

Figure 6: The power spectrum density (PSD) of EUR

(a) The power spectrum density (PSD) of EUR (before the Müller-Watson filtering)

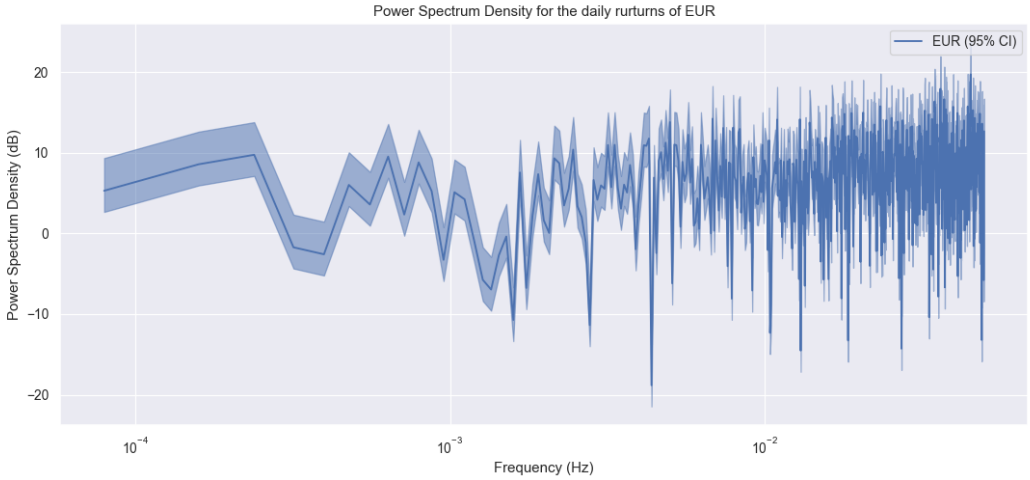

(b) The power spectrum density (PSD) of EUR (after the Müller-Watson filtering)

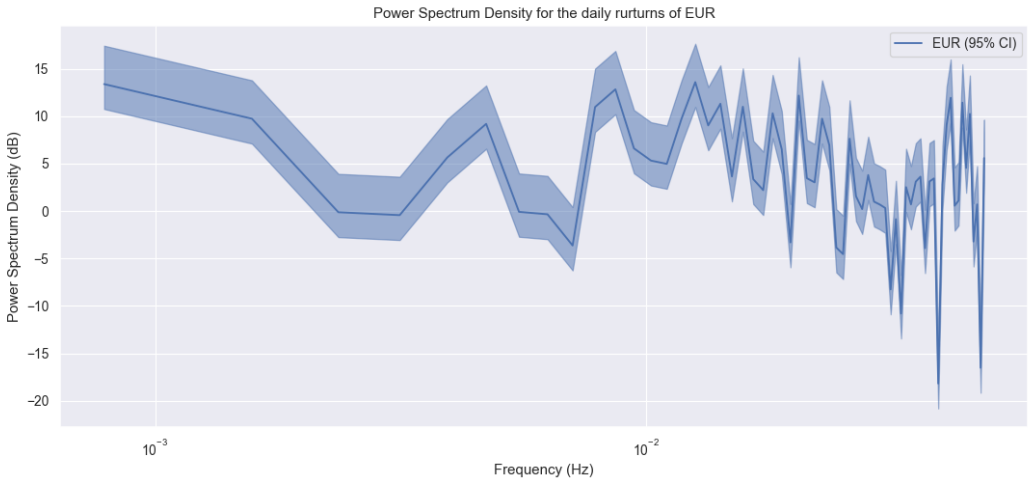

Figure 7: The power spectrum density (PSD) of GOLD

(a) The power spectrum density (PSD) of GOLD (before the Müller-Watson filtering)

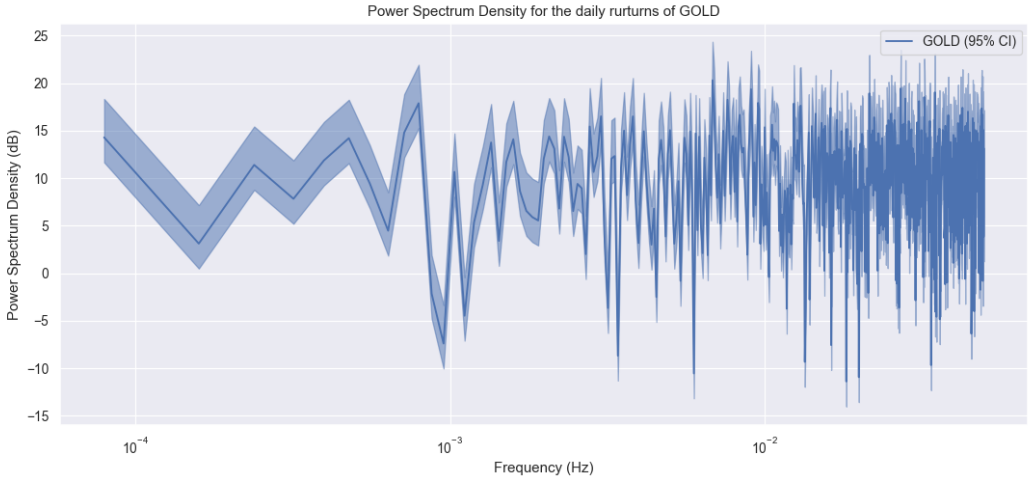

(b) The power spectrum density (PSD) of GOLD (after the Müller-Watson filtering)

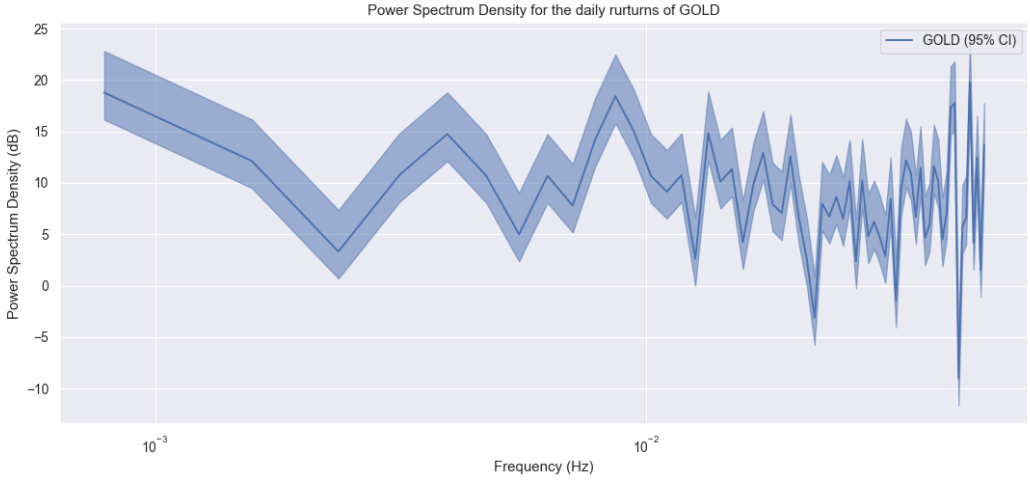

Figure 8: The power spectrum density (PSD) of S&P500

(a) The power spectrum density (PSD) of S&P500 (before the Müller-Watson filtering)

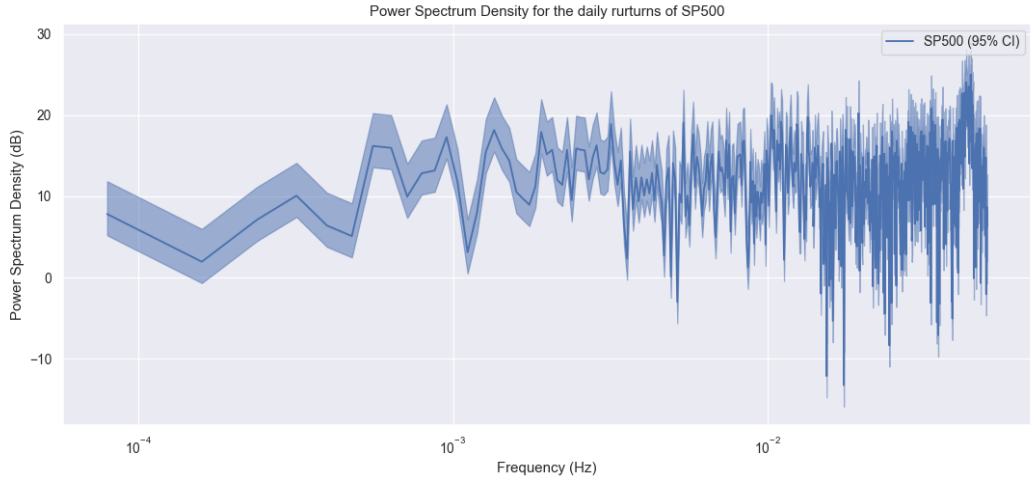

(b) The power spectrum density (PSD) of S&P500 (after the Müller-Watson filtering)

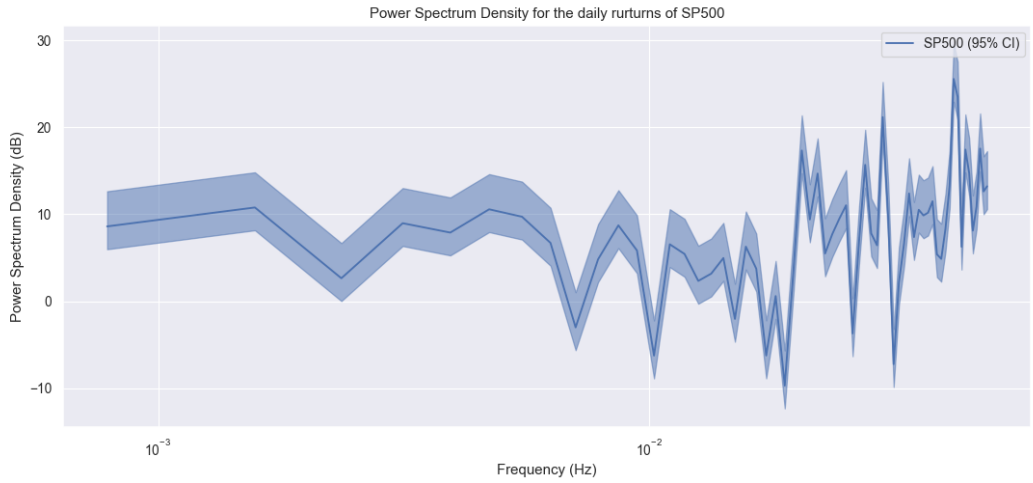

Figure 9: The power spectrum density (PSD) of MSCI

(a) The power spectrum density (PSD) of MSCI (before the Müller-Watson filtering)

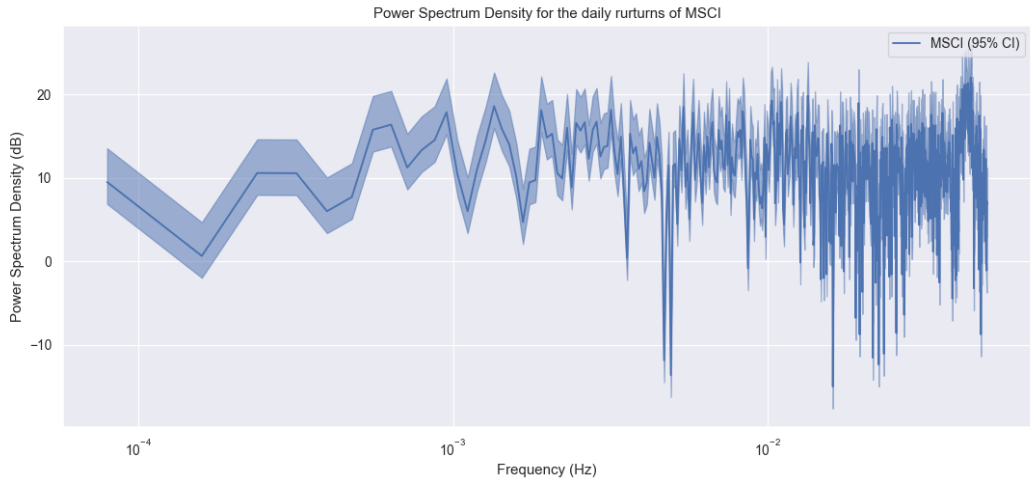

(b) The power spectrum density (PSD) of MSCI (after the Müller-Watson filtering)

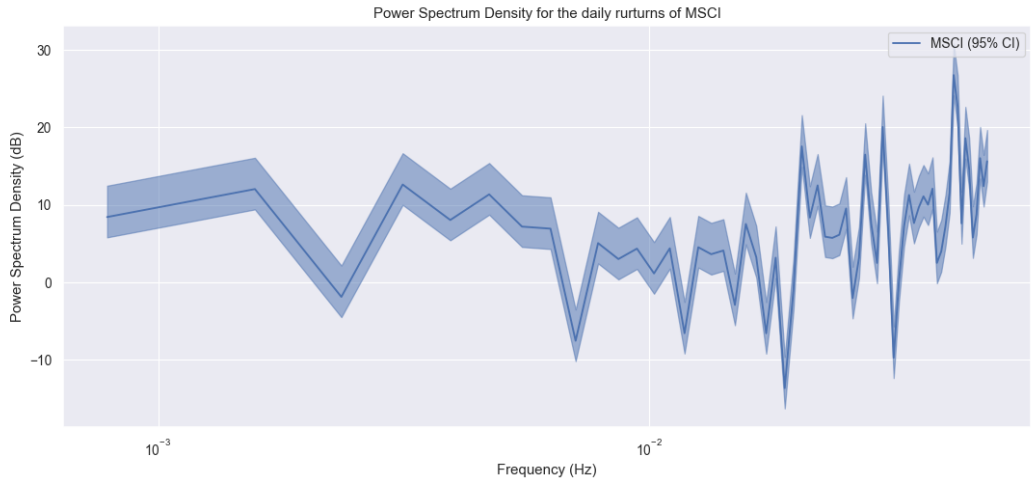

Figure 10: DTW alignment between BTC and GOLD in 2020

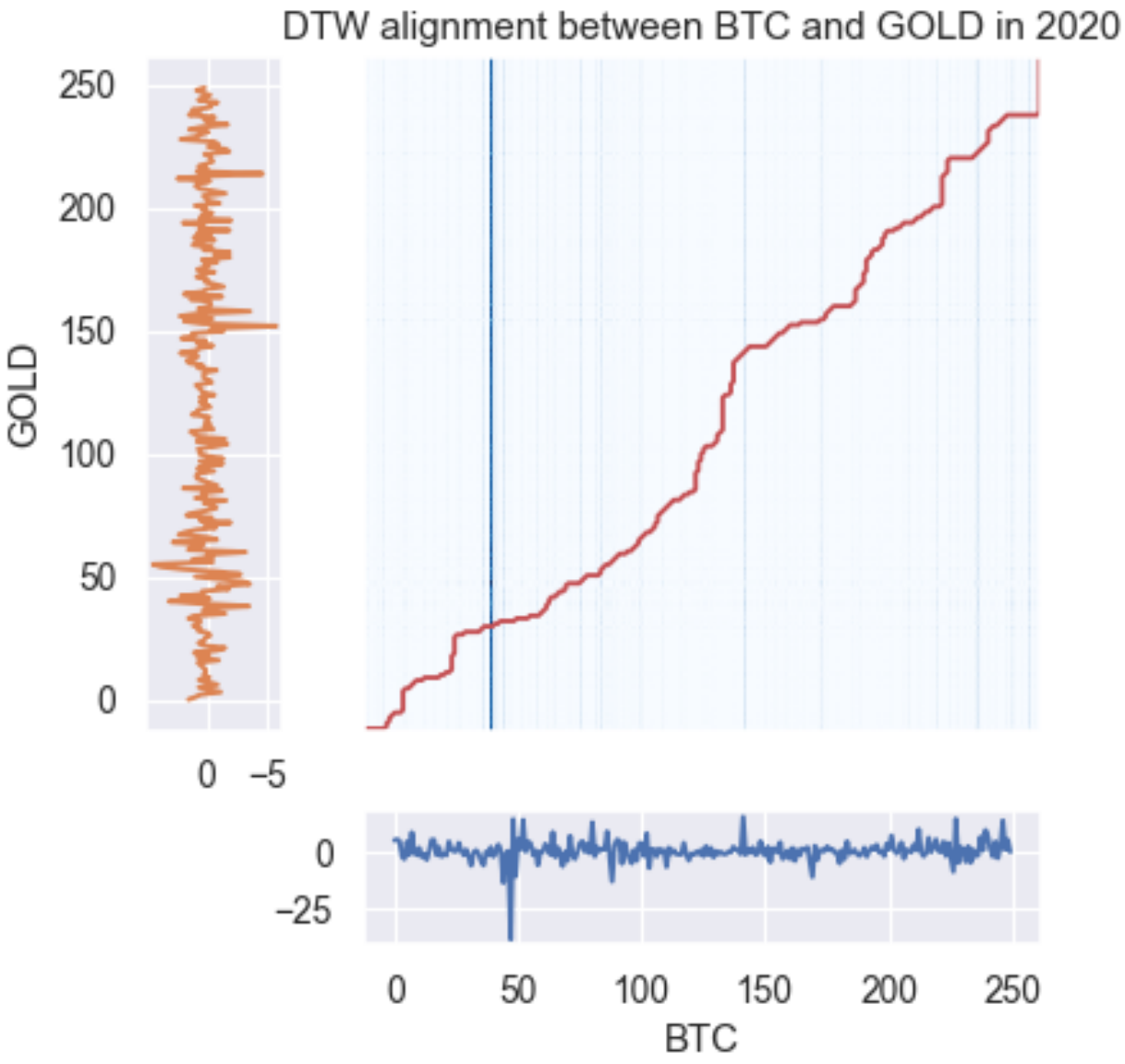

Figure 11: The OLS-CUSUM test of BTC (before the Müller-Watson filtering)

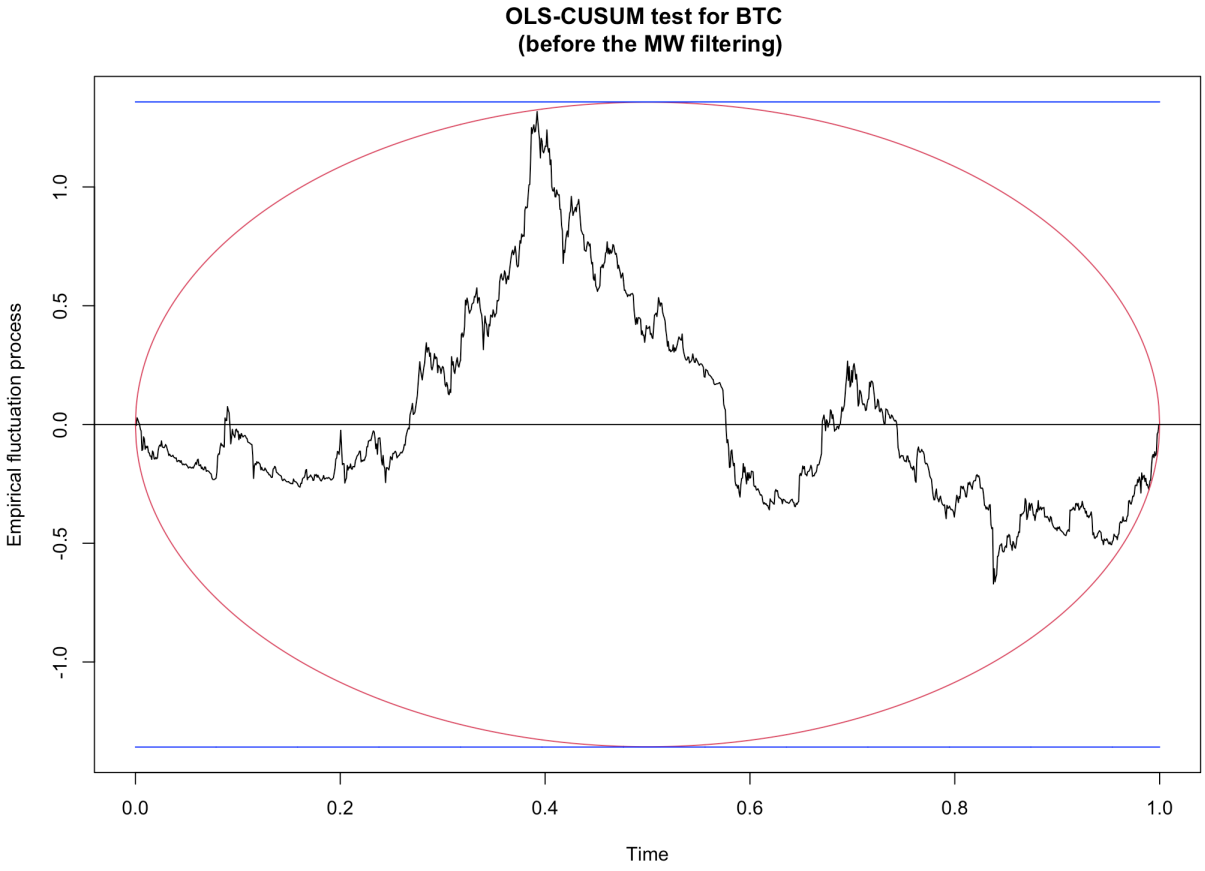

Figure 12: The OLS-CUSUM test of ETH (before the Müller-Watson filtering)

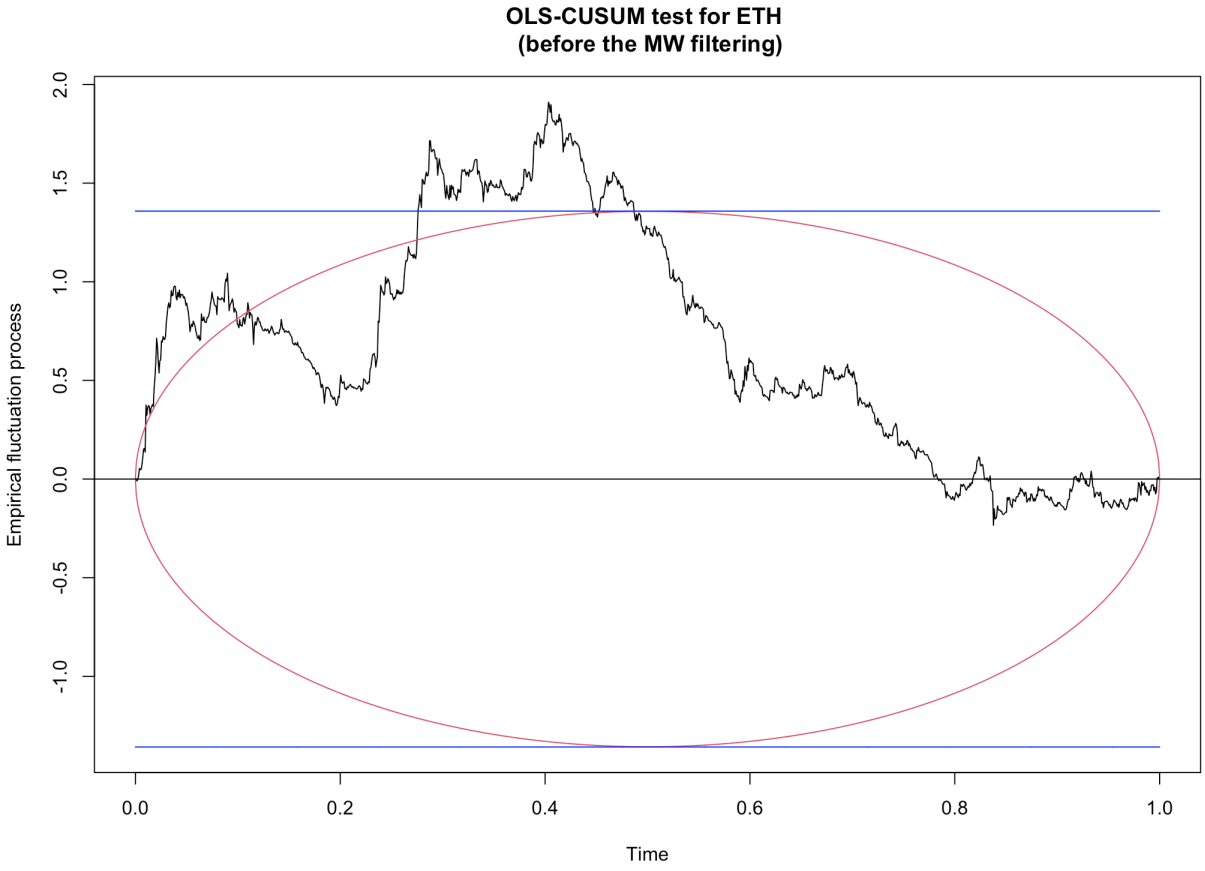

Figure 13: The OLS-CUSUM test of XRP (before the Müller-Watson filtering)

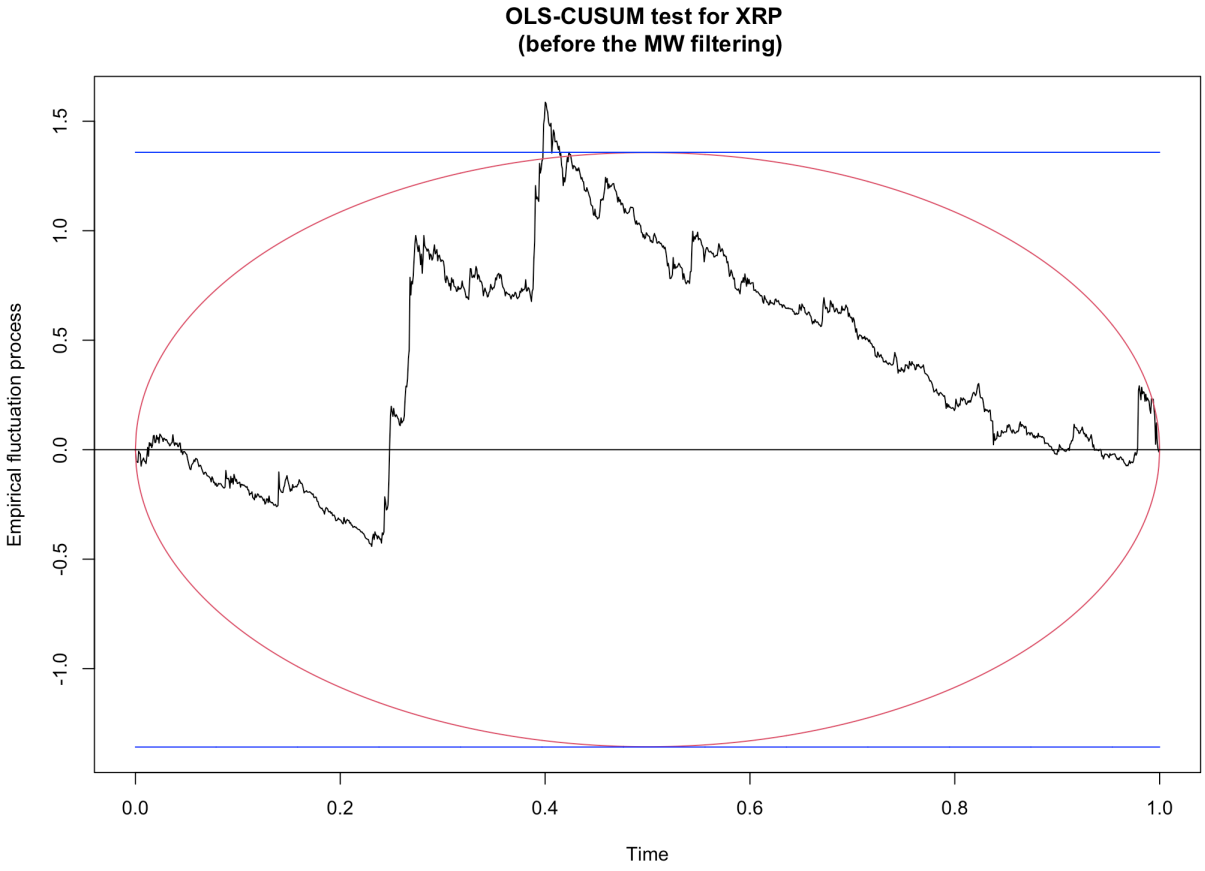

Figure 14: The OLS-CUSUM test of JPY (before the Müller-Watson filtering)

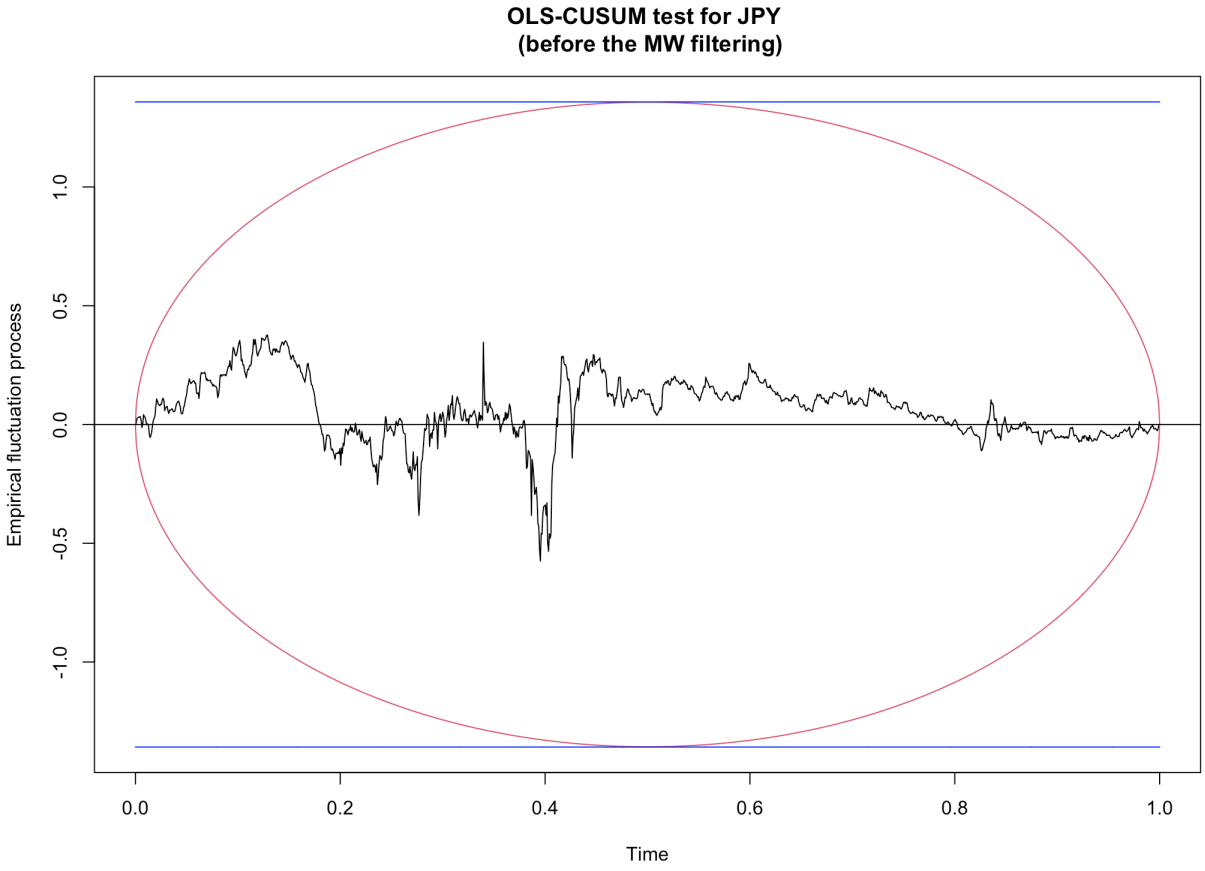

Figure 15: The OLS-CUSUM test of EUR (before the Müller-Watson filtering)

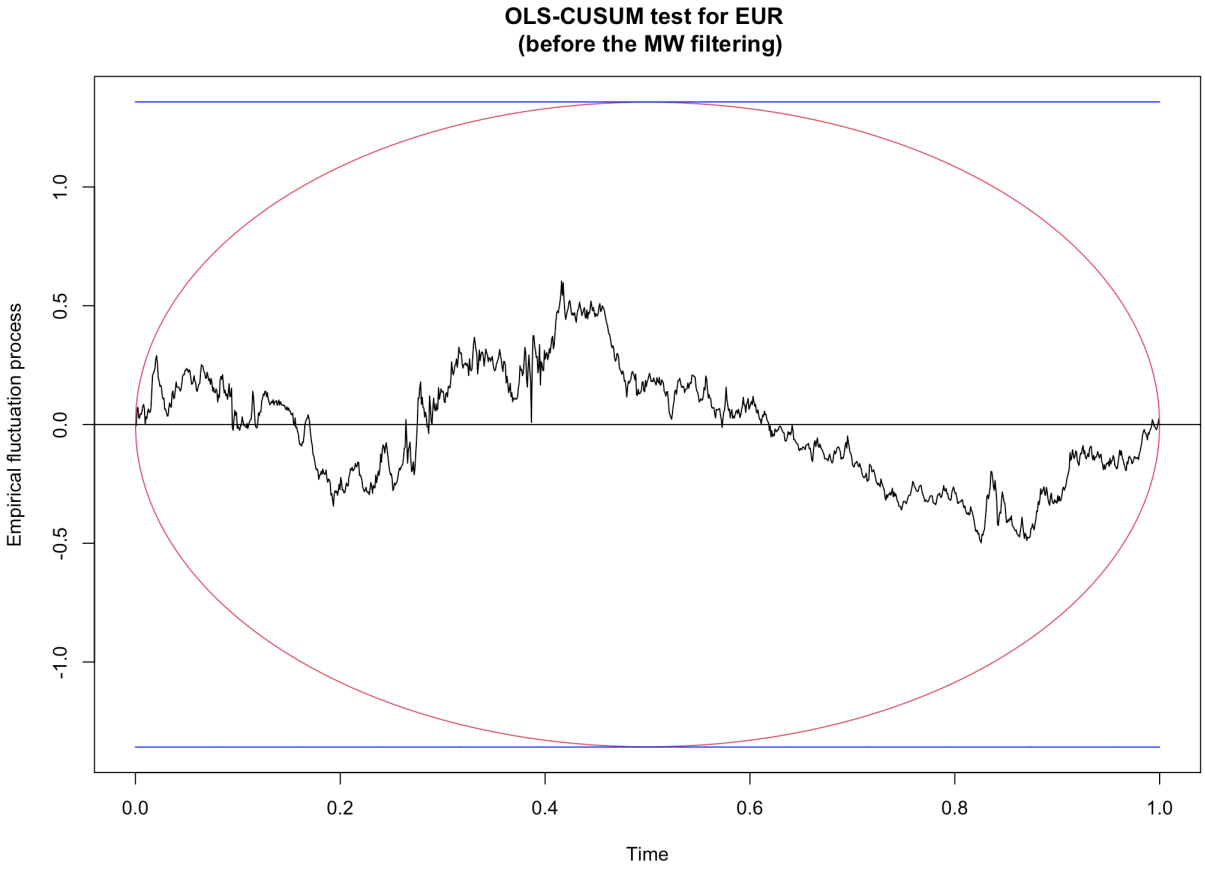

Figure 16: The OLS-CUSUM test of GOLD (before the Müller-Watson filtering)

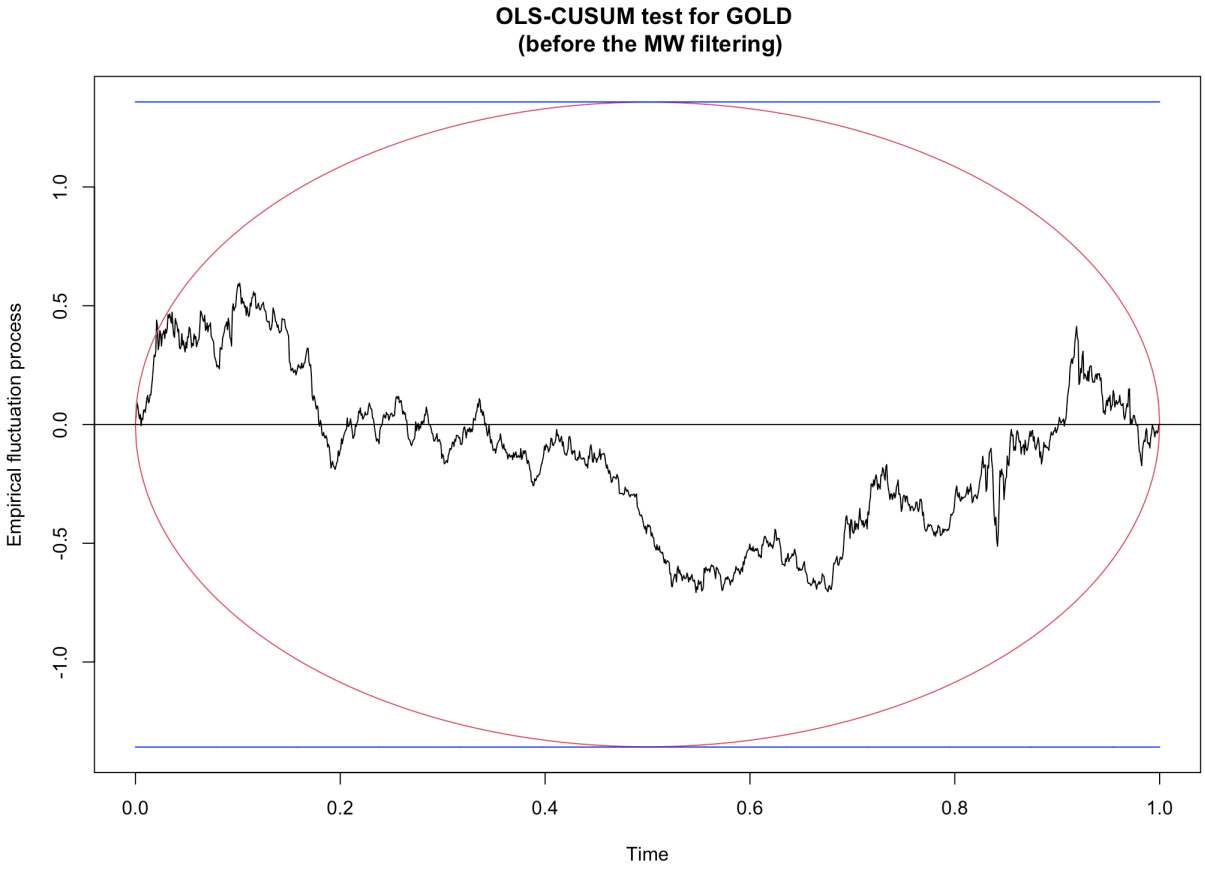

Figure 17: The OLS-CUSUM test of S&P500 (before the Müller-Watson filtering)

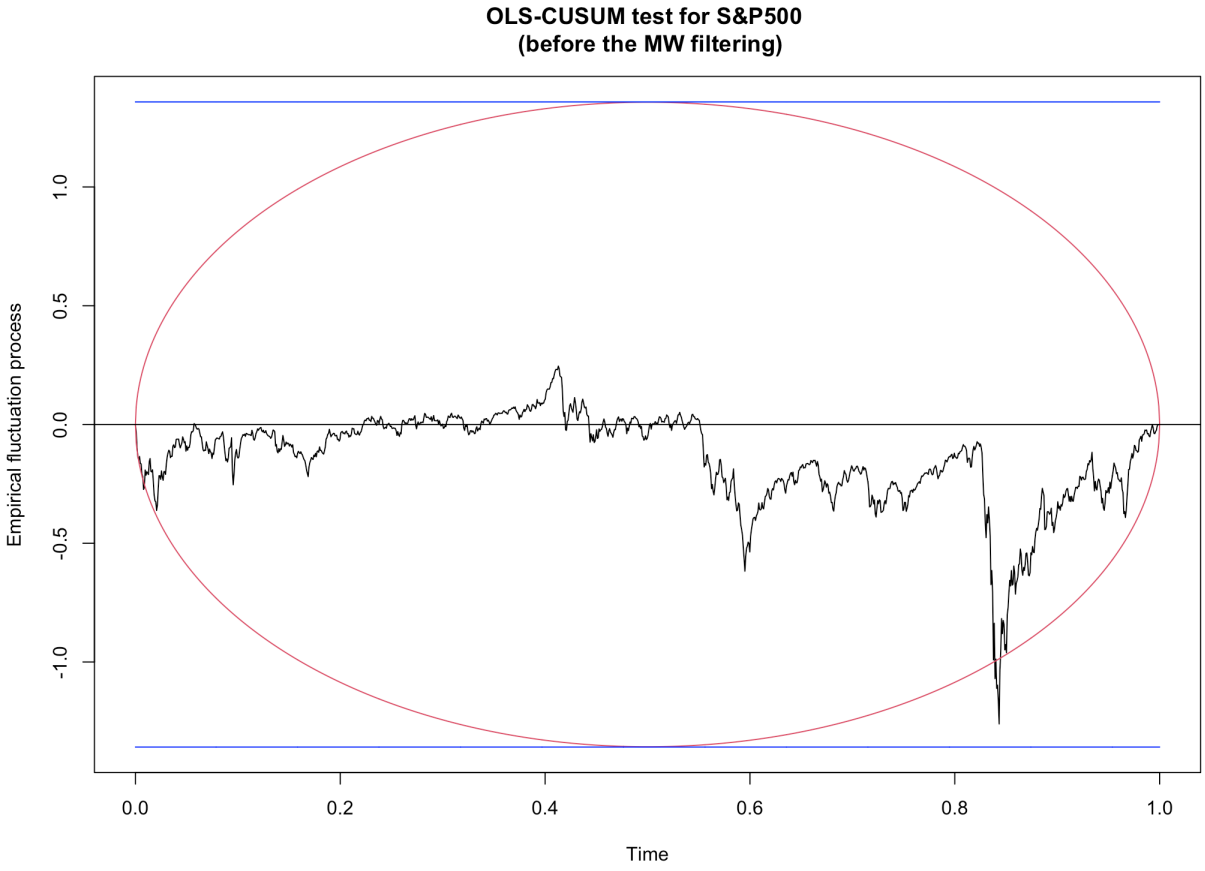

Figure 18: The OLS-CUSUM test of MSCI (before the Müller-Watson filtering)

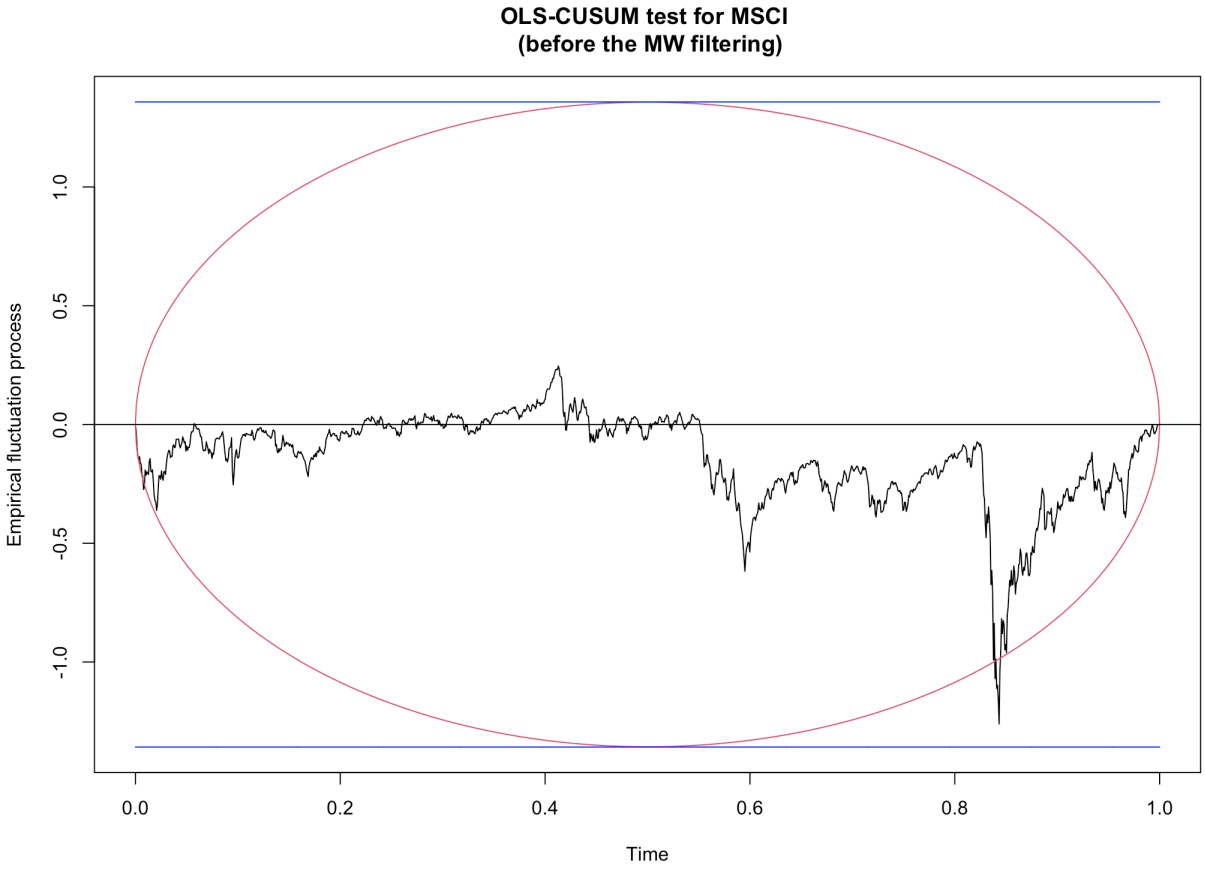

Figure 19: The OLS-CUSUM test of BTC (after the Müller-Watson filtering)

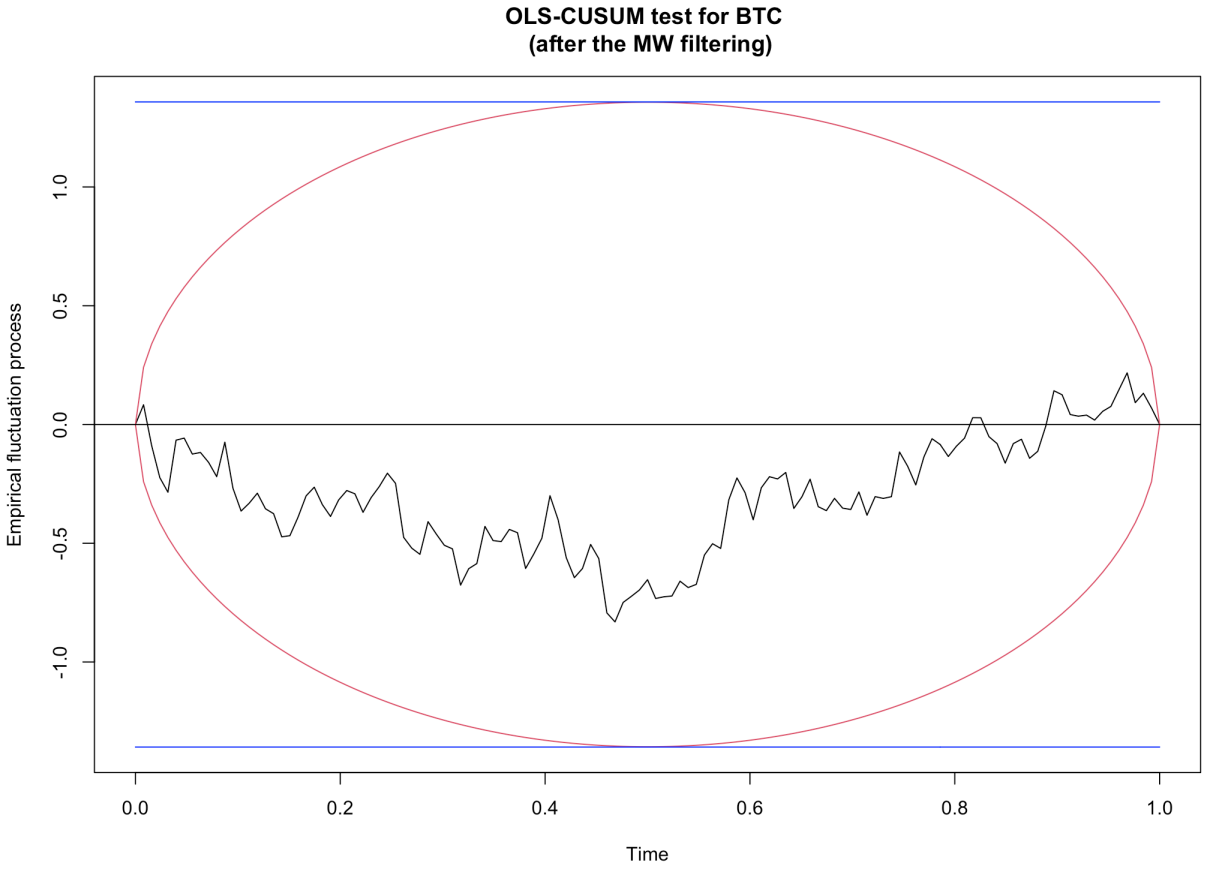

Figure 20: The OLS-CUSUM test of ETH (after the Müller-Watson filtering)

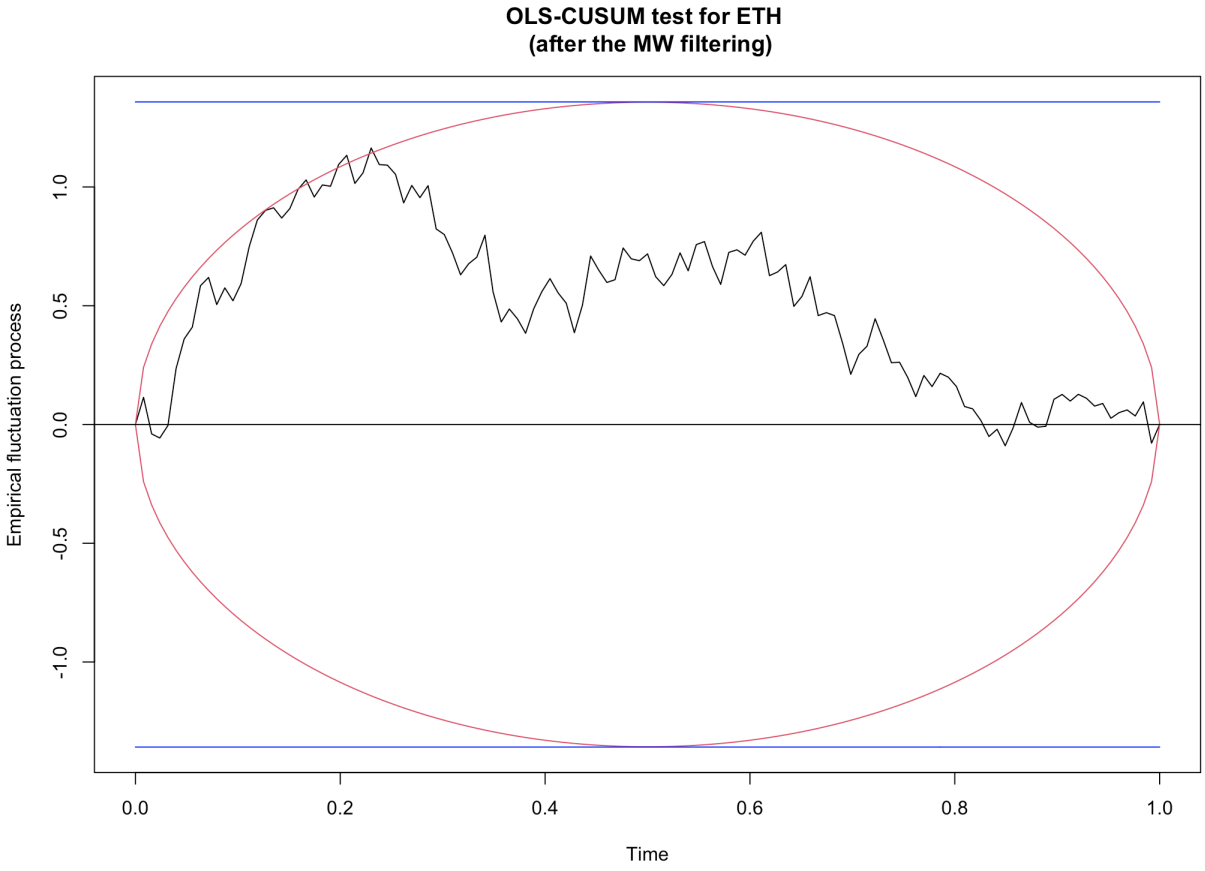

Figure 21: The OLS-CUSUM test of XRP (after the Müller-Watson filtering)

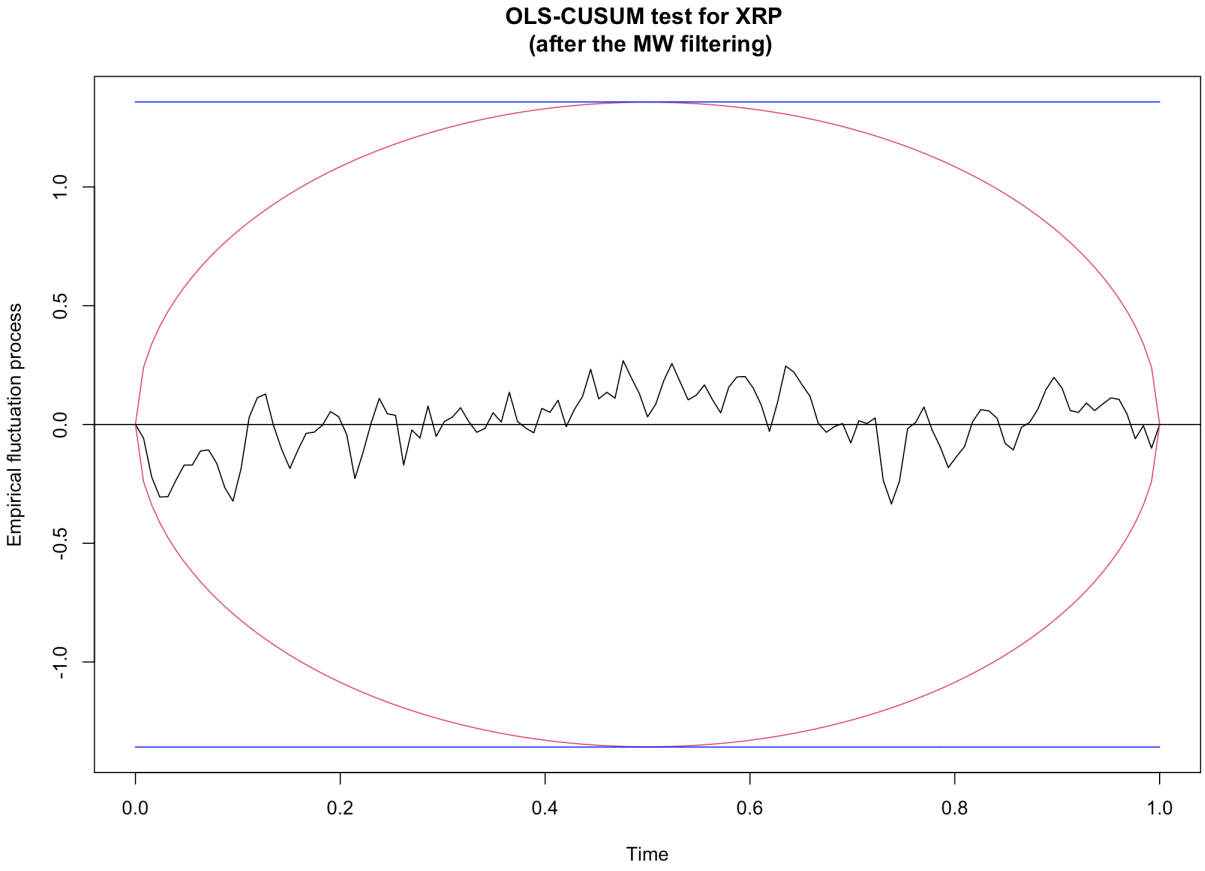

Figure 22: The OLS-CUSUM test of JPY (after the Müller-Watson filtering)

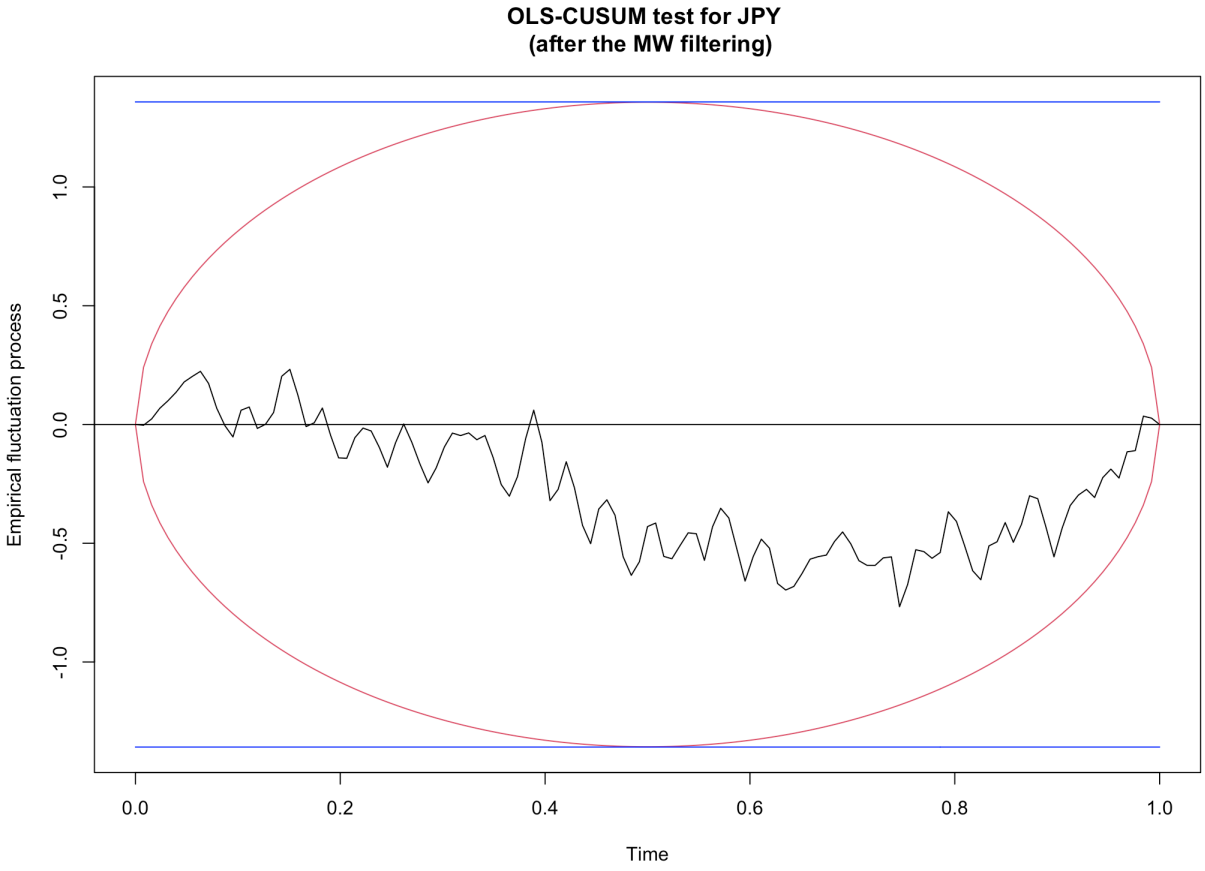

Figure 23: The OLS-CUSUM test of EUR (after the Müller-Watson filtering)

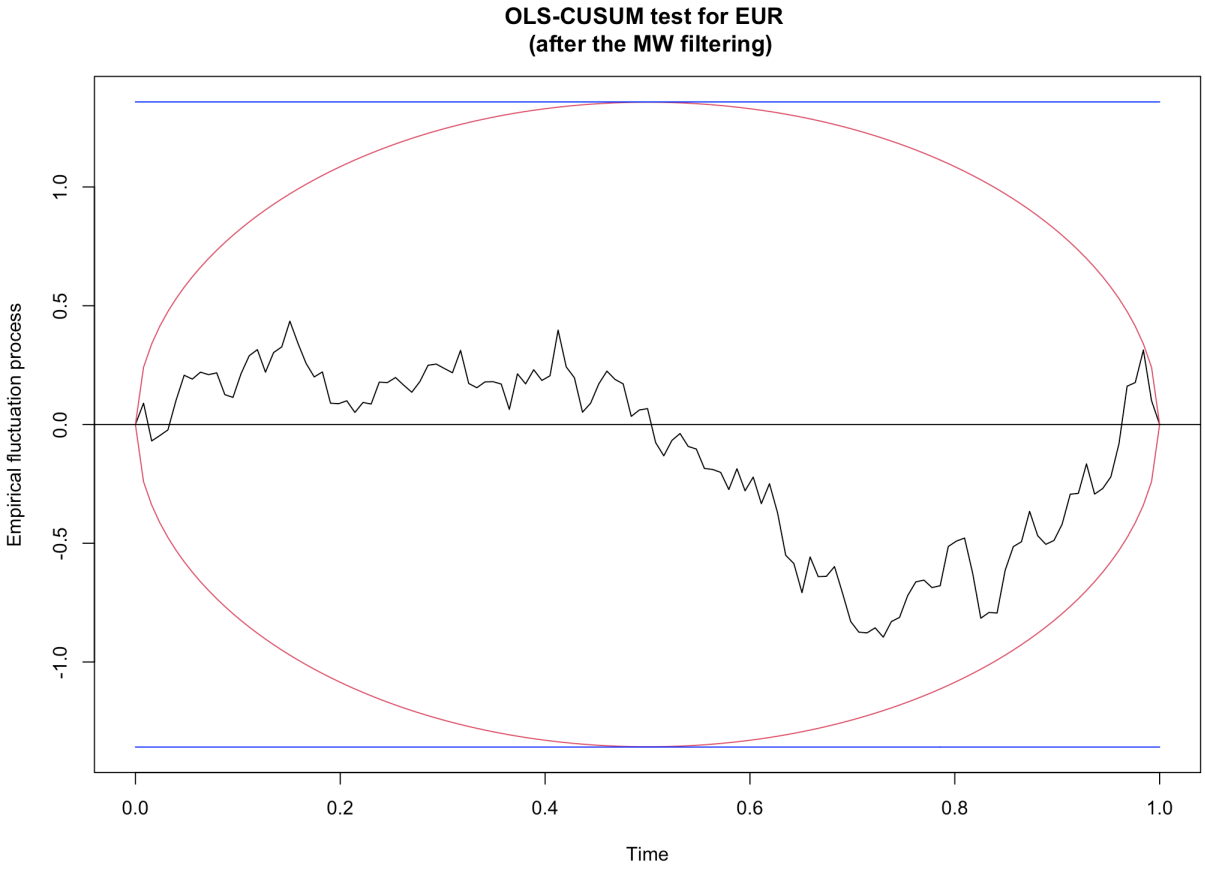

Figure 24: The OLS-CUSUM test of GOLD (after the Müller-Watson filtering)

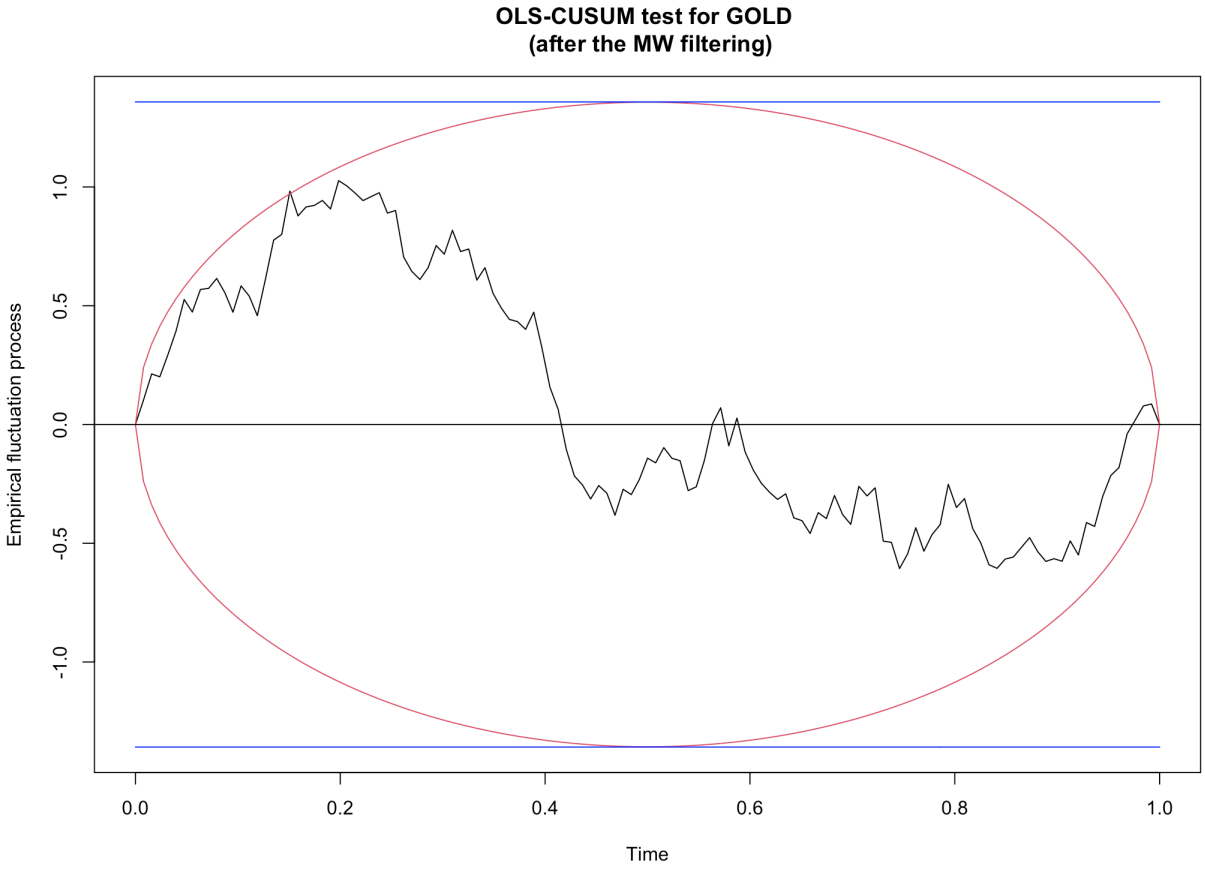

Figure 25: The OLS-CUSUM test of S&P500 (after the Müller-Watson filtering)

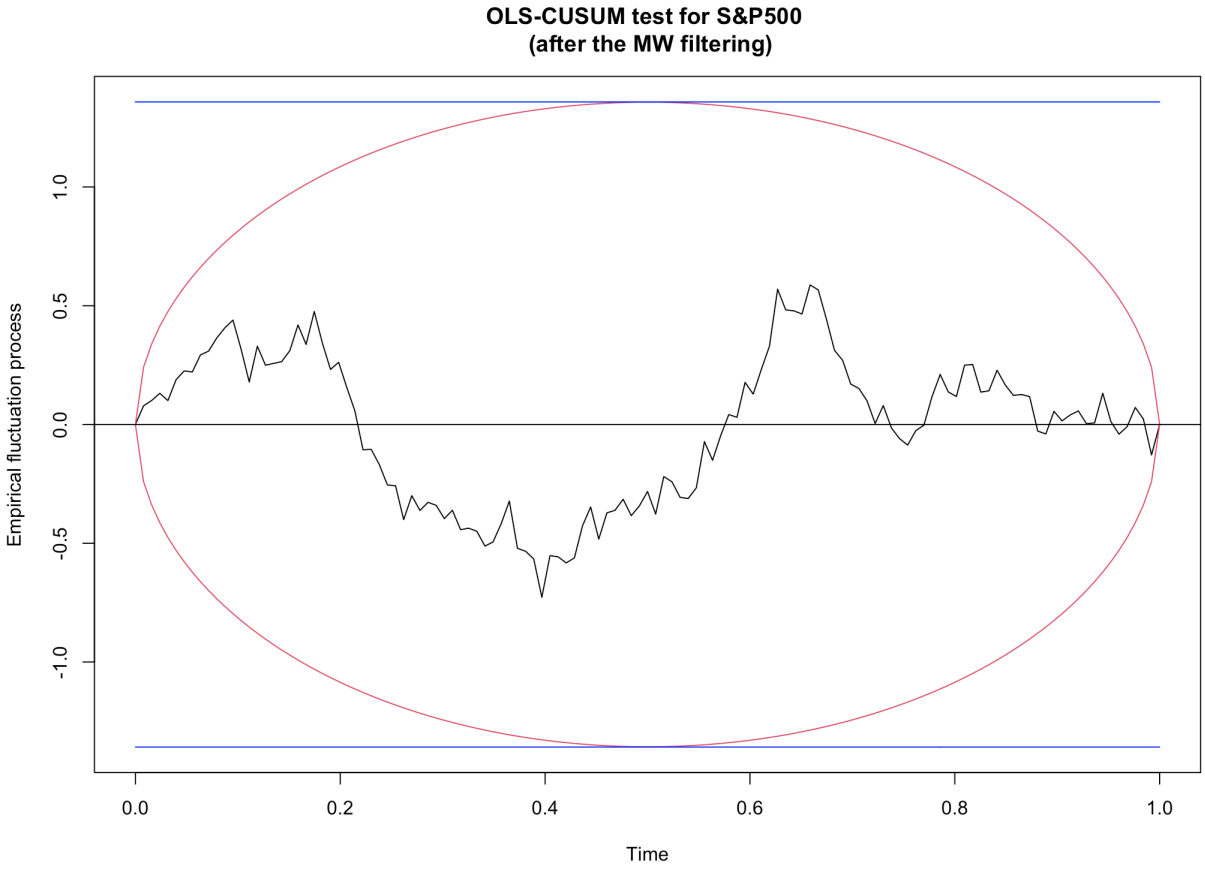

Figure 26: The OLS-CUSUM test of MSCI (after the Müller-Watson filtering)

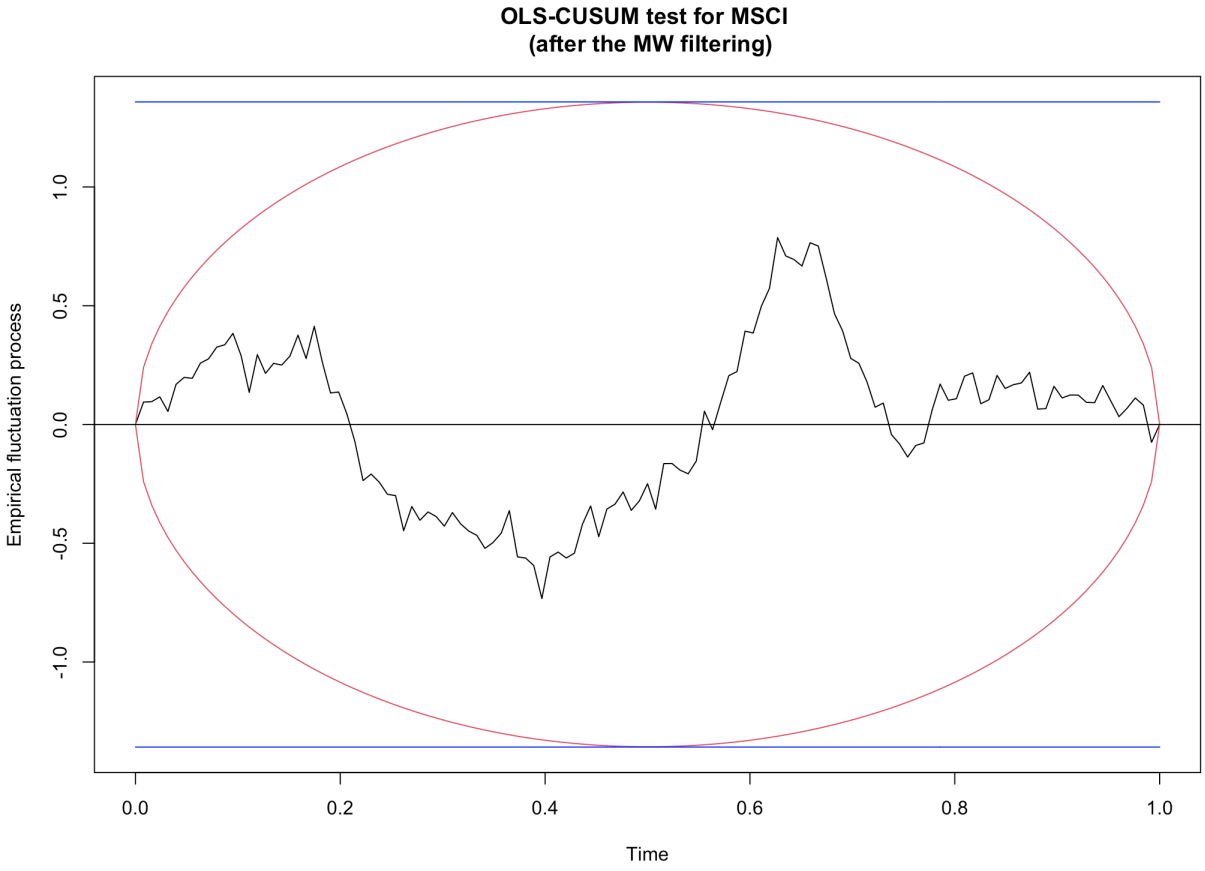

Figure 27: The Rec-CUSUM test of BTC [2016-2020] (before the Müller-Watson filtering)

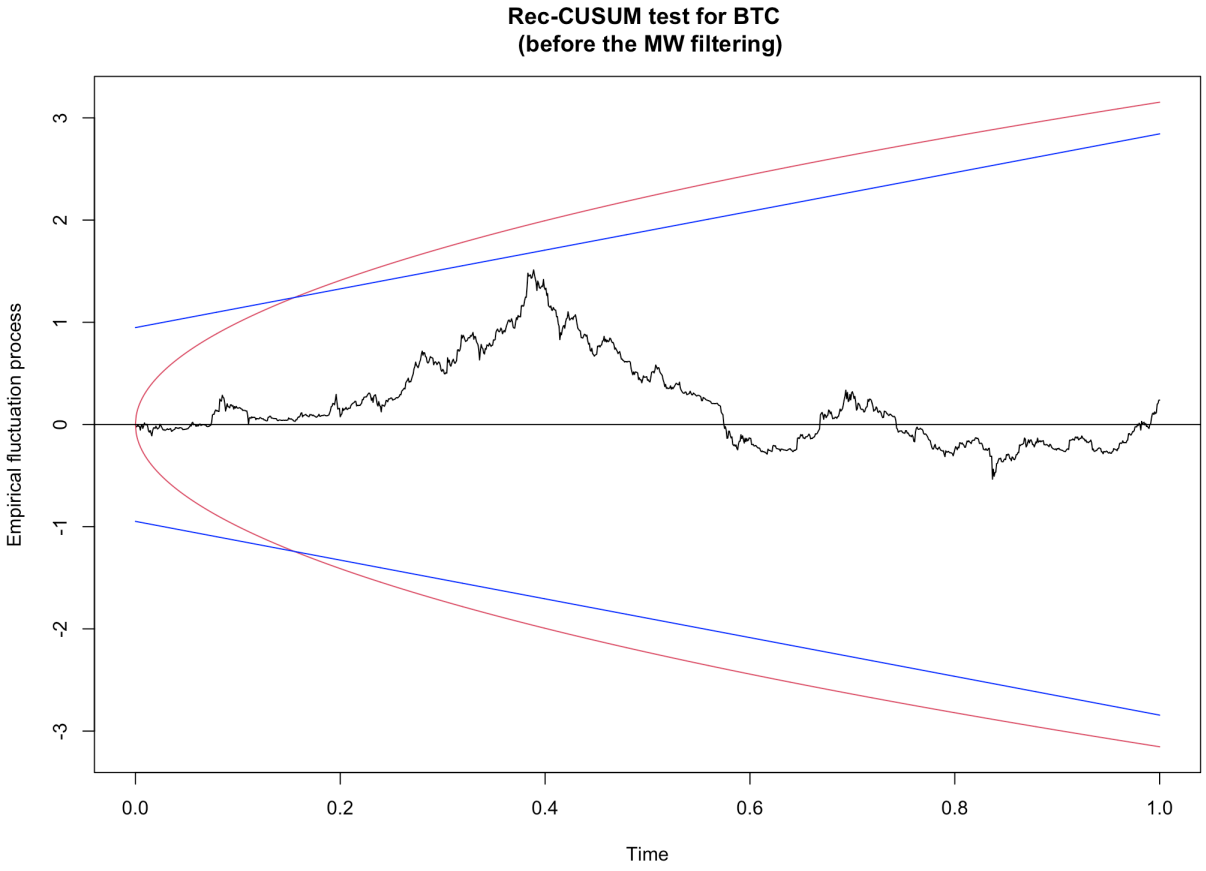

Figure 28: The Rec-CUSUM test of BTC [2017-2020] (before the Müller-Watson filtering)

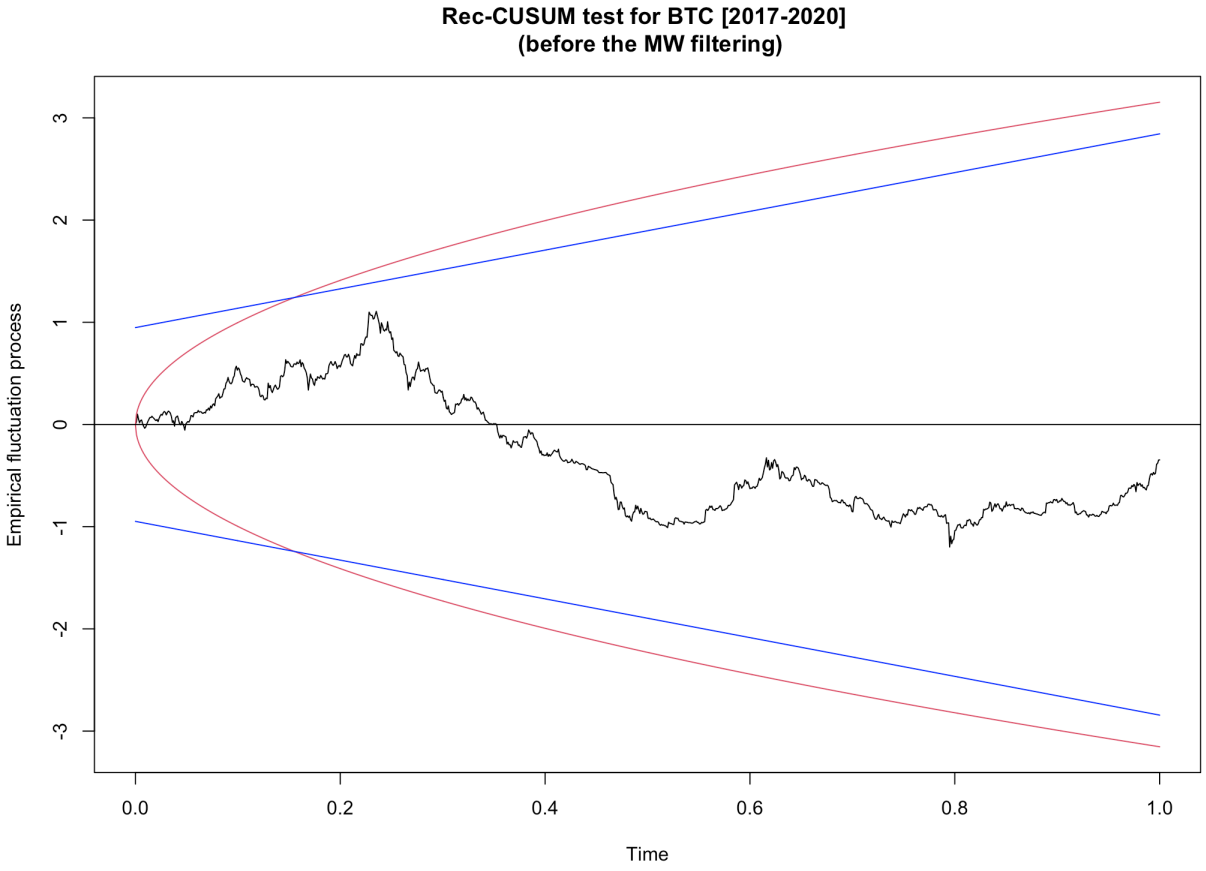

Figure 29: The Rec-CUSUM test of BTC [2018-2020] (before the Müller-Watson filtering)

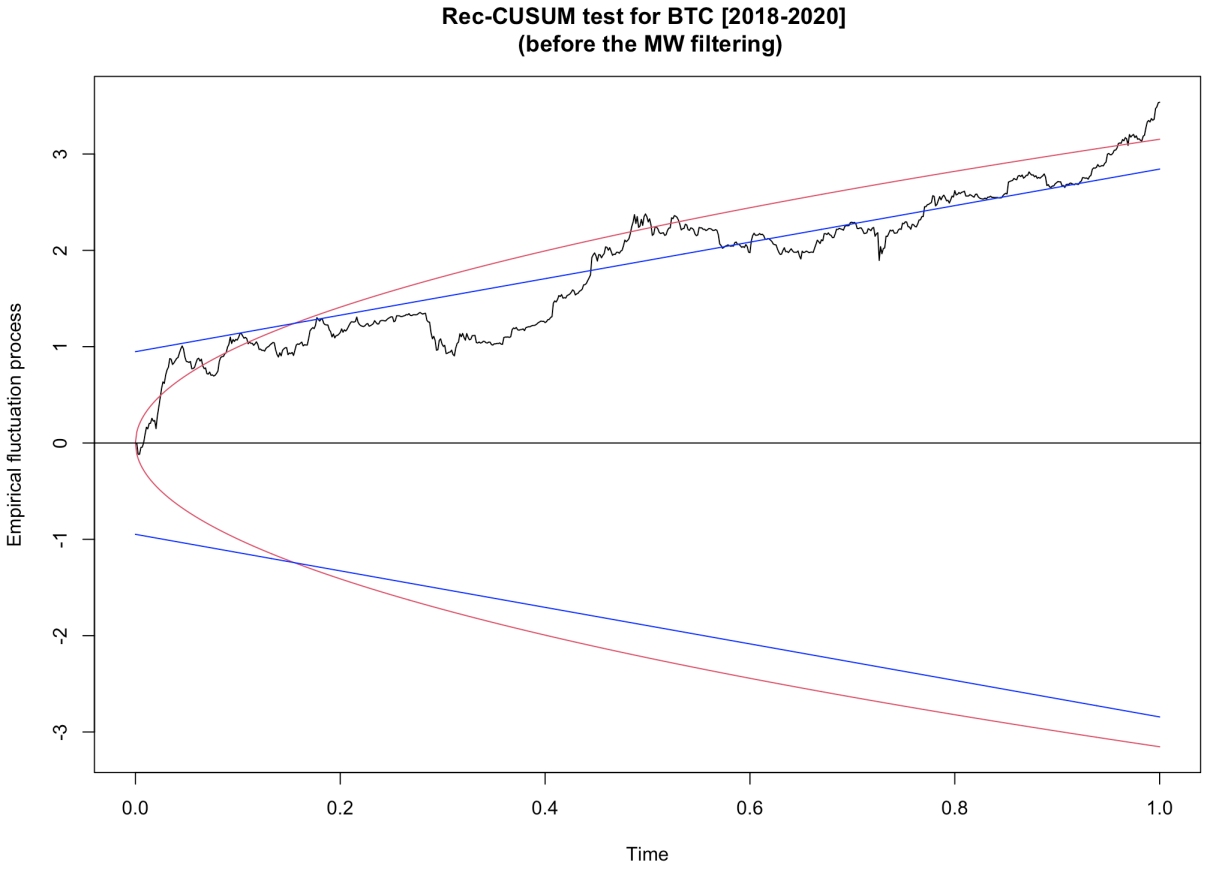

Figure 30: The Rec-CUSUM test of BTC [2019-2020] (before the Müller-Watson filtering)

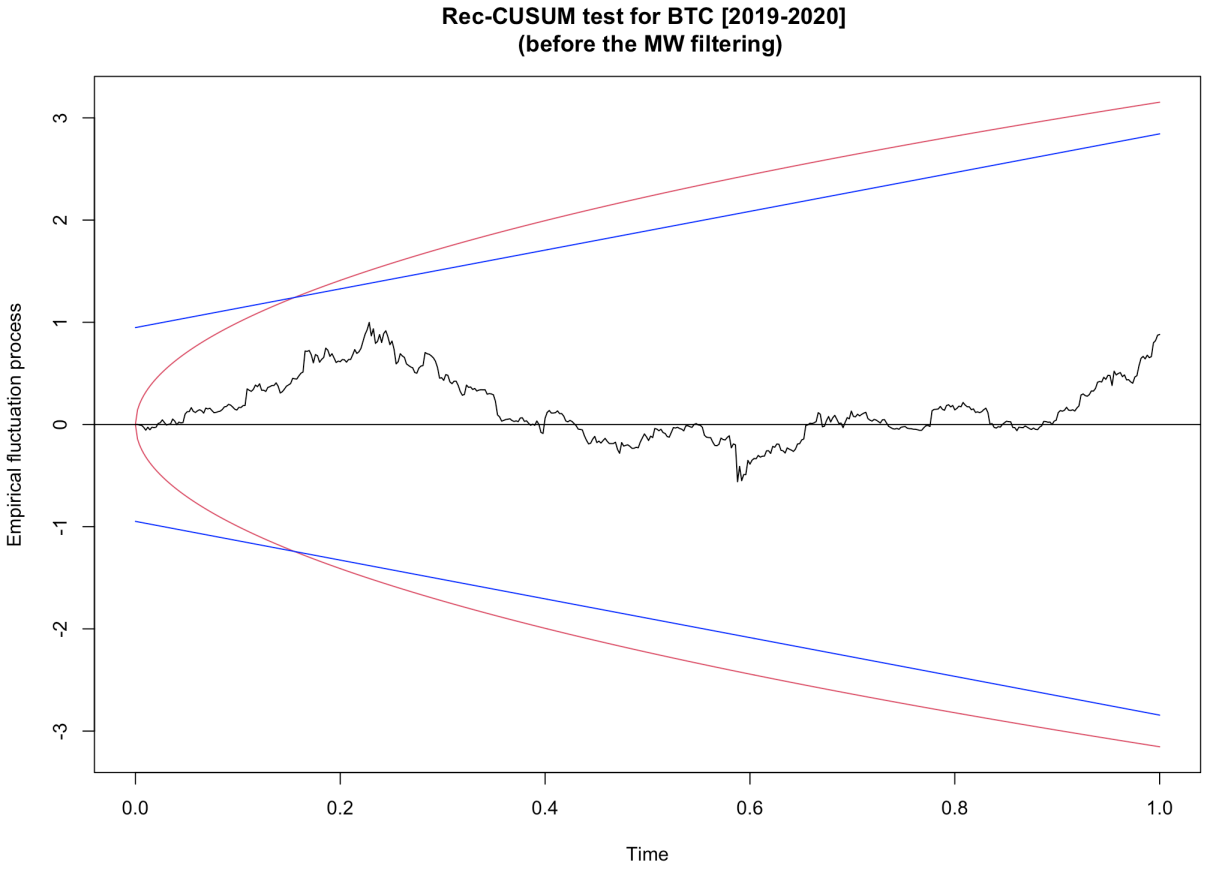

Figure 31: The Rec-CUSUM test of ETH [2016-2020] (before the Müller-Watson filtering)

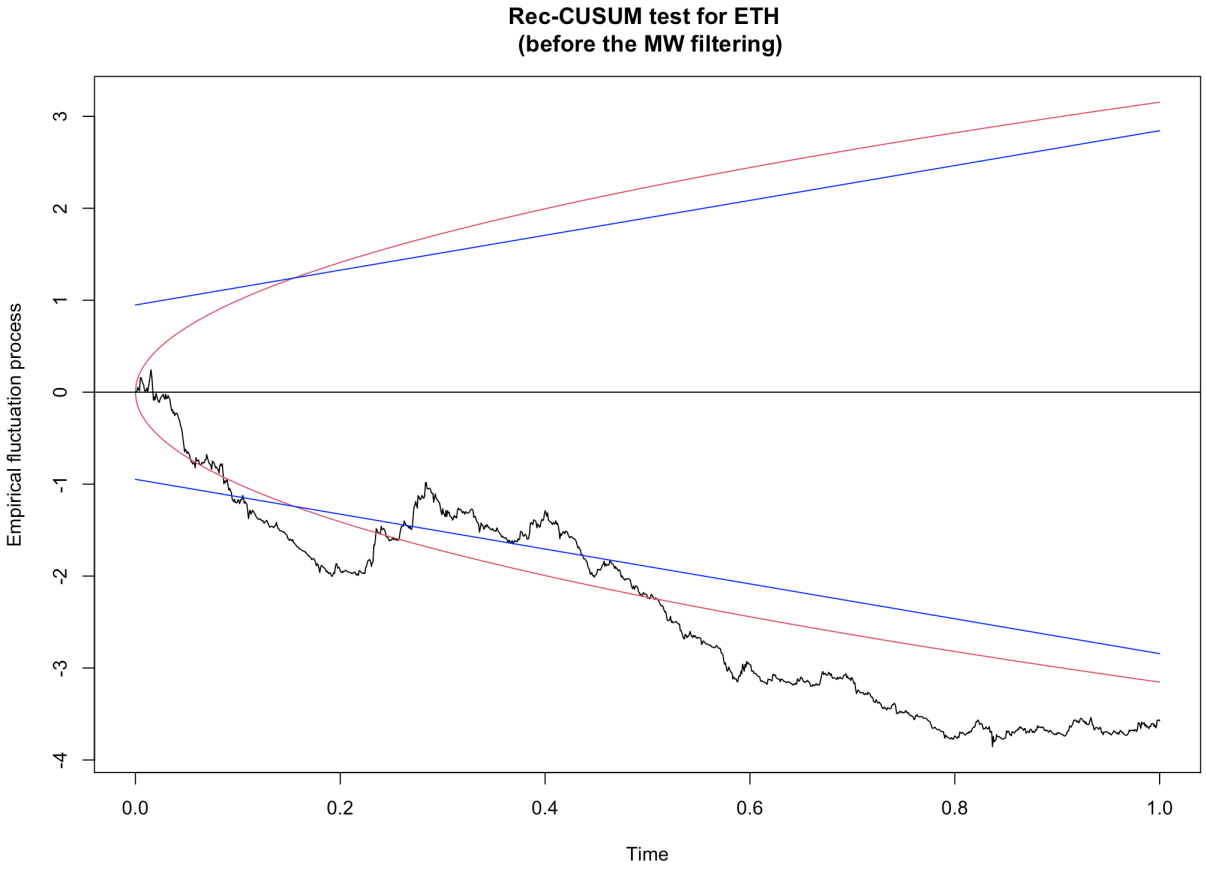

Figure 32: The Rec-CUSUM test of ETH [2017-2020] (before the Müller-Watson filtering)

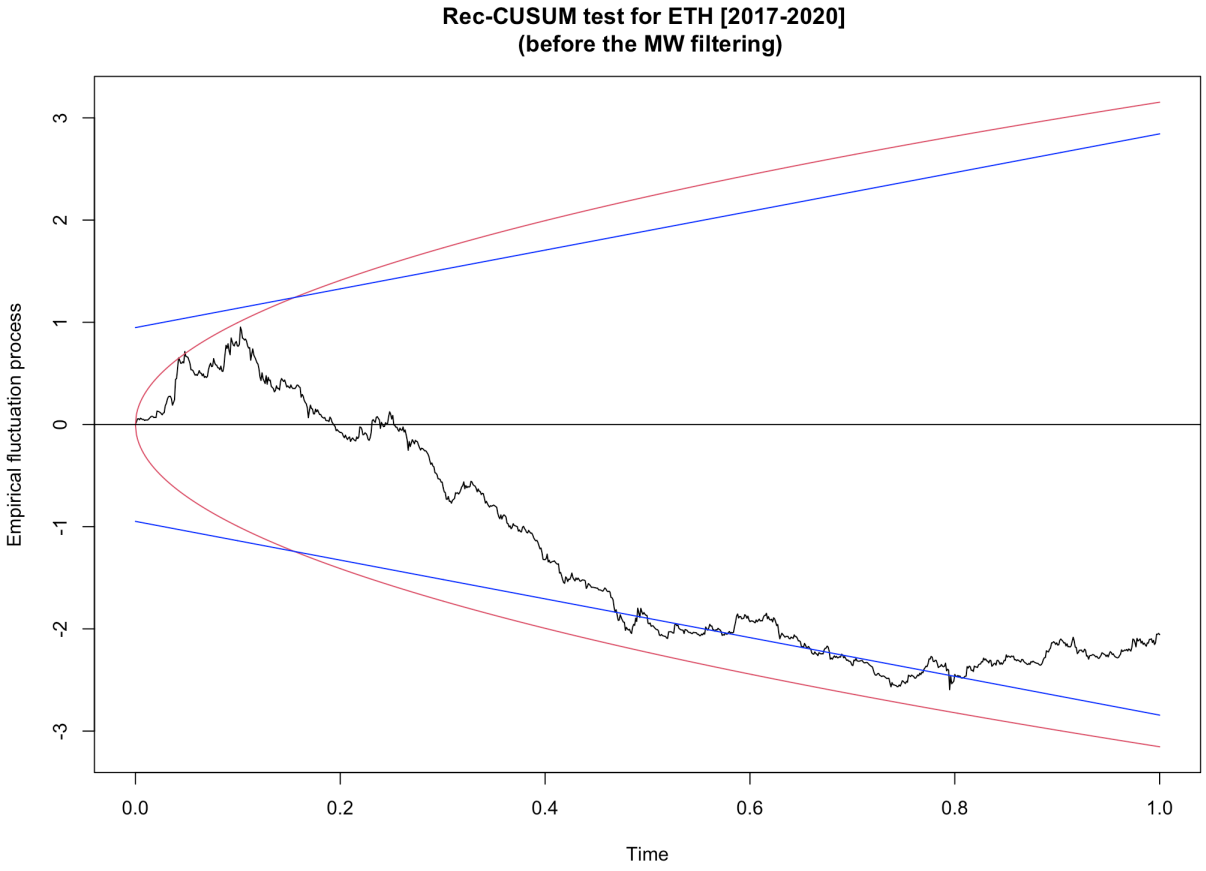

Figure 33: The Rec-CUSUM test of ETH [2018-2020] (before the Müller-Watson filtering)

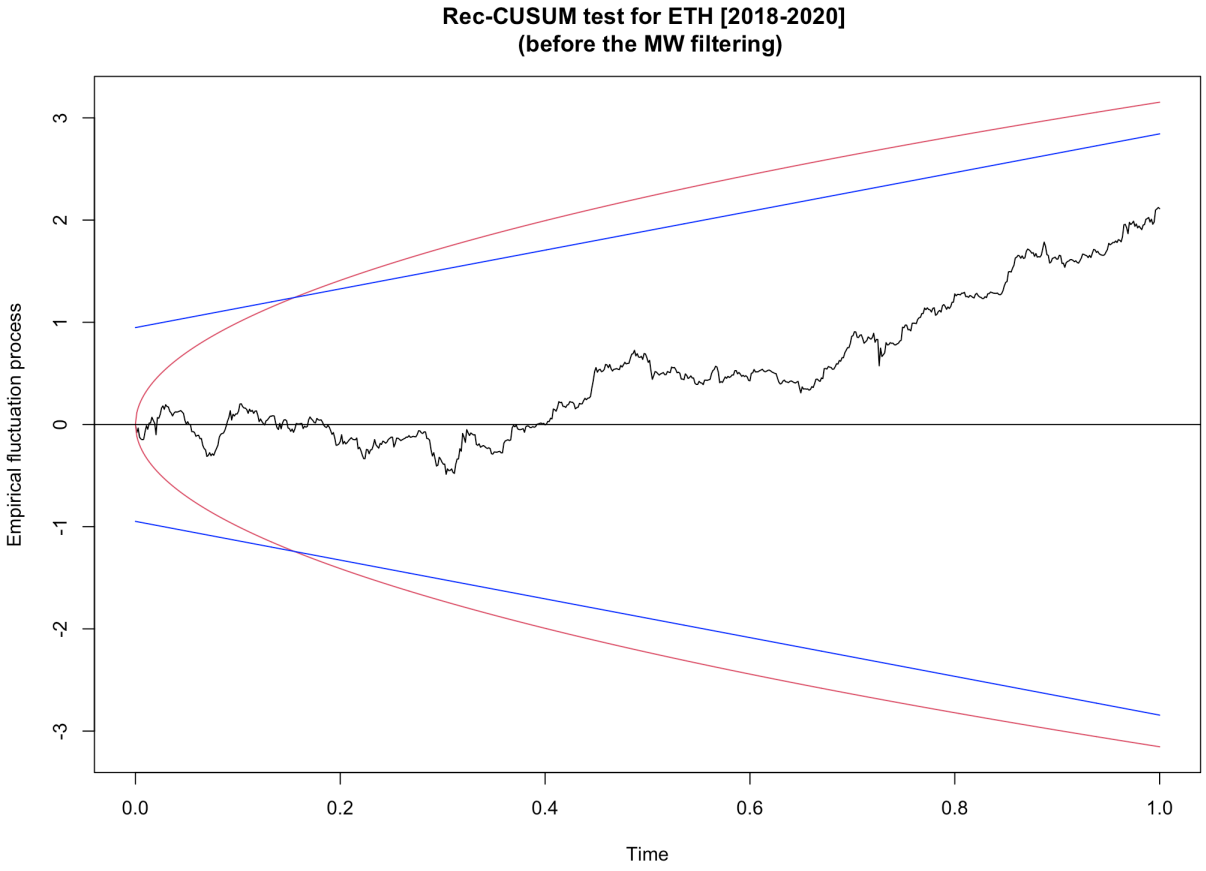

Figure 34: The Rec-CUSUM test of ETH [2019-2020] (before the Müller-Watson filtering)

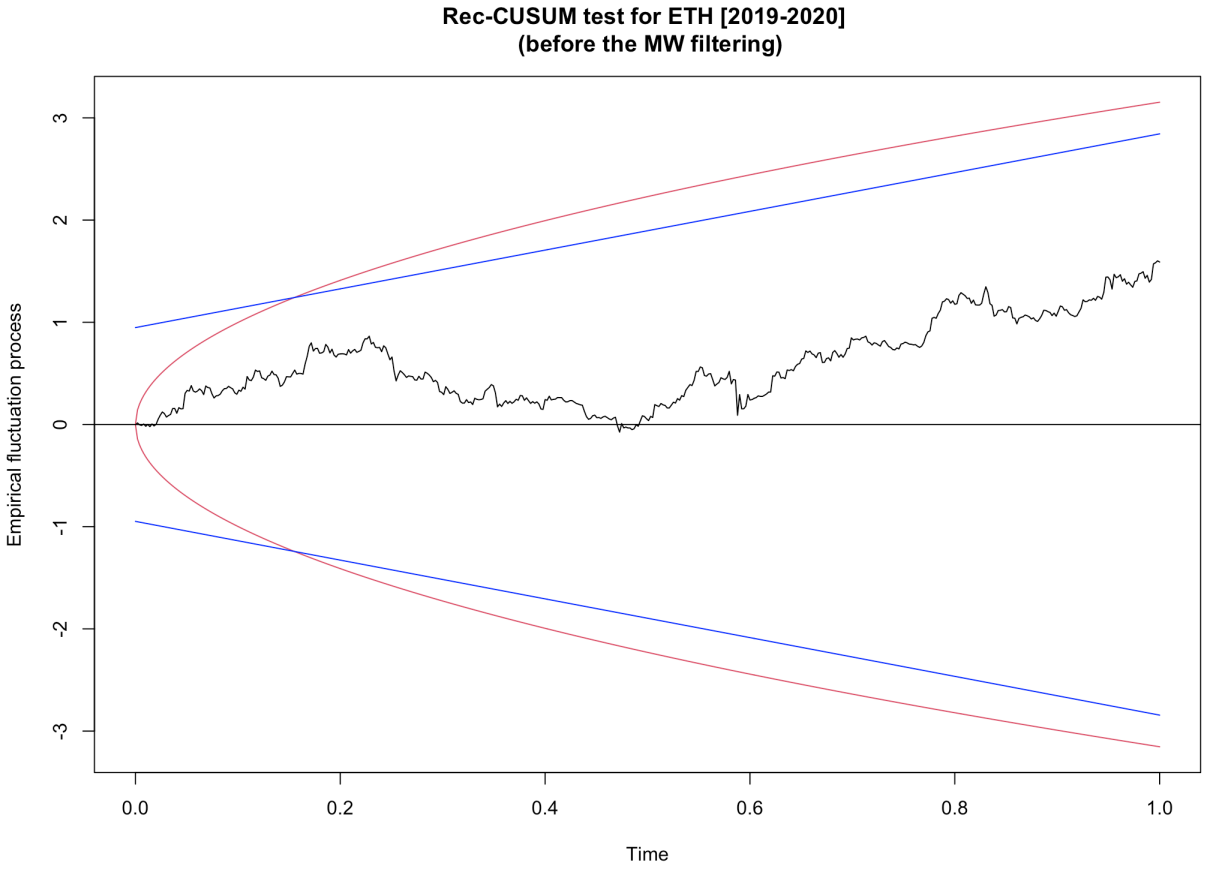

Figure 35: The Rec-CUSUM test of XRP [2016-2020] (before the Müller-Watson filtering)

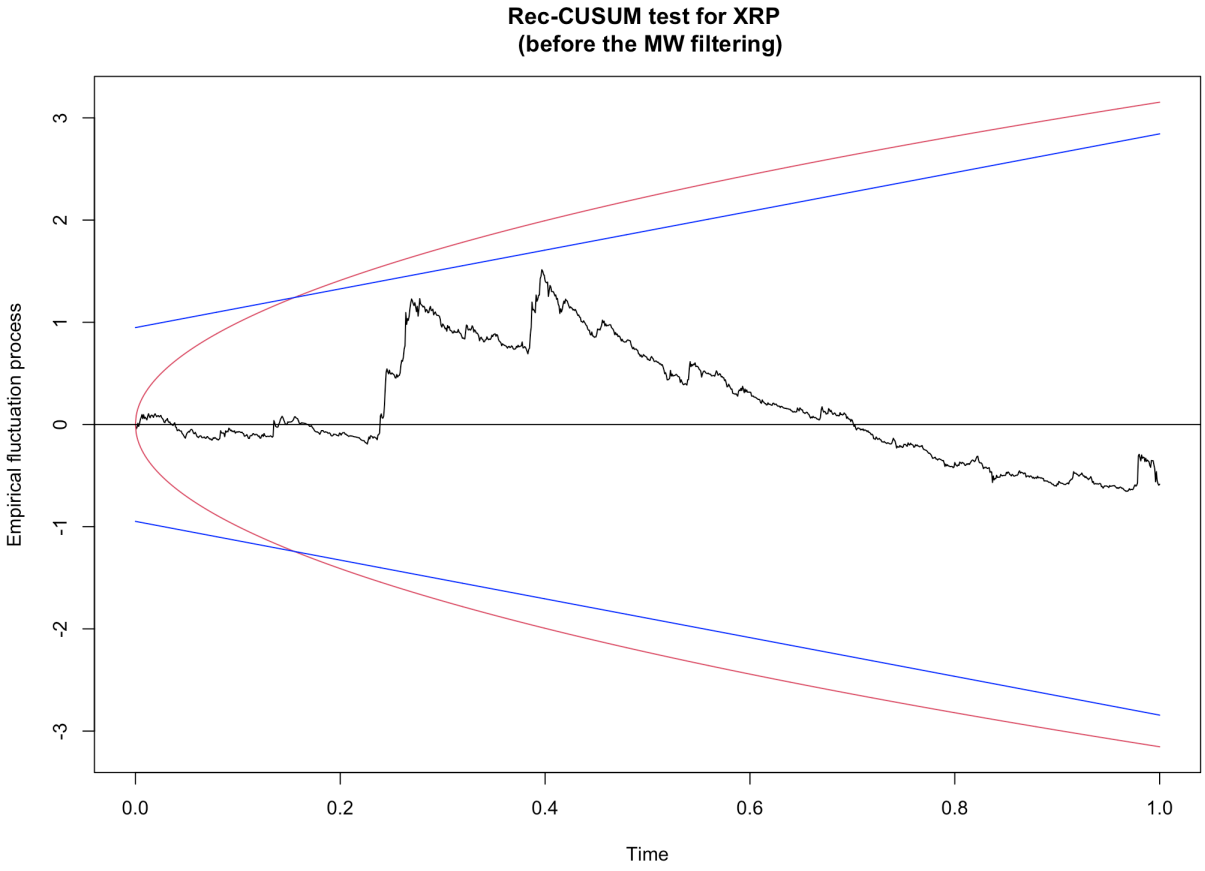

Figure 36: The Rec-CUSUM test of XRP [2017-2020] (before the Müller-Watson filtering)

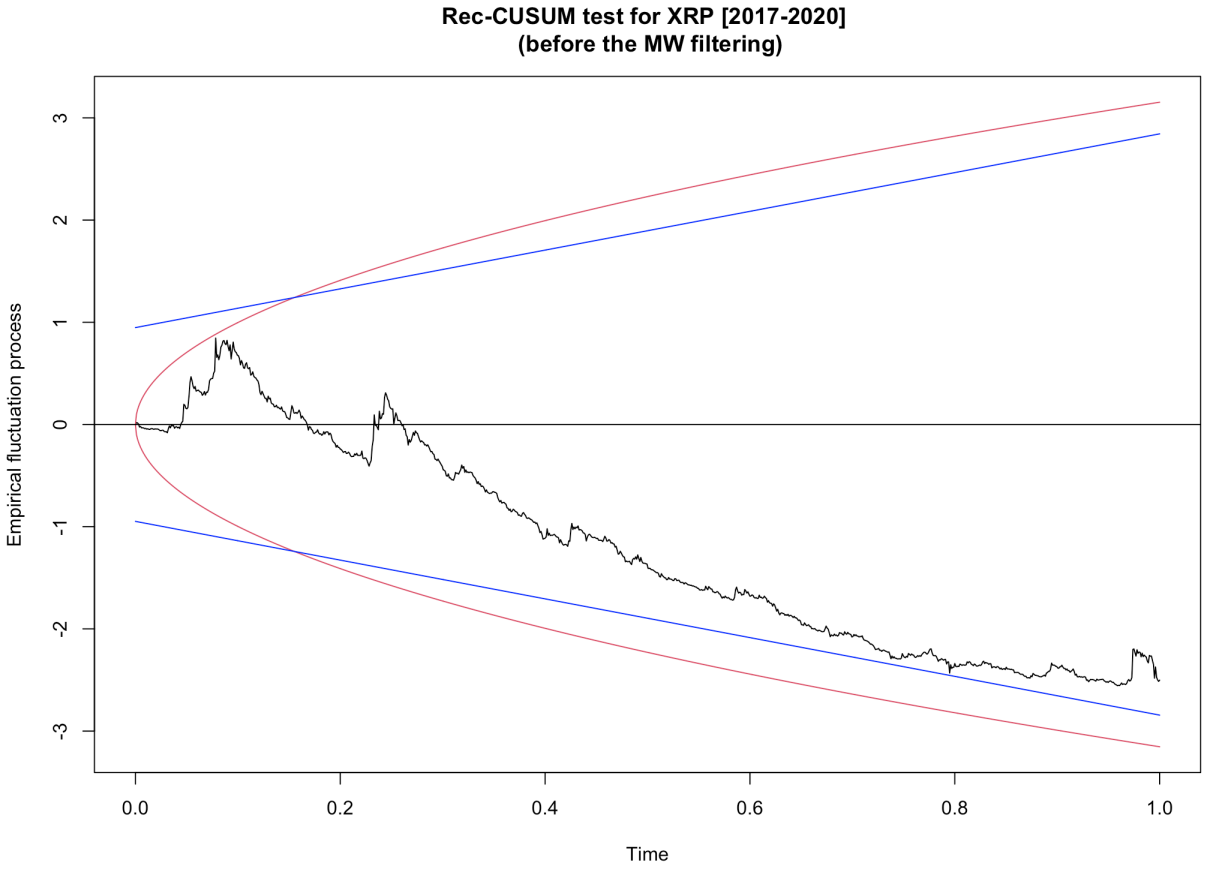

Figure 37: The Rec-CUSUM test of XRP [2018-2020] (before the Müller-Watson filtering)

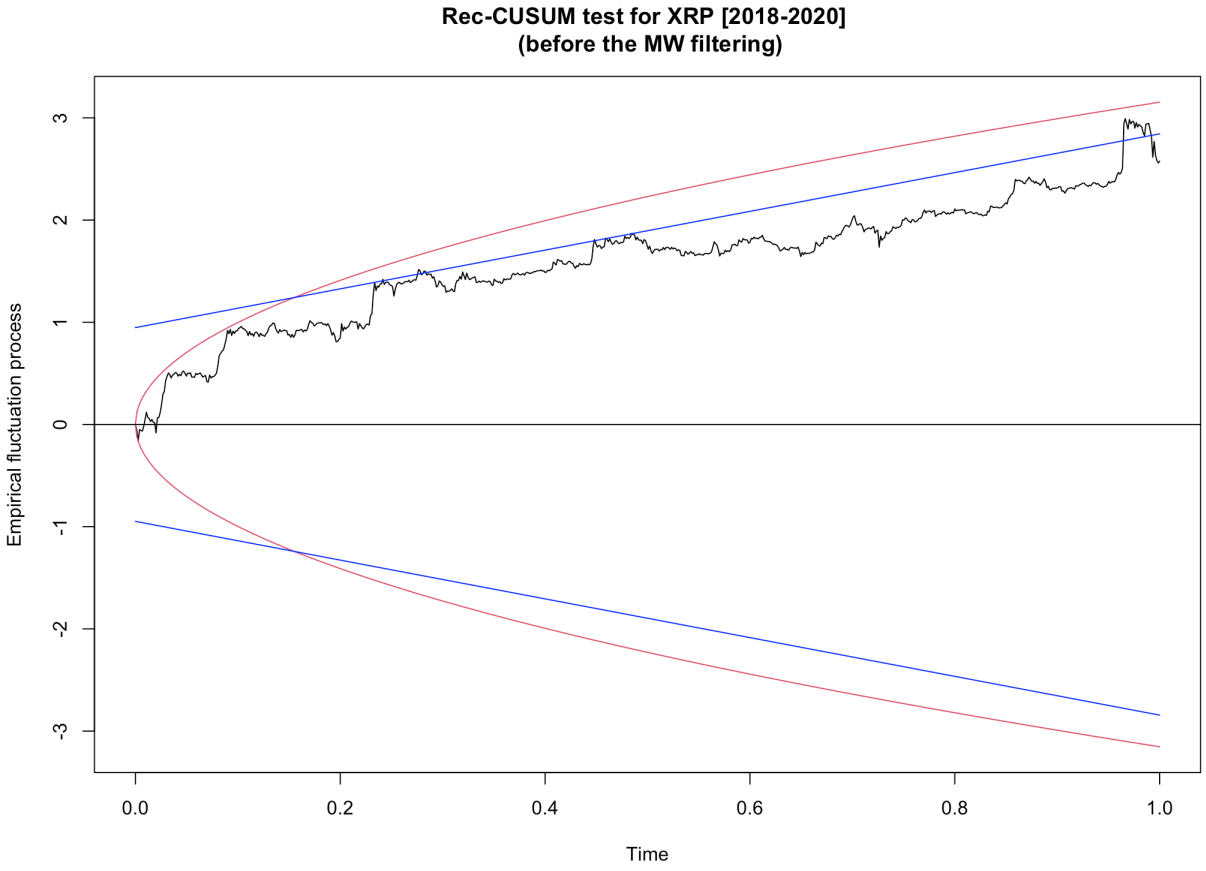

Figure 38: The Rec-CUSUM test of XRP [2019-2020] (before the Müller-Watson filtering)

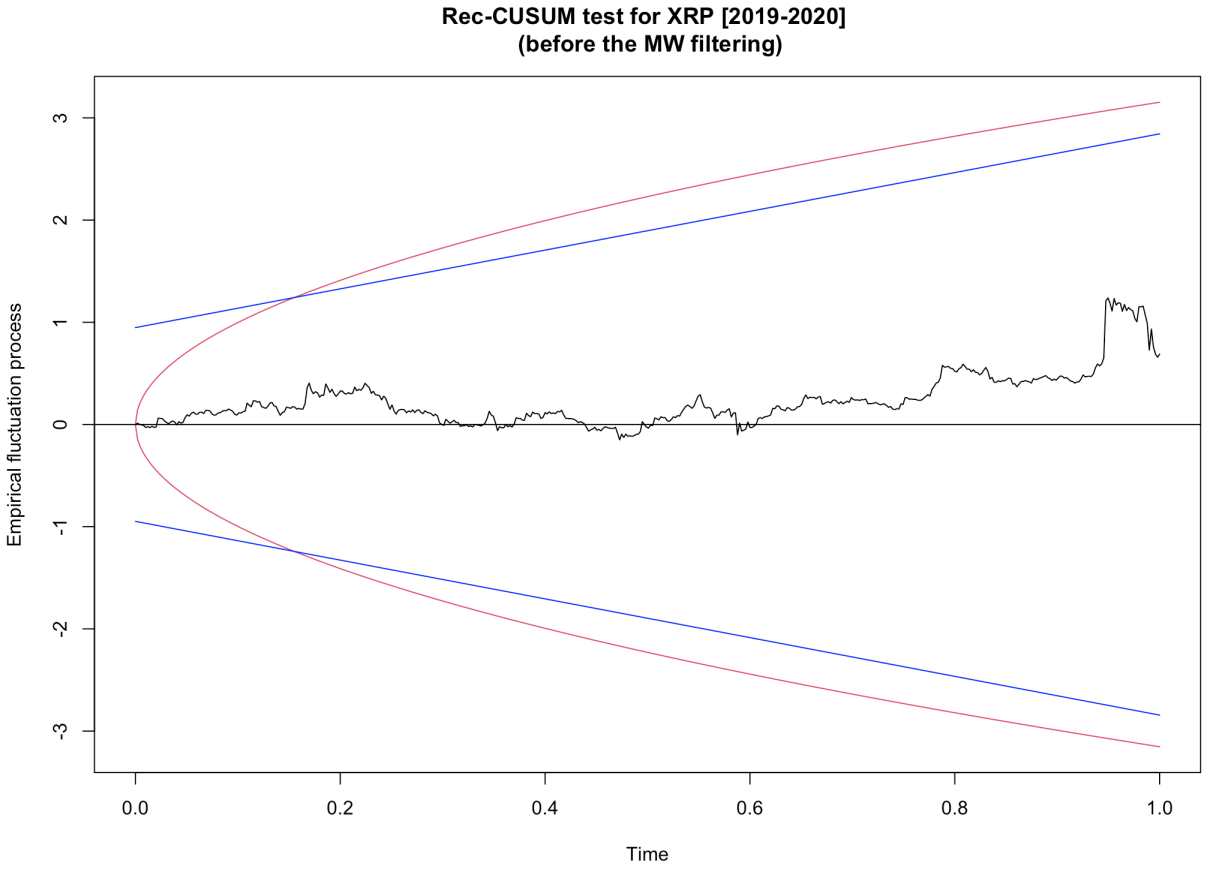

Figure 39: The Rec-CUSUM test of JPY [2016-2020] (before the Müller-Watson filtering)

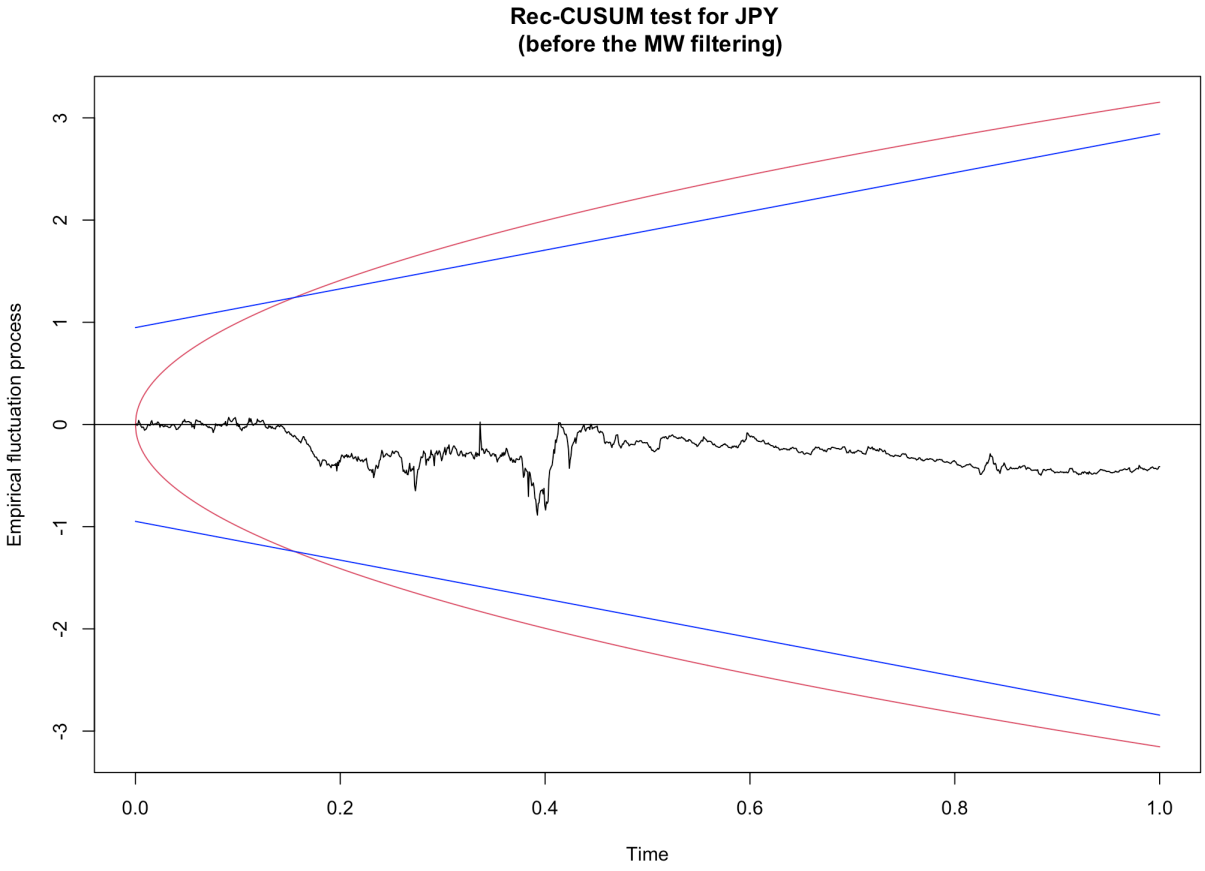

Figure 40: The Rec-CUSUM test of JPY [2017-2020] (before the Müller-Watson filtering)

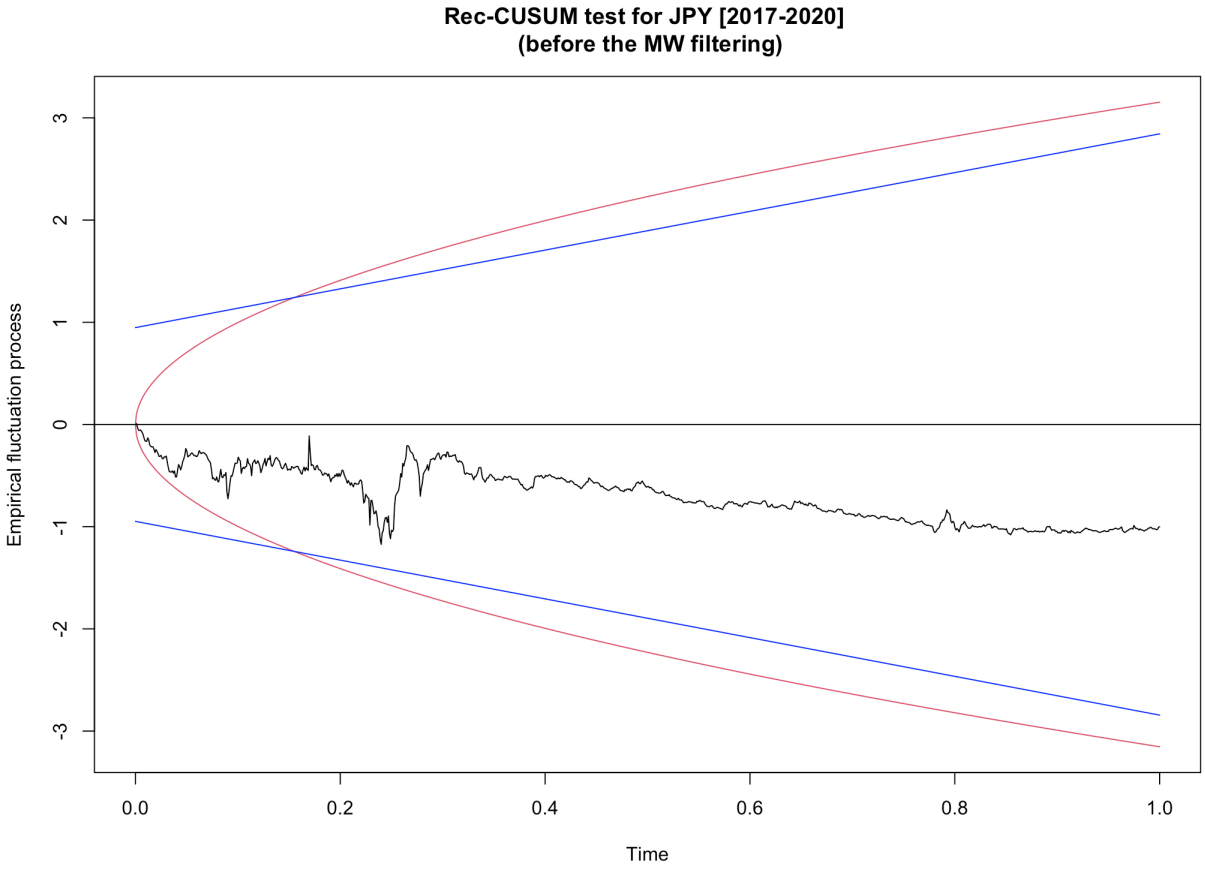

Figure 41: The Rec-CUSUM test of JPY [2018-2020] (before the Müller-Watson filtering)

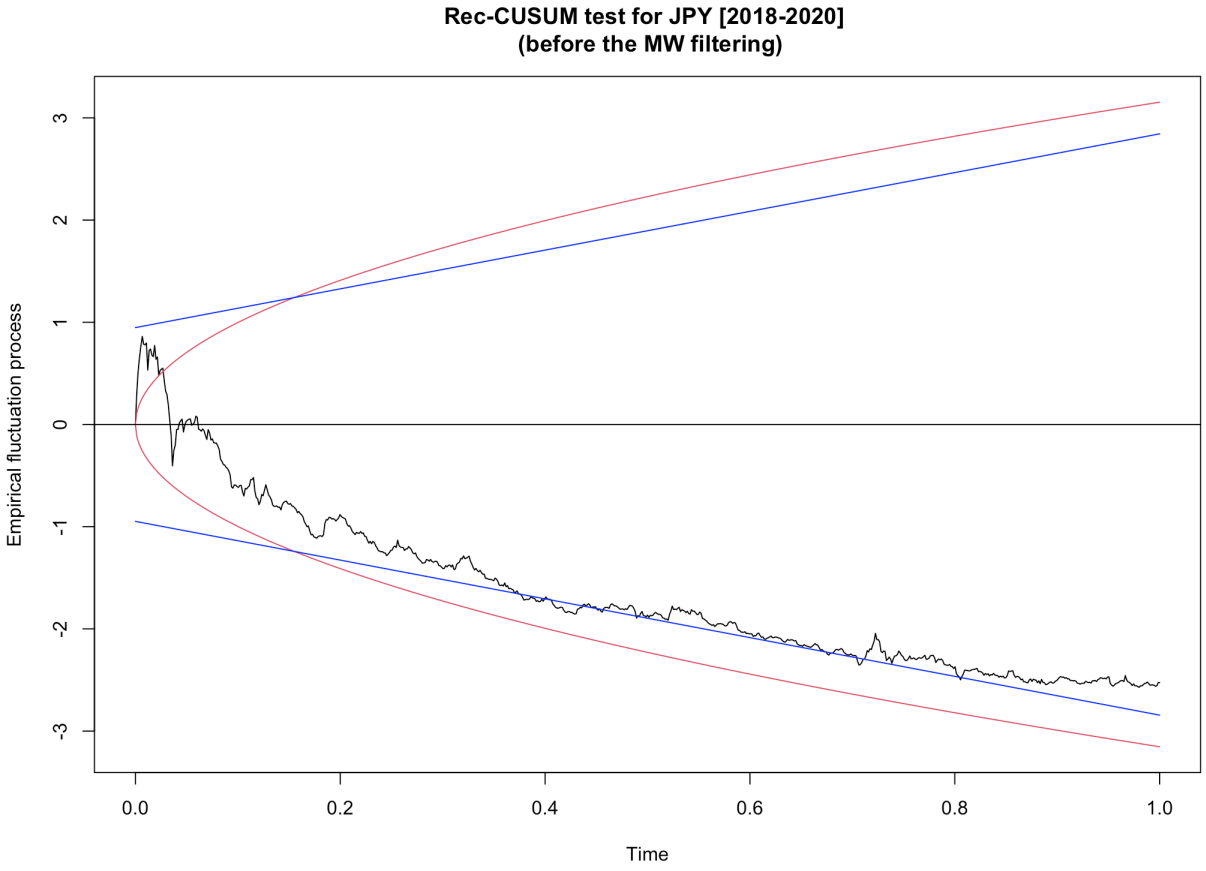

Figure 42: The Rec-CUSUM test of JPY [2019-2020] (before the Müller-Watson filtering)

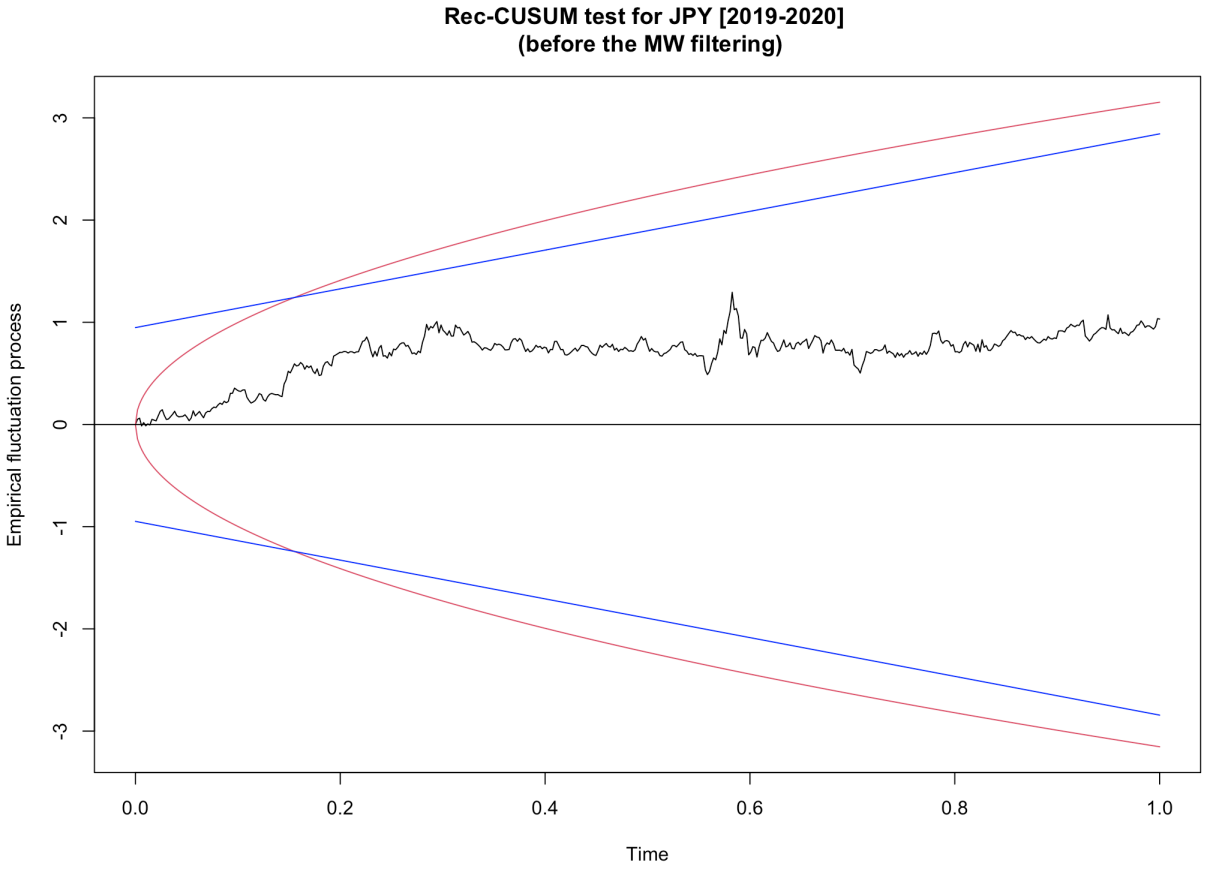

Figure 43: The Rec-CUSUM test of EUR [2016-2020] (before the Müller-Watson filtering)

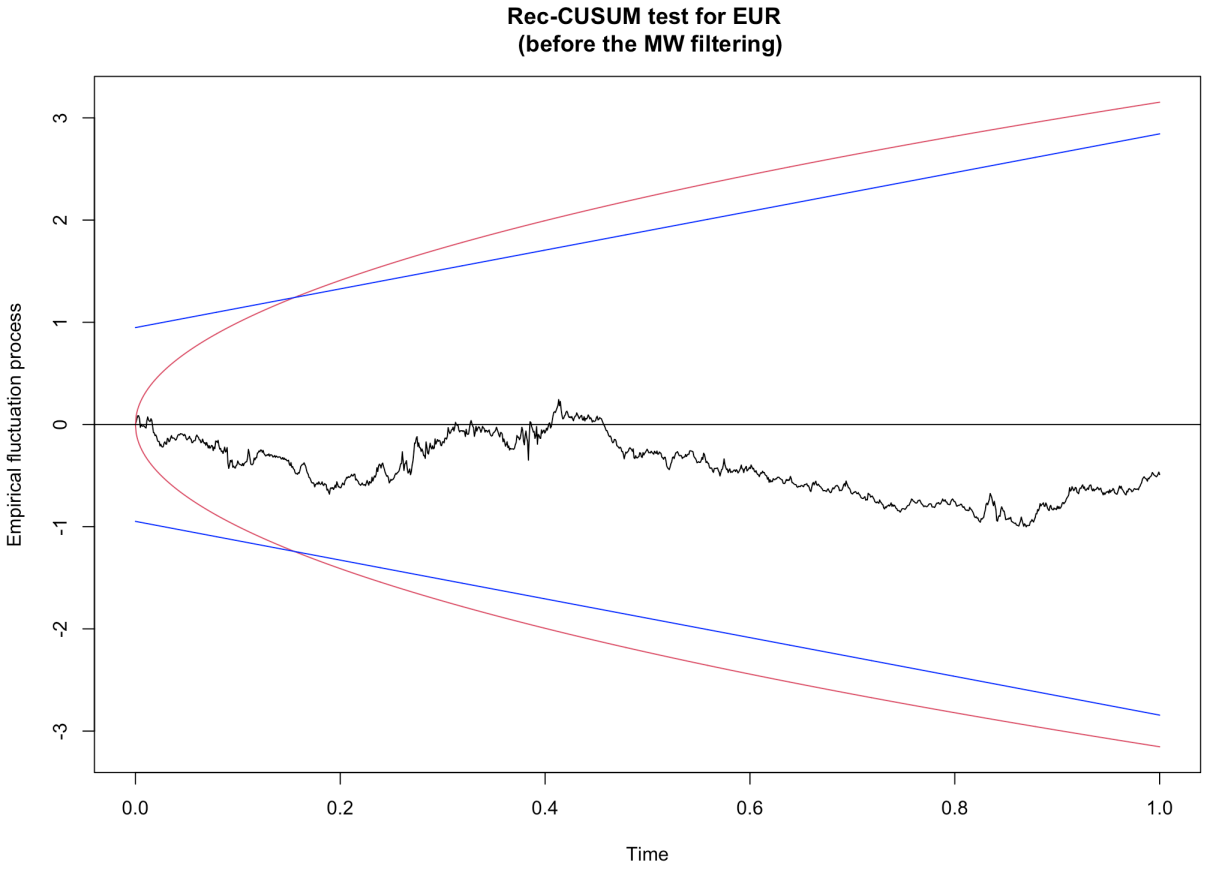

Figure 44: The Rec-CUSUM test of EUR [2017-2020] (before the Müller-Watson filtering)

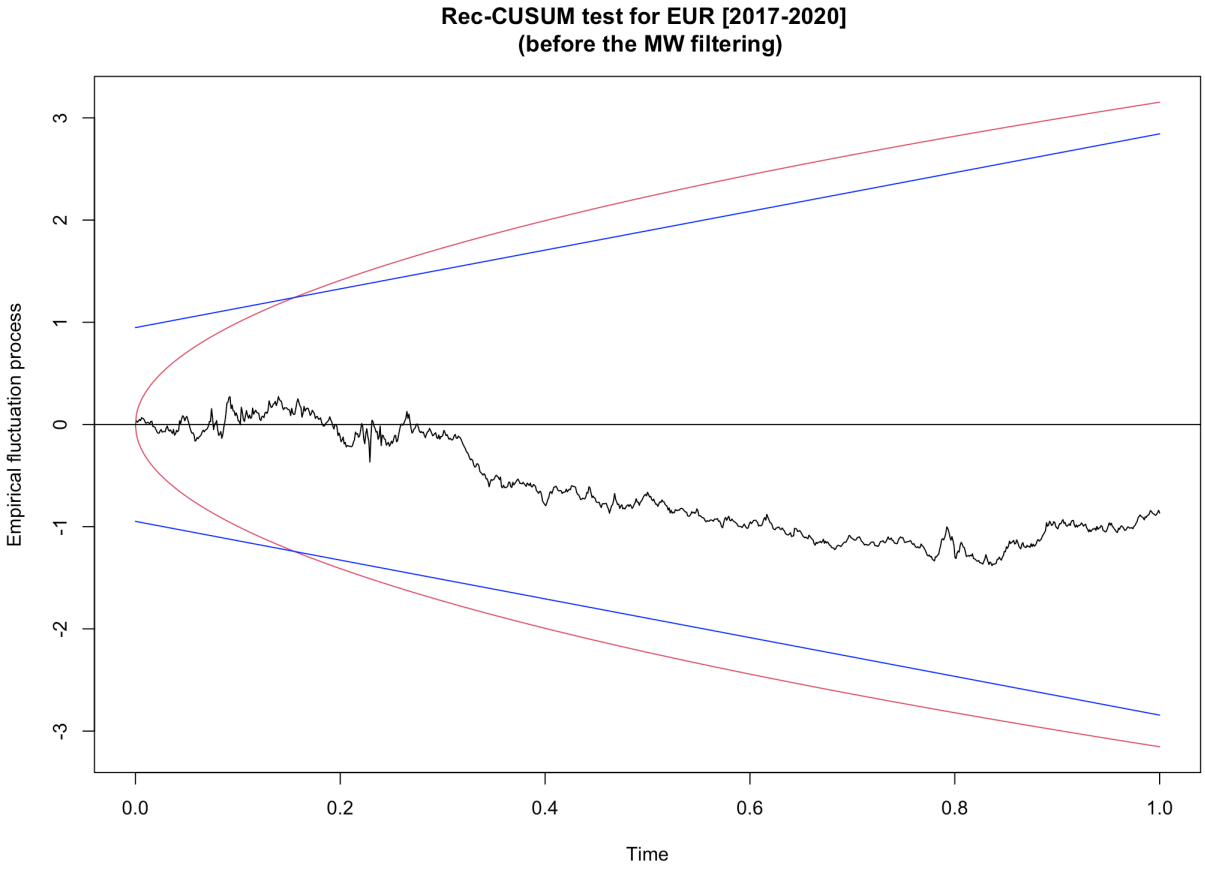

Figure 45: The Rec-CUSUM test of EUR [2018-2020] (before the Müller-Watson filtering)

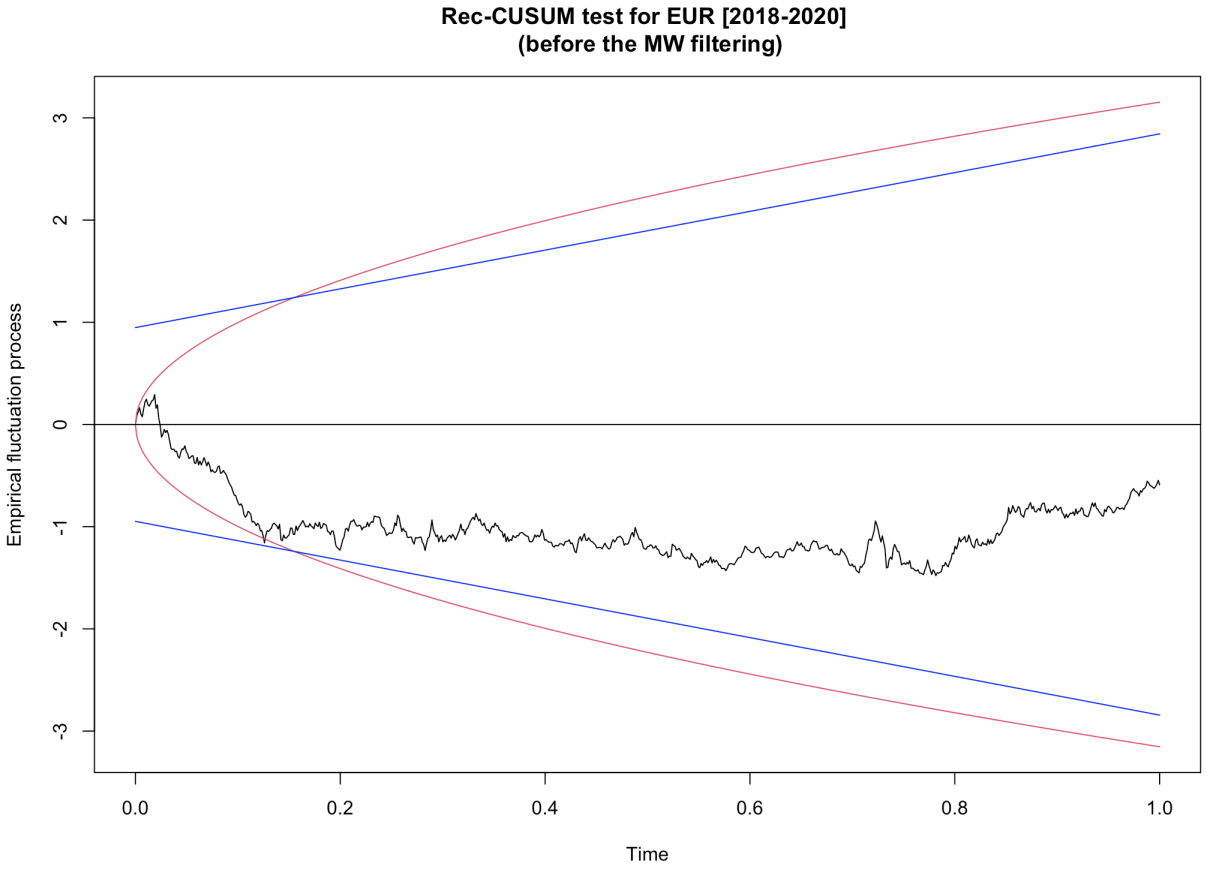

Figure 46: The Rec-CUSUM test of EUR [2019-2020] (before the Müller-Watson filtering)

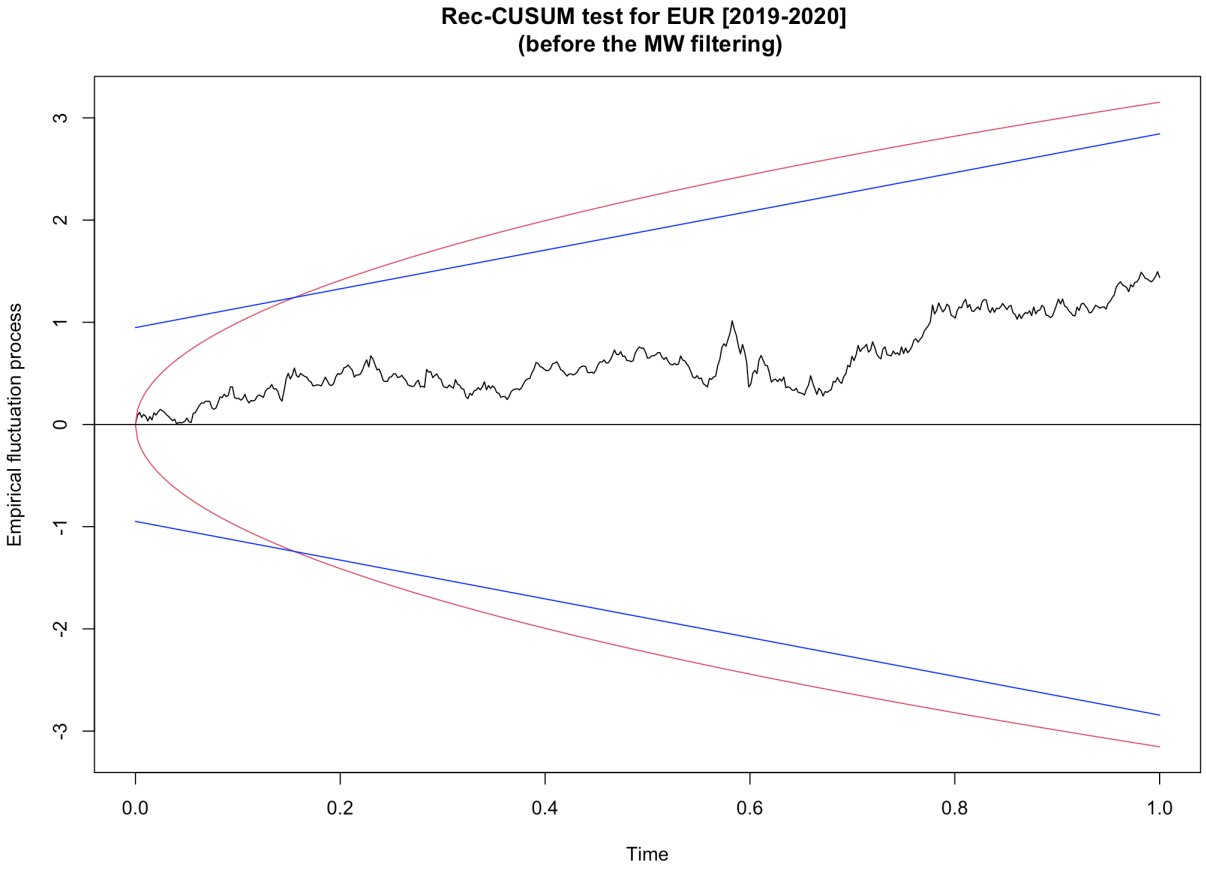

Figure 47: The Rec-CUSUM test of GOLD [2016-2020] (before the Müller-Watson filtering)

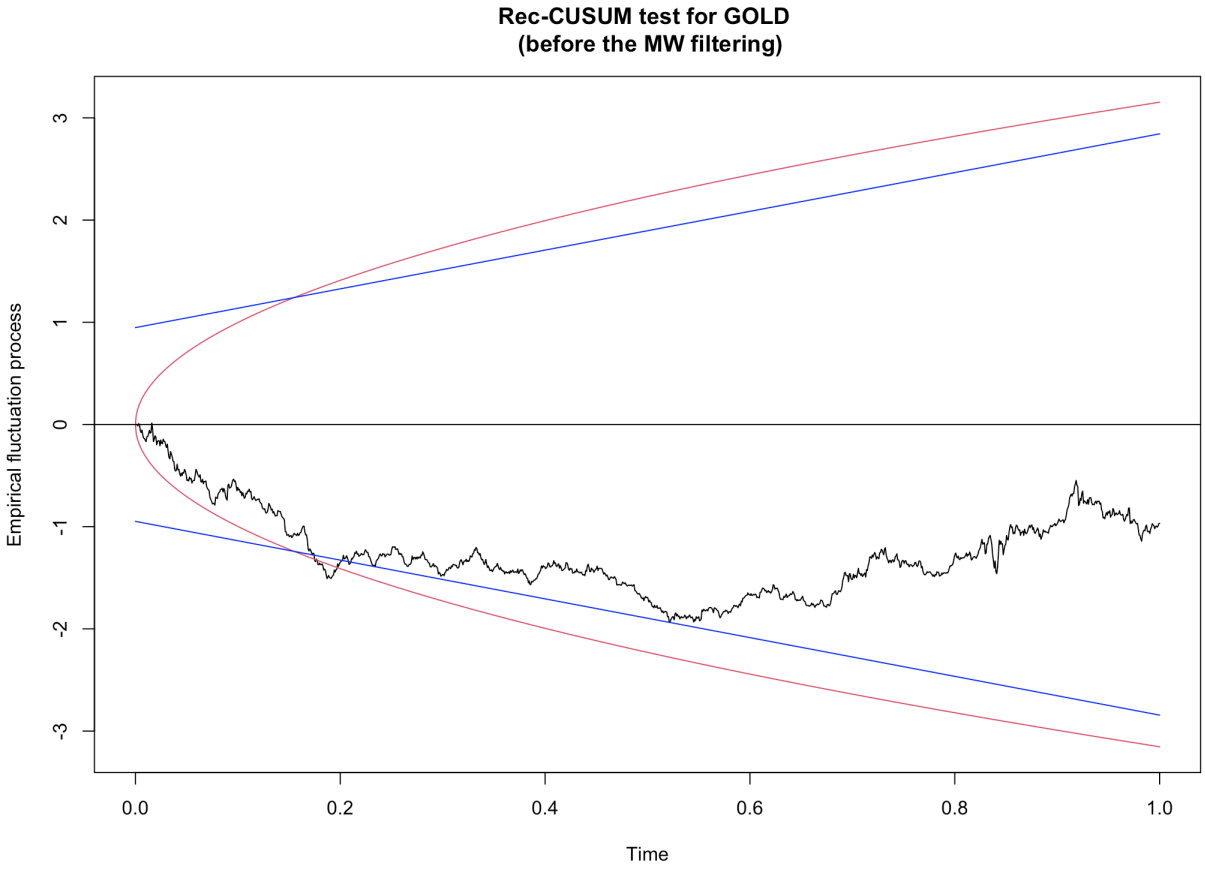

Figure 48: The Rec-CUSUM test of GOLD [2017-2020] (before the Müller-Watson filtering)

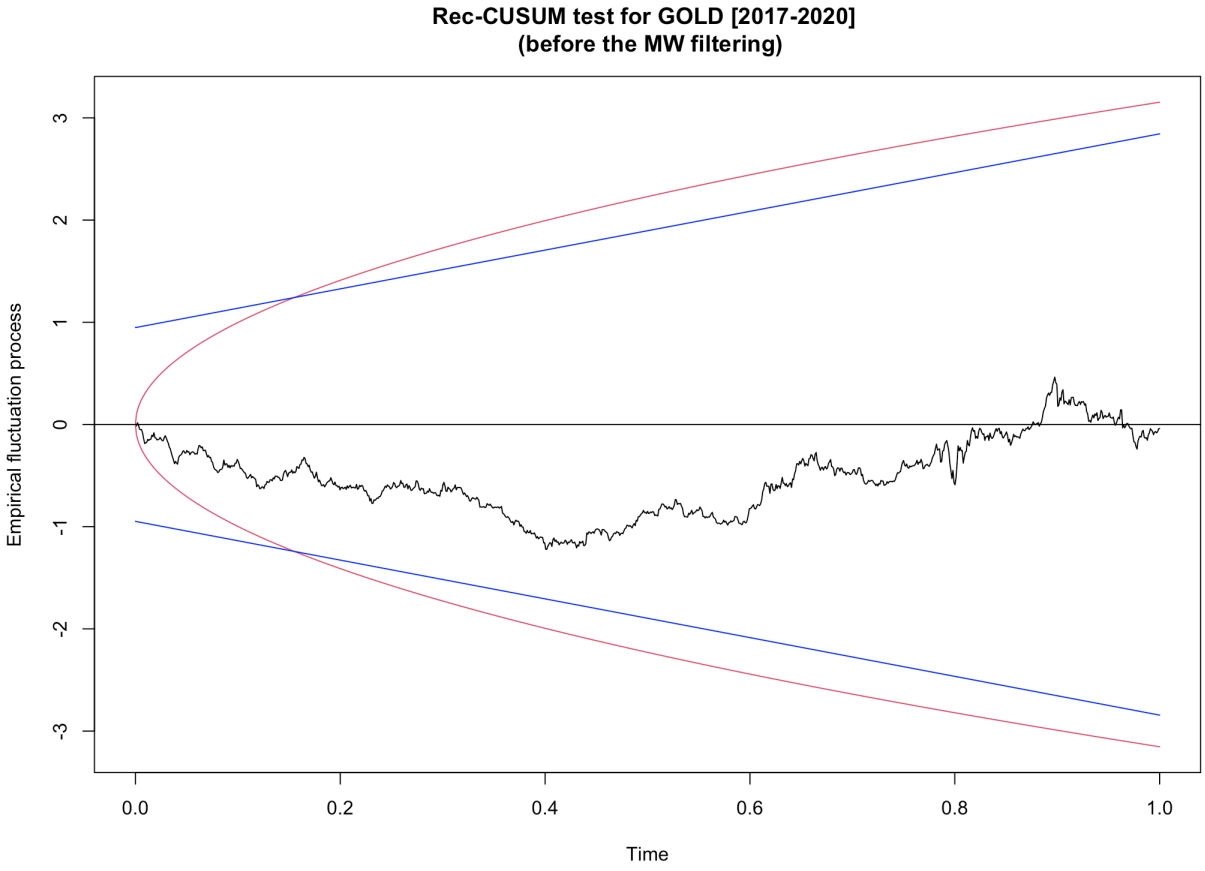

Figure 49: The Rec-CUSUM test of GOLD [2018-2020] (before the Müller-Watson filtering)

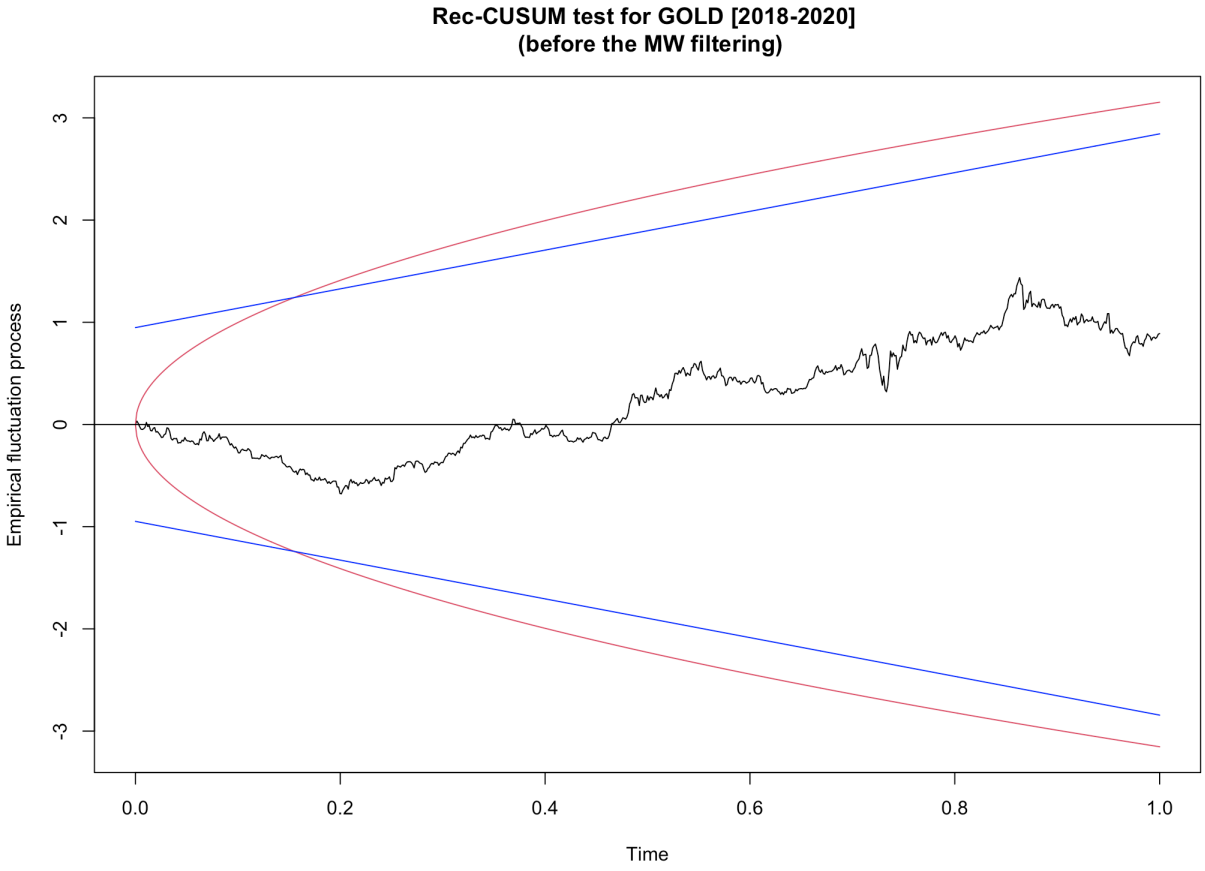

Figure 50: The Rec-CUSUM test of GOLD [2019-2020] (before the Müller-Watson filtering)

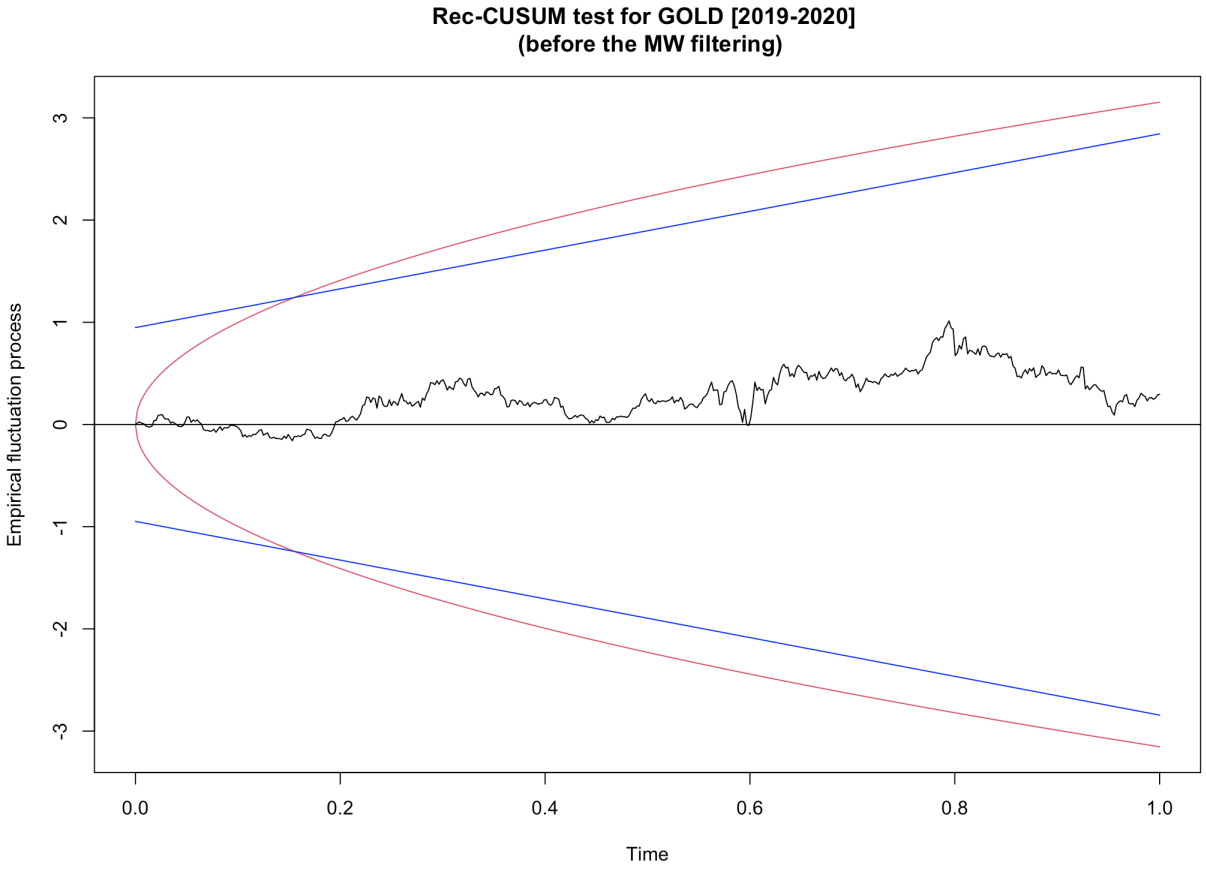

Figure 51: The Rec-CUSUM test of S&P500 [2016-2020] (before the Müller-Watson filtering)

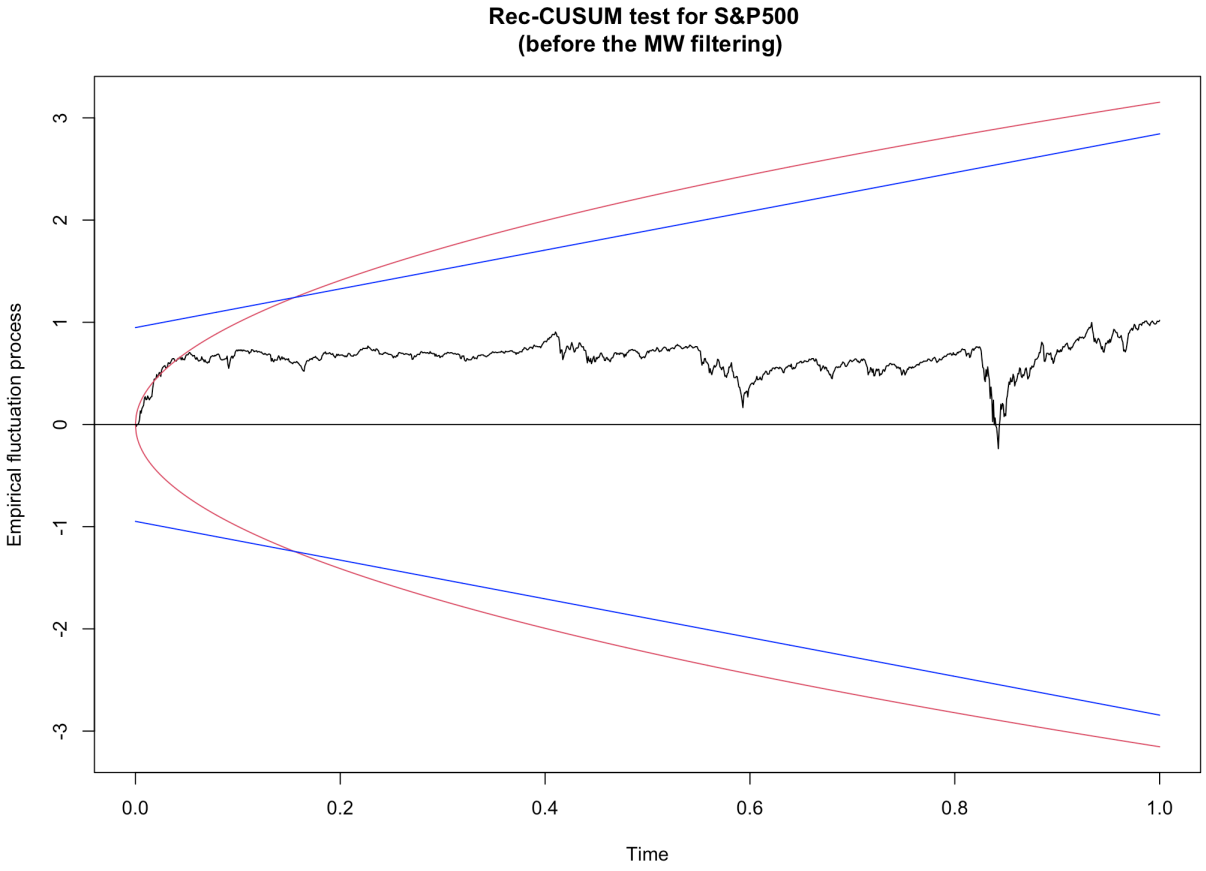

Figure 52: The Rec-CUSUM test of S&P500 [2017-2020] (before the Müller-Watson filtering)

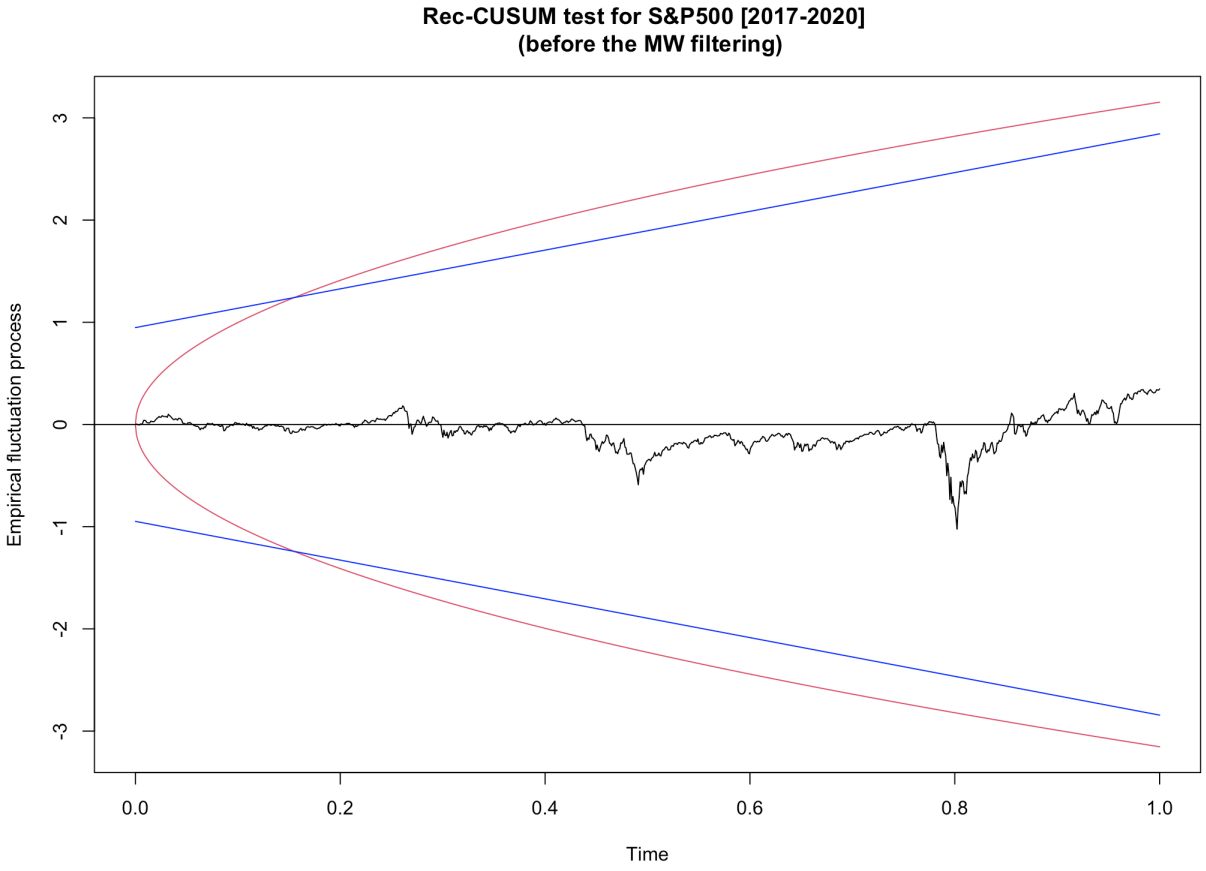

Figure 53: The Rec-CUSUM test of S&P500 [2018-2020] (before the Müller-Watson filtering)

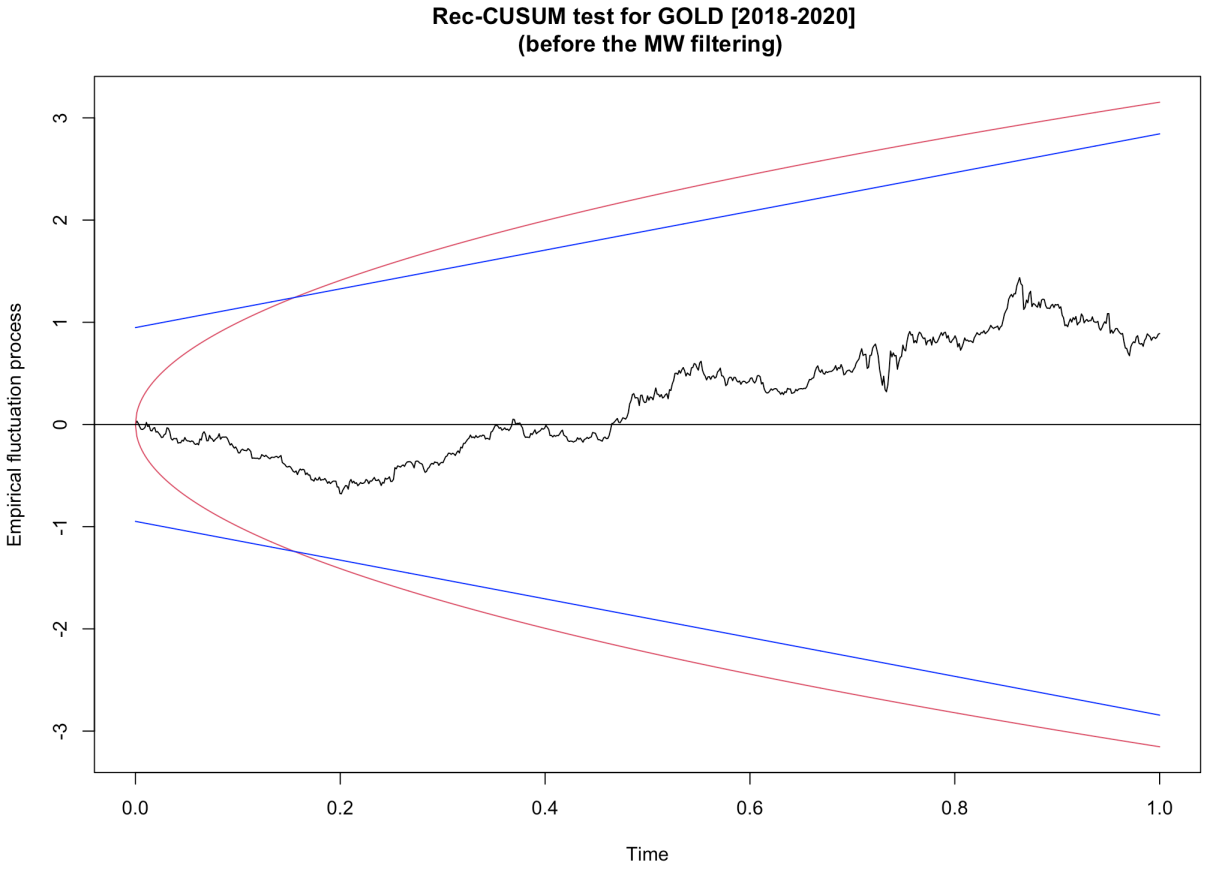

Figure 54: The Rec-CUSUM test of S&P500 [2019-2020] (before the Müller-Watson filtering)

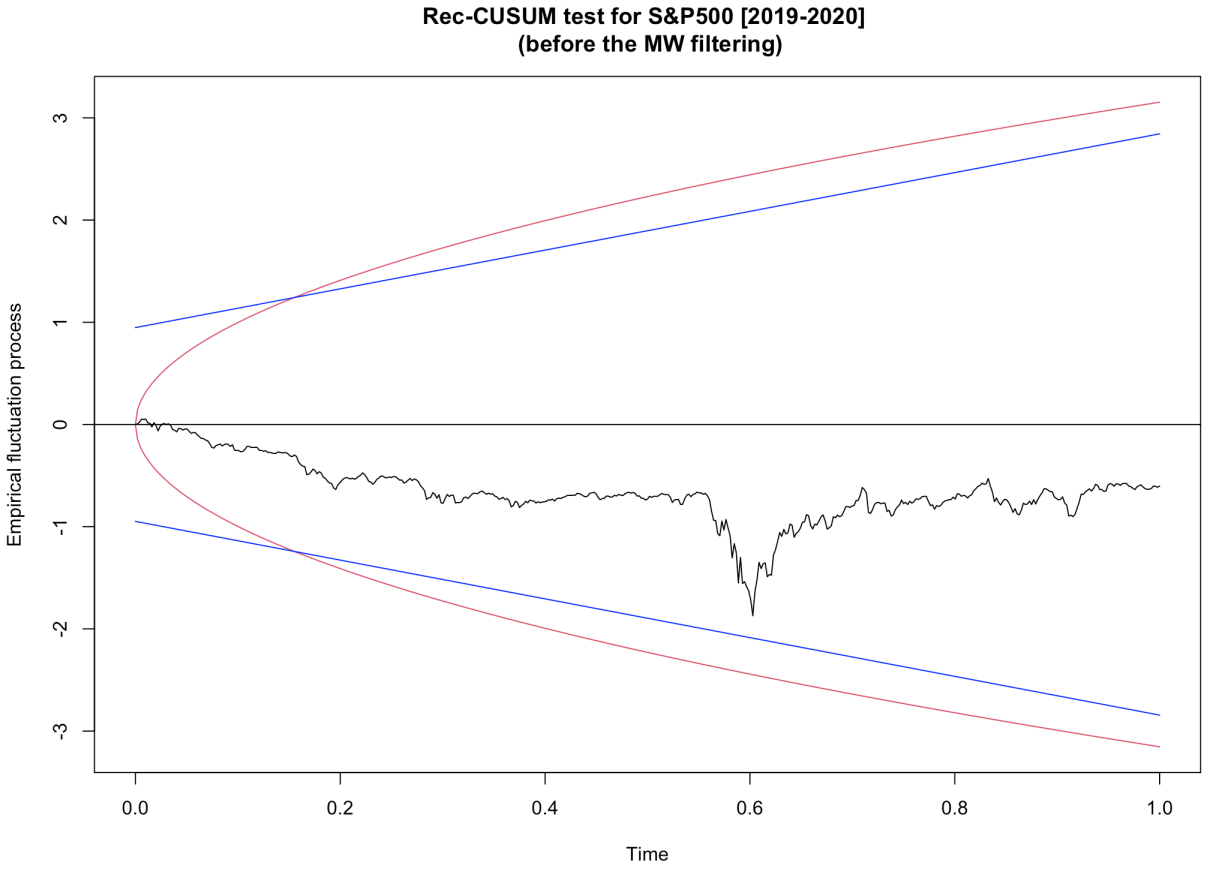

Figure 55: The Rec-CUSUM test of MSCI [2016-2020] (before the Müller-Watson filtering)

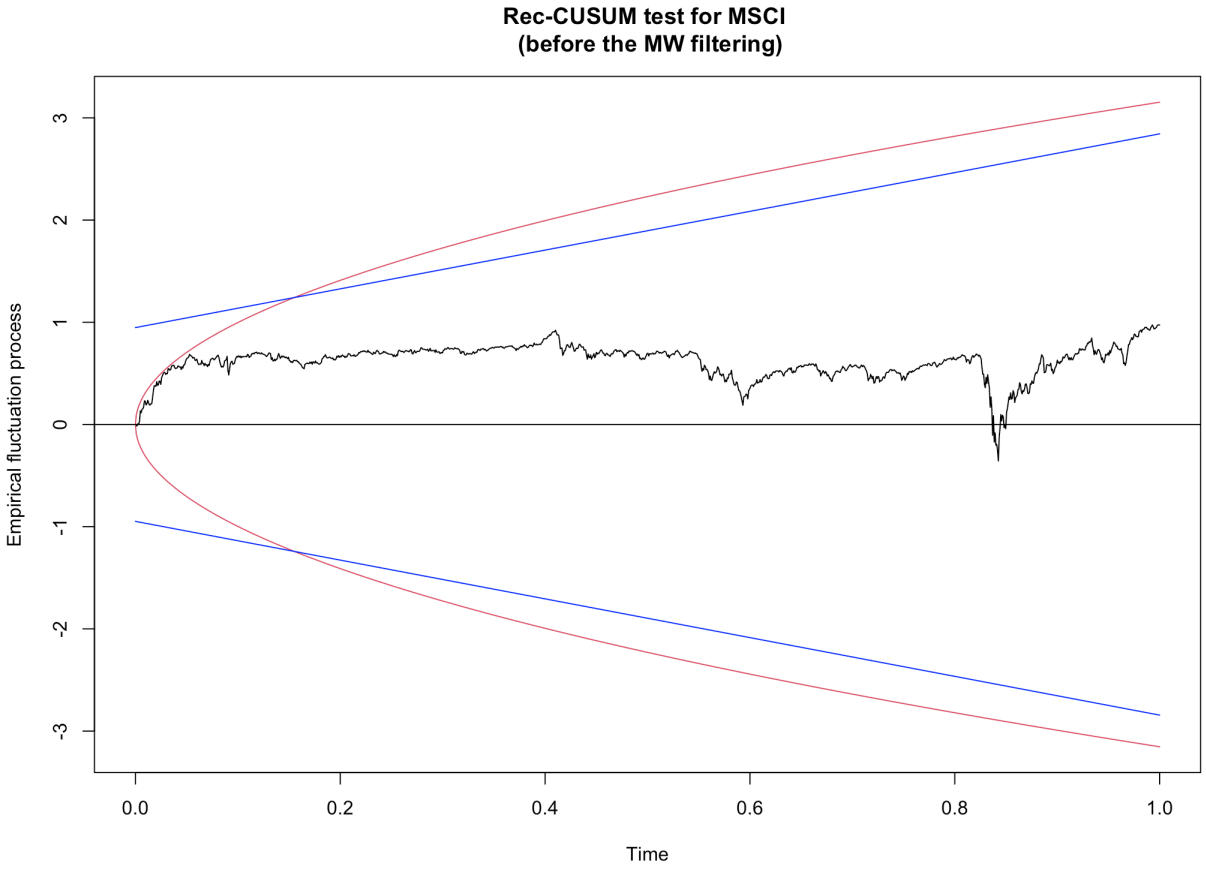

Figure 56: The Rec-CUSUM test of MSCI [2017-2020] (before the Müller-Watson filtering)

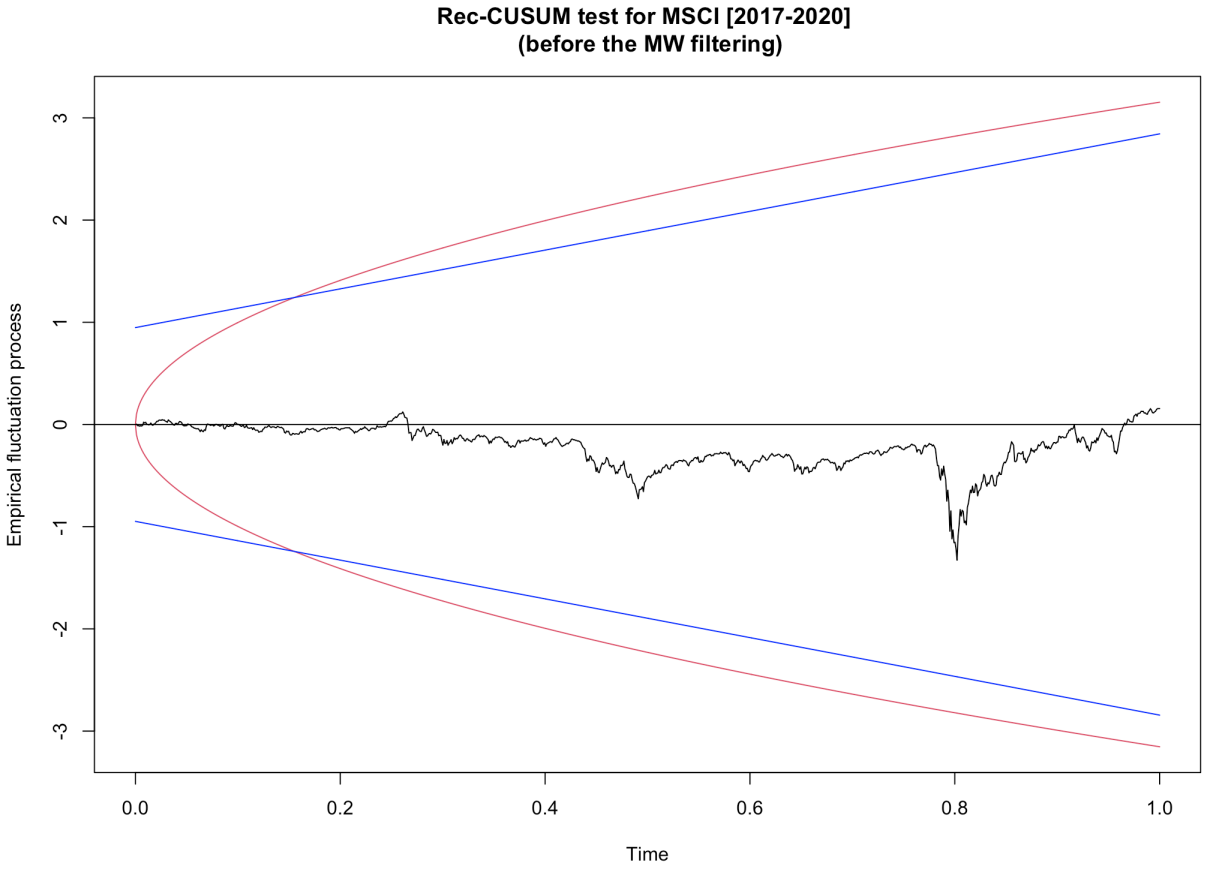

Figure 57: The Rec-CUSUM test of MSCI [2018-2020] (before the Müller-Watson filtering)

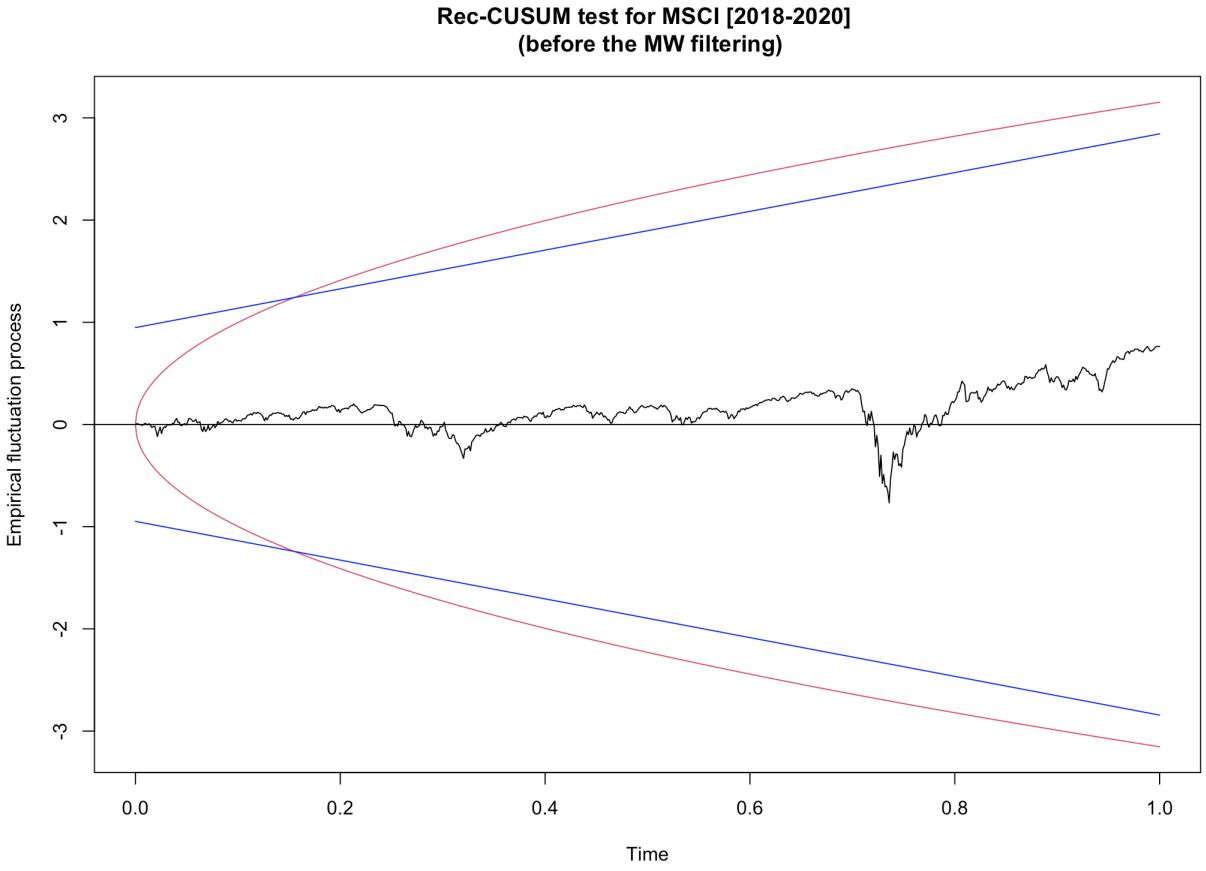

Figure 58: The Rec-CUSUM test of MSCI [2019-2020] (before the Müller-Watson filtering)

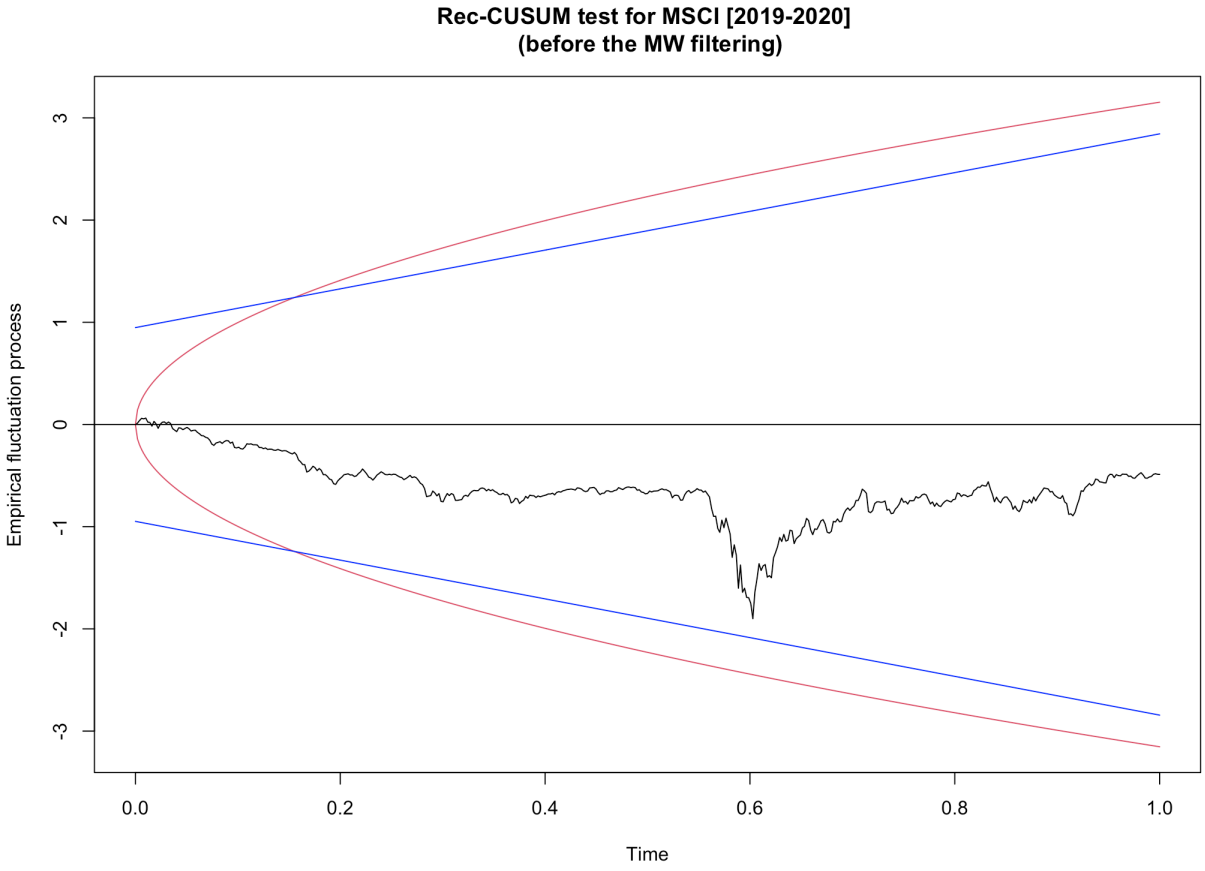

Figure 59: The Rec-CUSUM test of BTC [2016-2020] (after the Müller-Watson filtering)

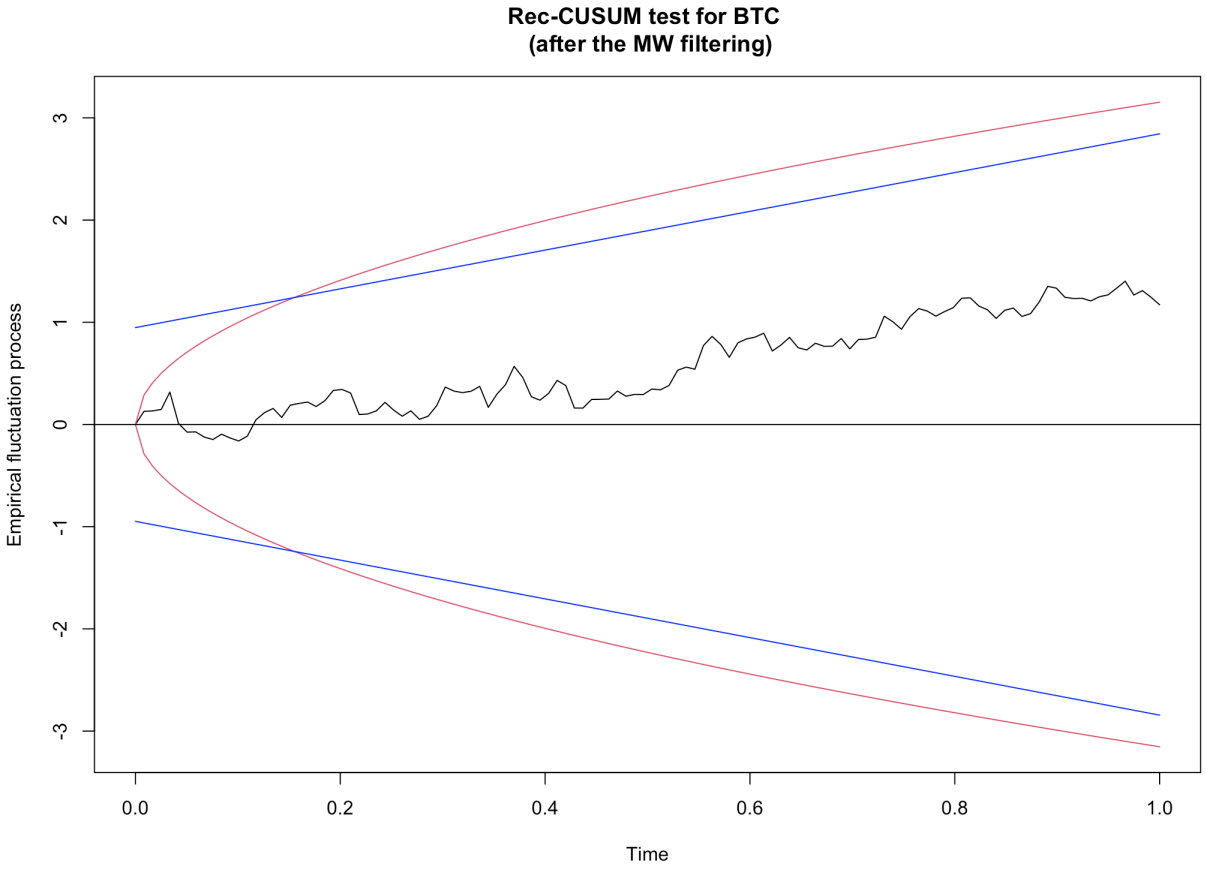

Figure 60: The Rec-CUSUM test of BTC [2017-2020] (after the Müller-Watson filtering)

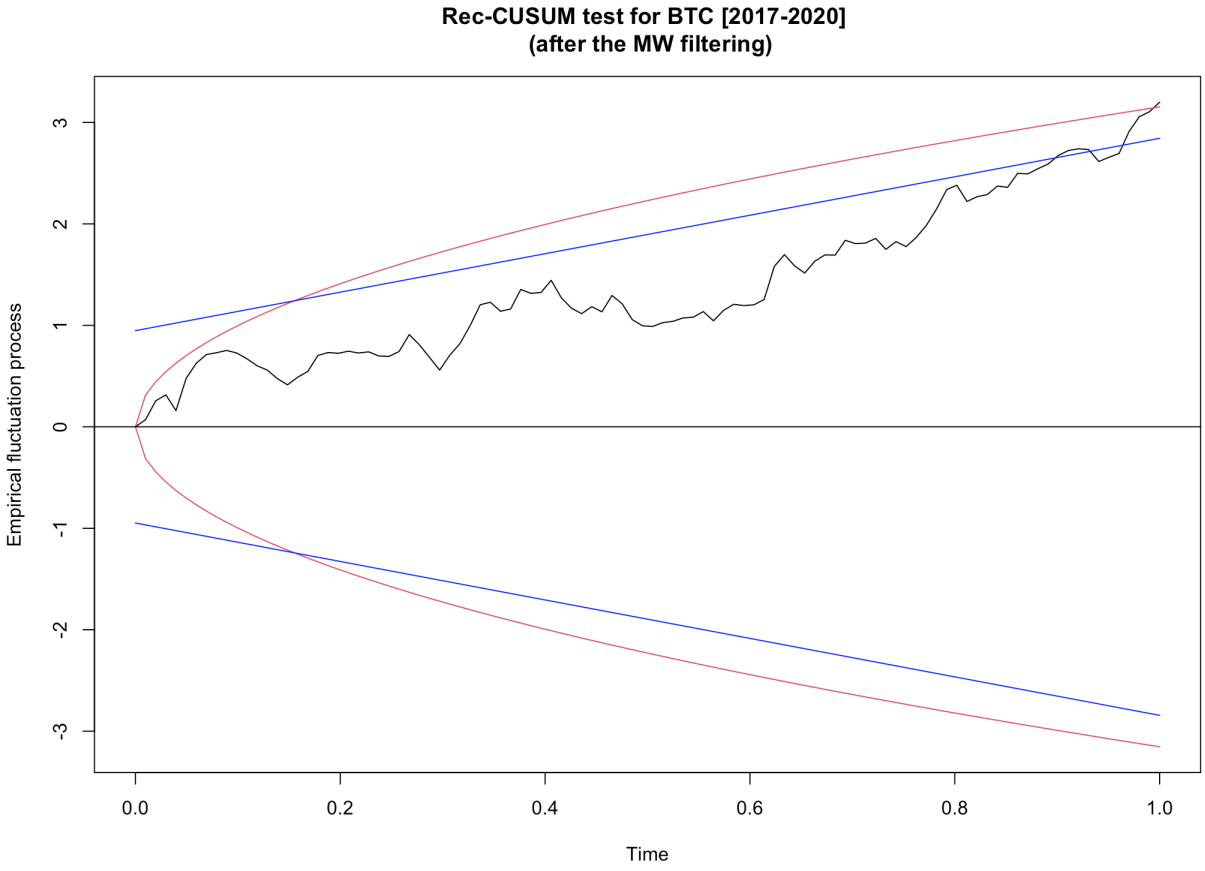

Figure 61: The Rec-CUSUM test of BTC [2018-2020] (after the Müller-Watson filtering)

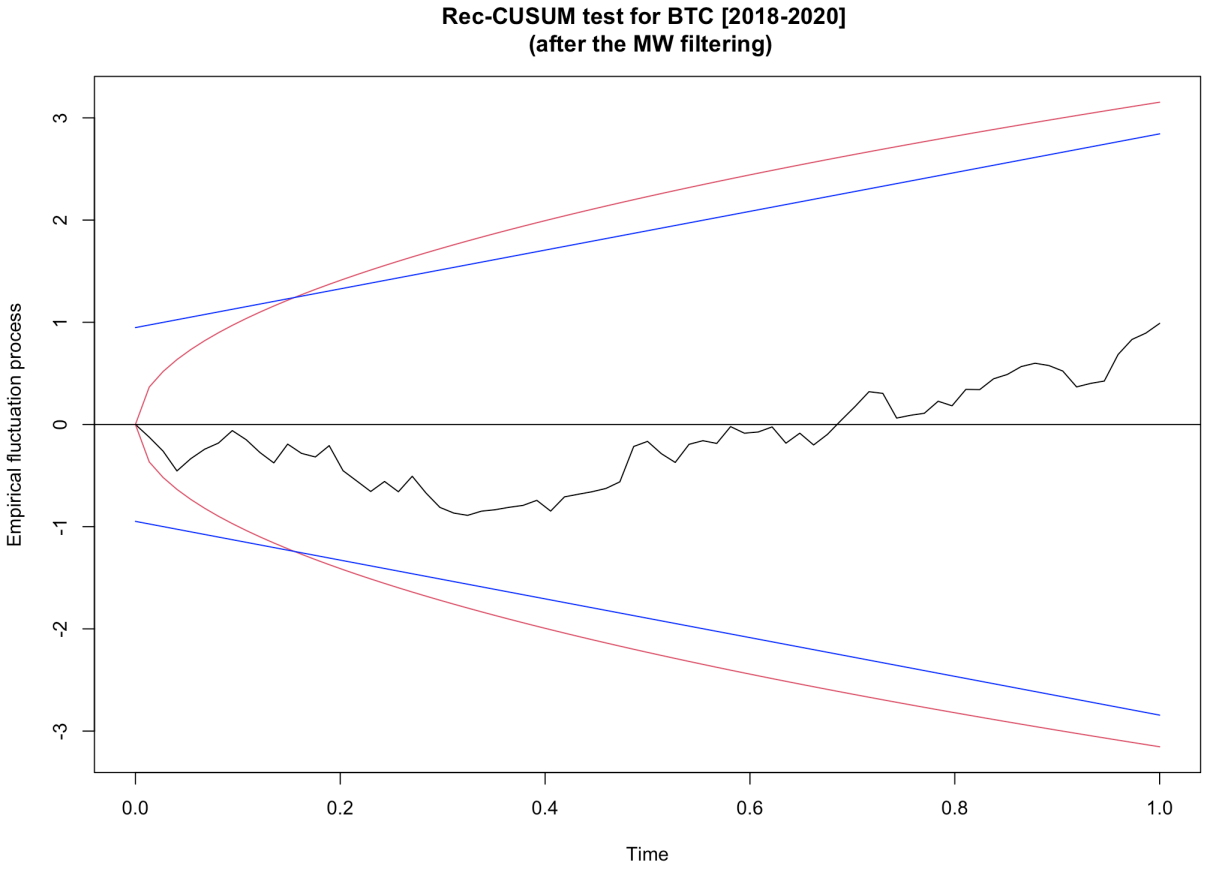

Figure 62: The Rec-CUSUM test of BTC [2019-2020] (after the Müller-Watson filtering)

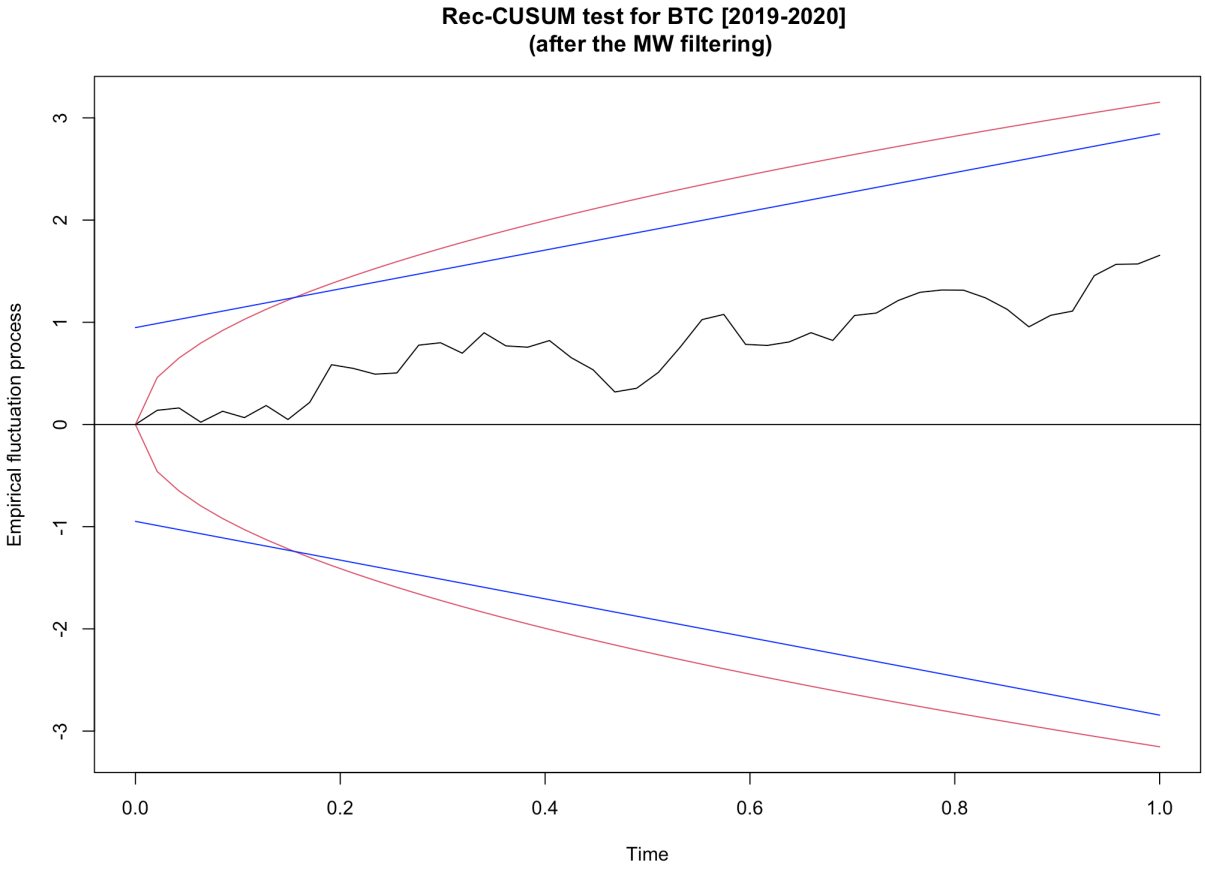

Figure 63: The Rec-CUSUM test of ETH [2016-2020] (after the Müller-Watson filtering)

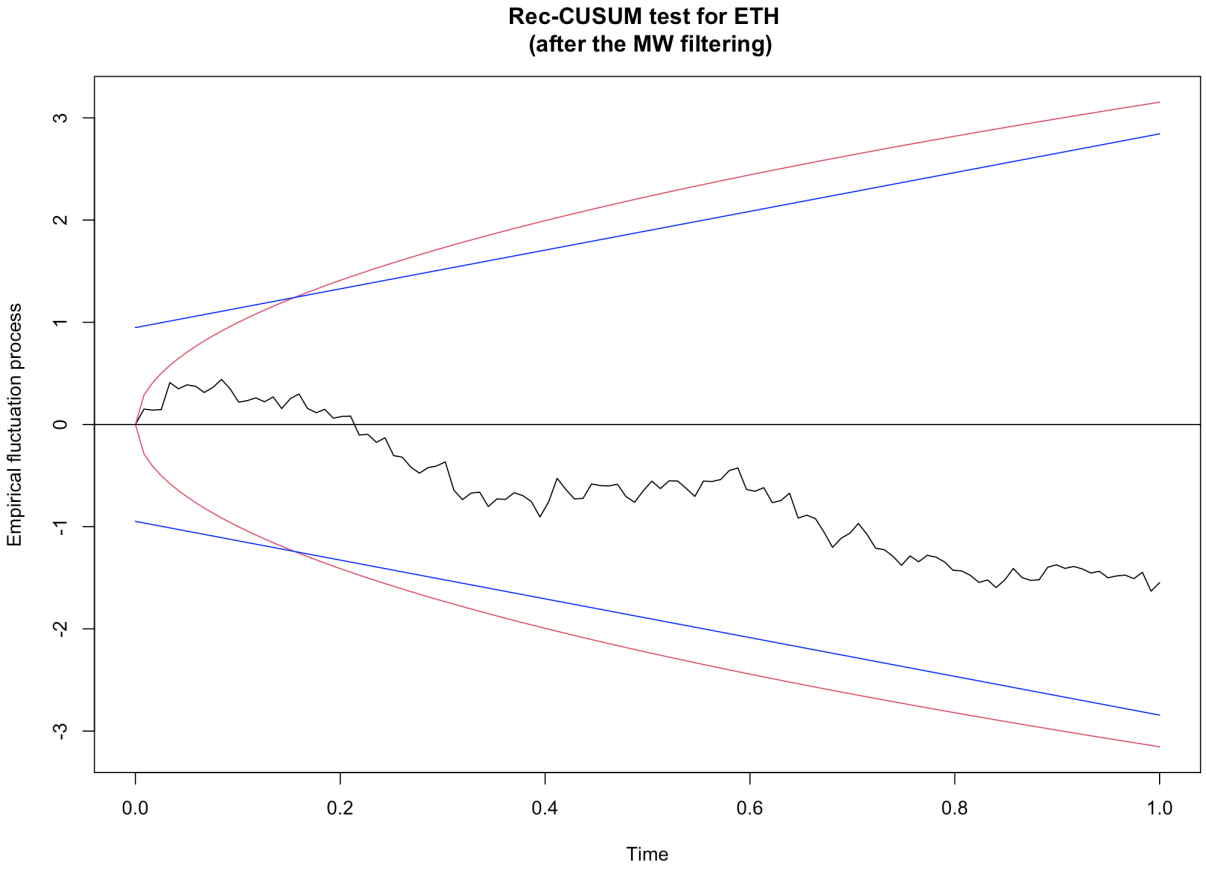

Figure 64: The Rec-CUSUM test of ETH [2017-2020] (after the Müller-Watson filtering)

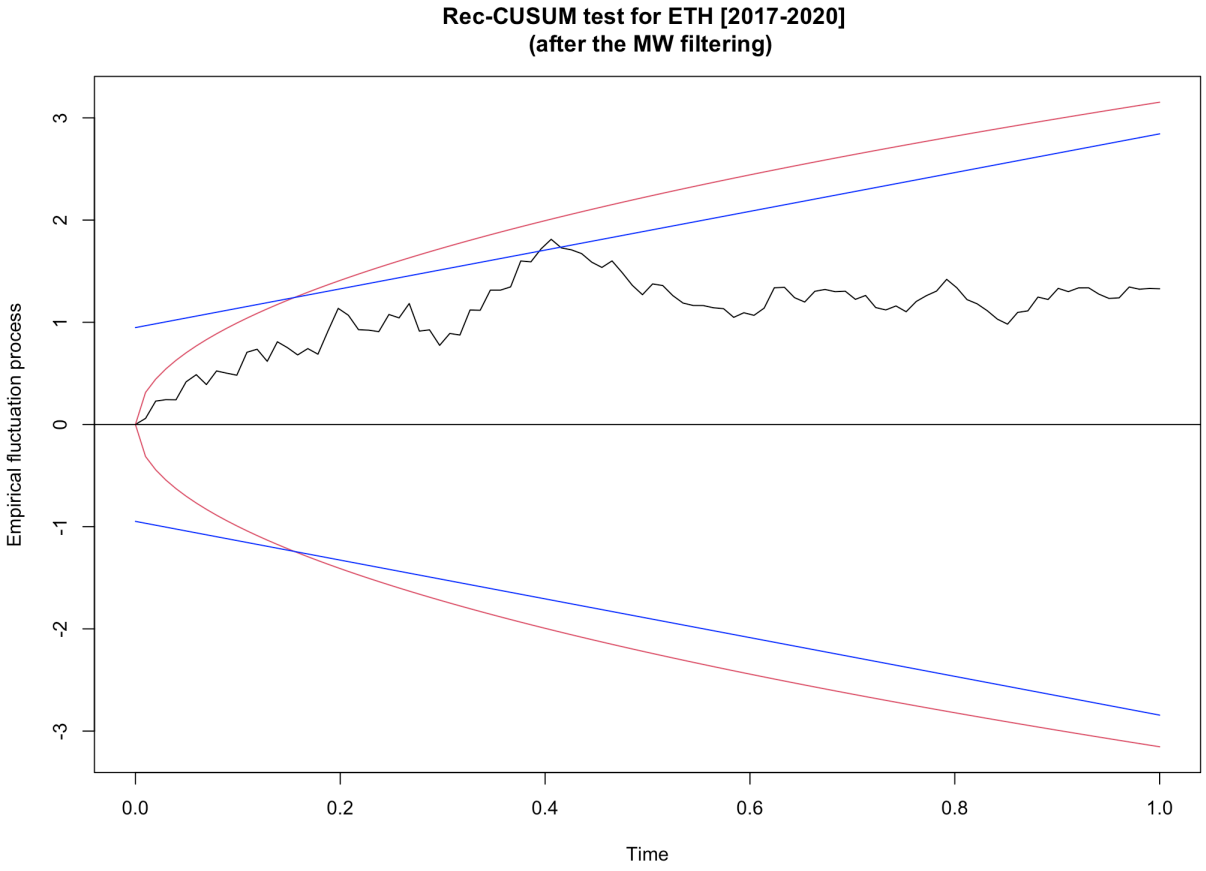

Figure 65: The Rec-CUSUM test of ETH [2018-2020] (after the Müller-Watson filtering)

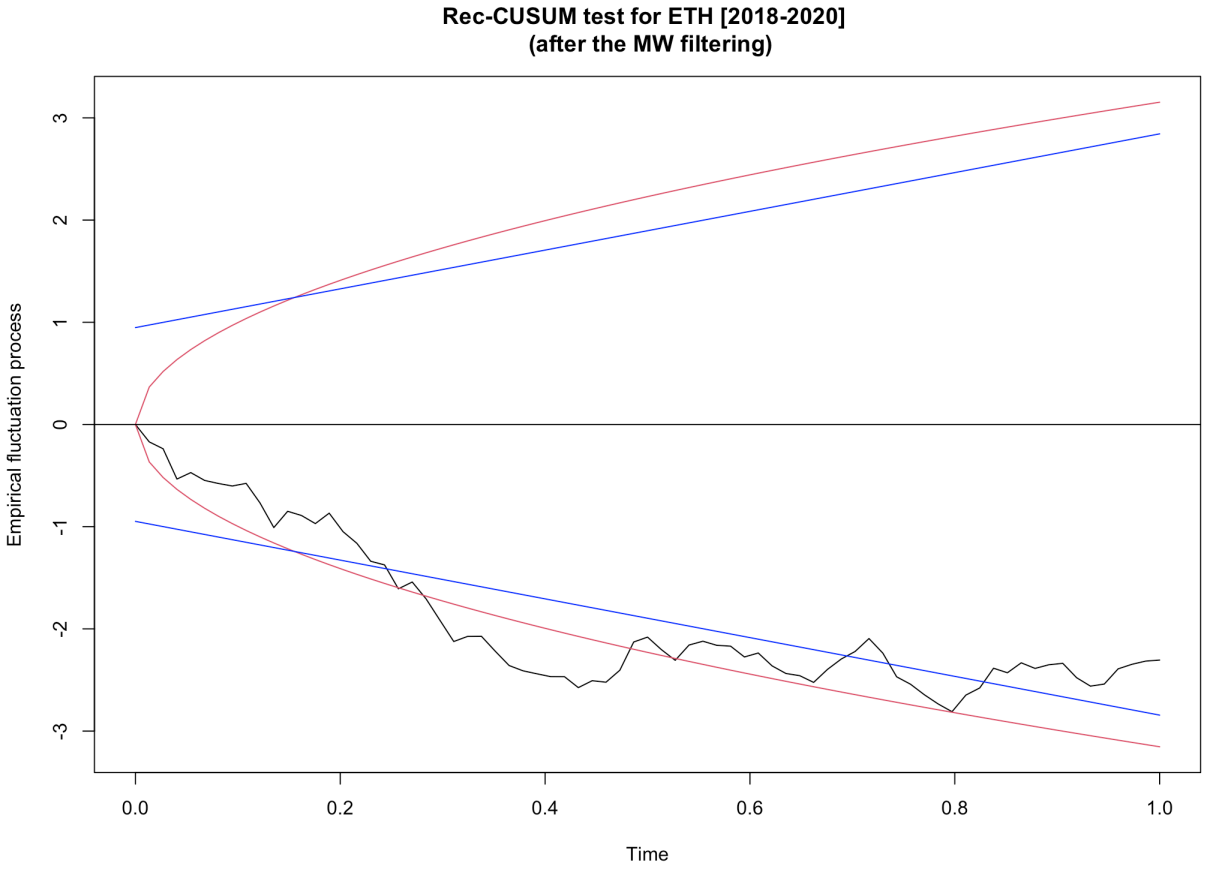

Figure 66: The Rec-CUSUM test of ETH [2019-2020] (after the Müller-Watson filtering)

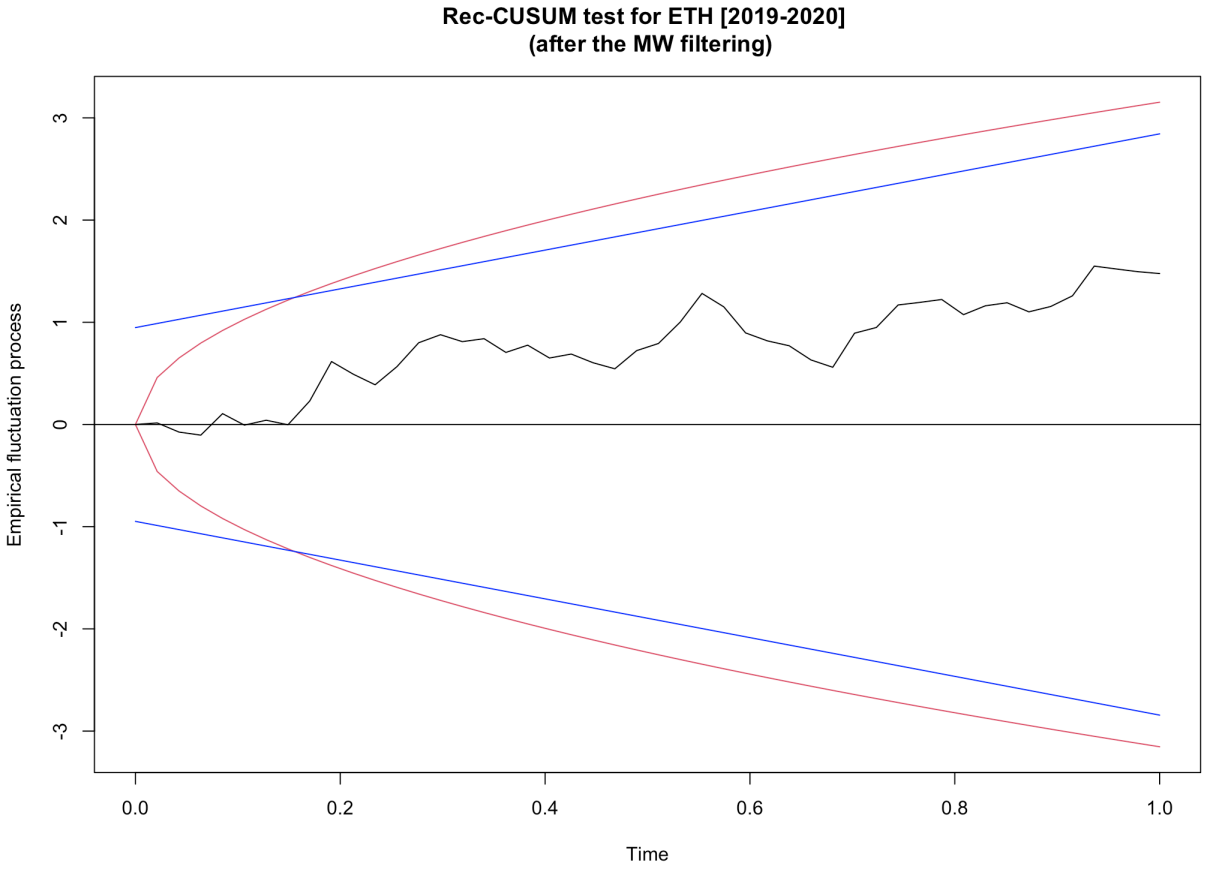

Figure 67: The Rec-CUSUM test of XRP [2016-2020] (after the Müller-Watson filtering)

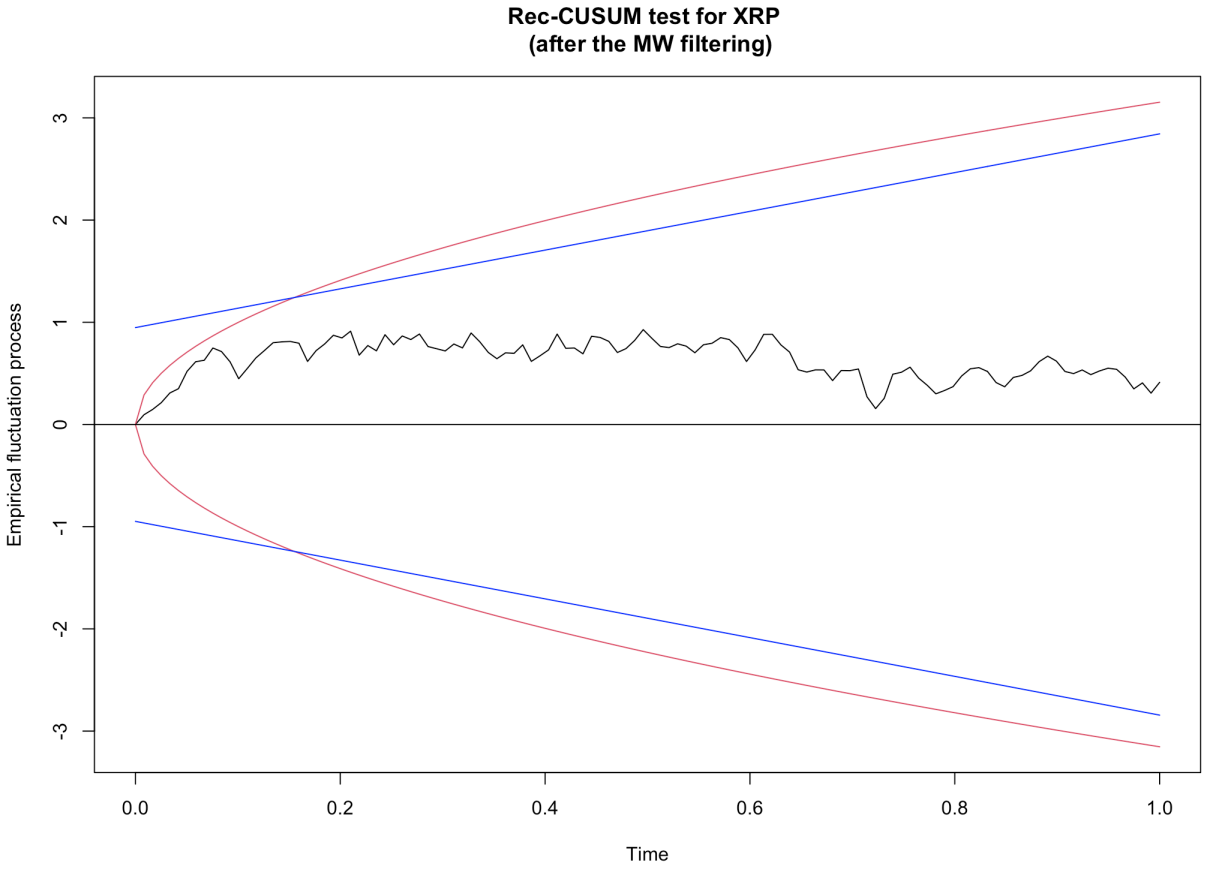

Figure 68: The Rec-CUSUM test of XRP [2017-2020] (after the Müller-Watson filtering)

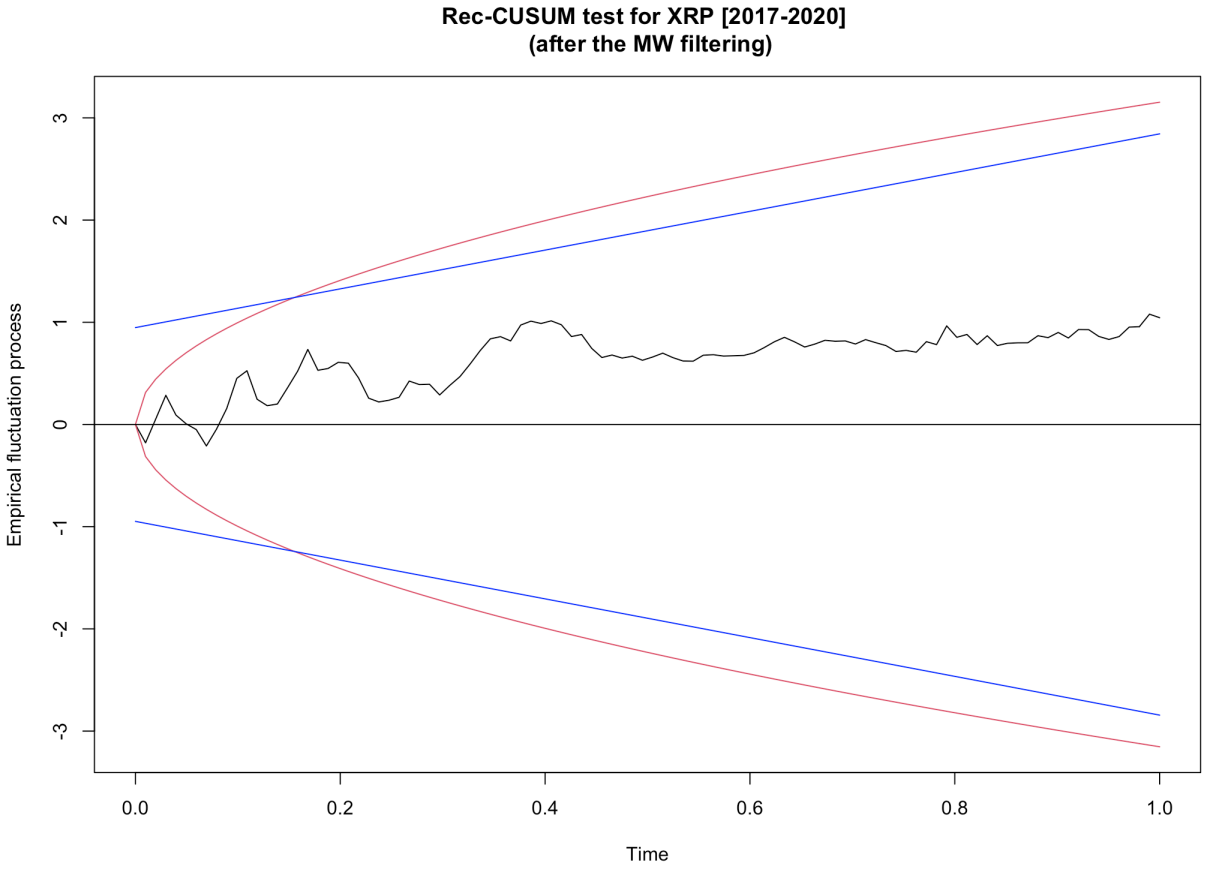

Figure 69: The Rec-CUSUM test of XRP [2018-2020] (after the Müller-Watson filtering)

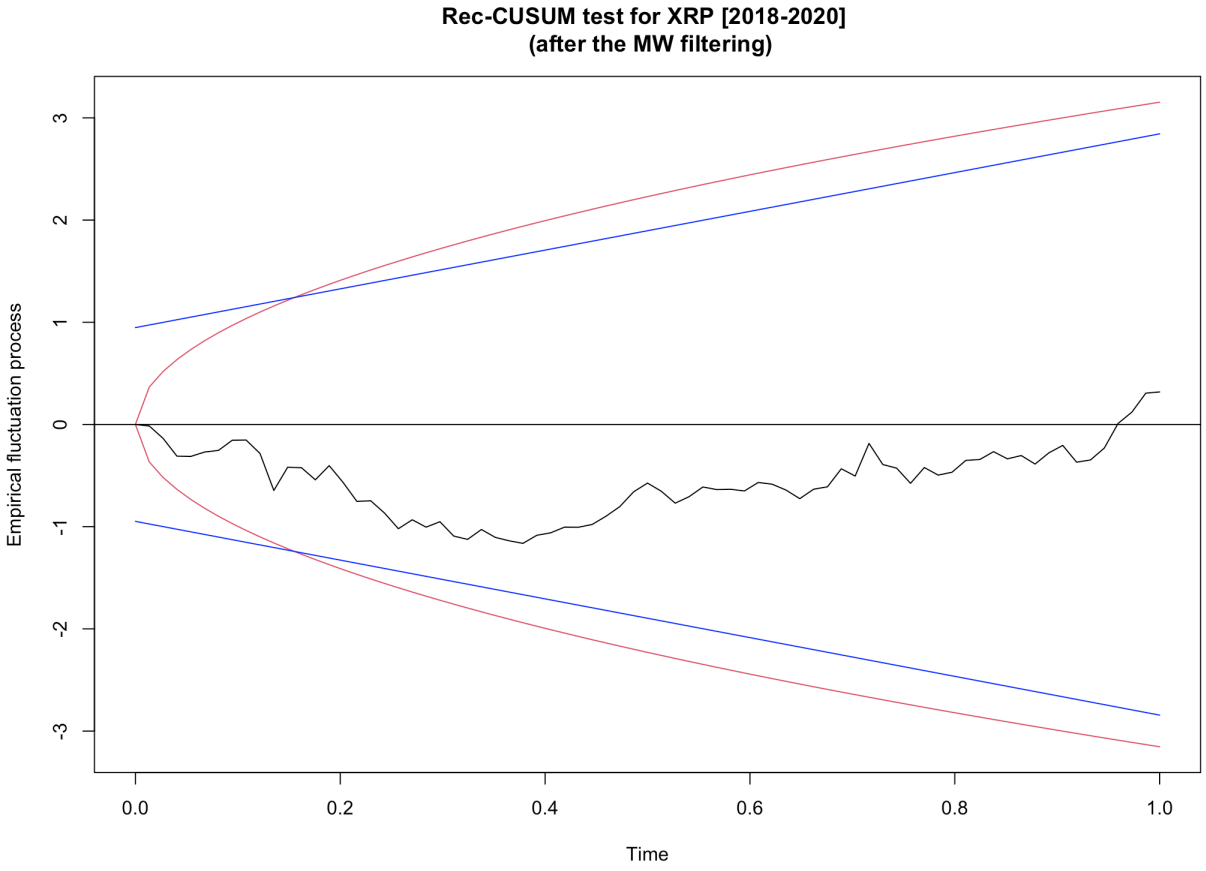

Figure 70: The Rec-CUSUM test of XRP [2019-2020] (after the Müller-Watson filtering)

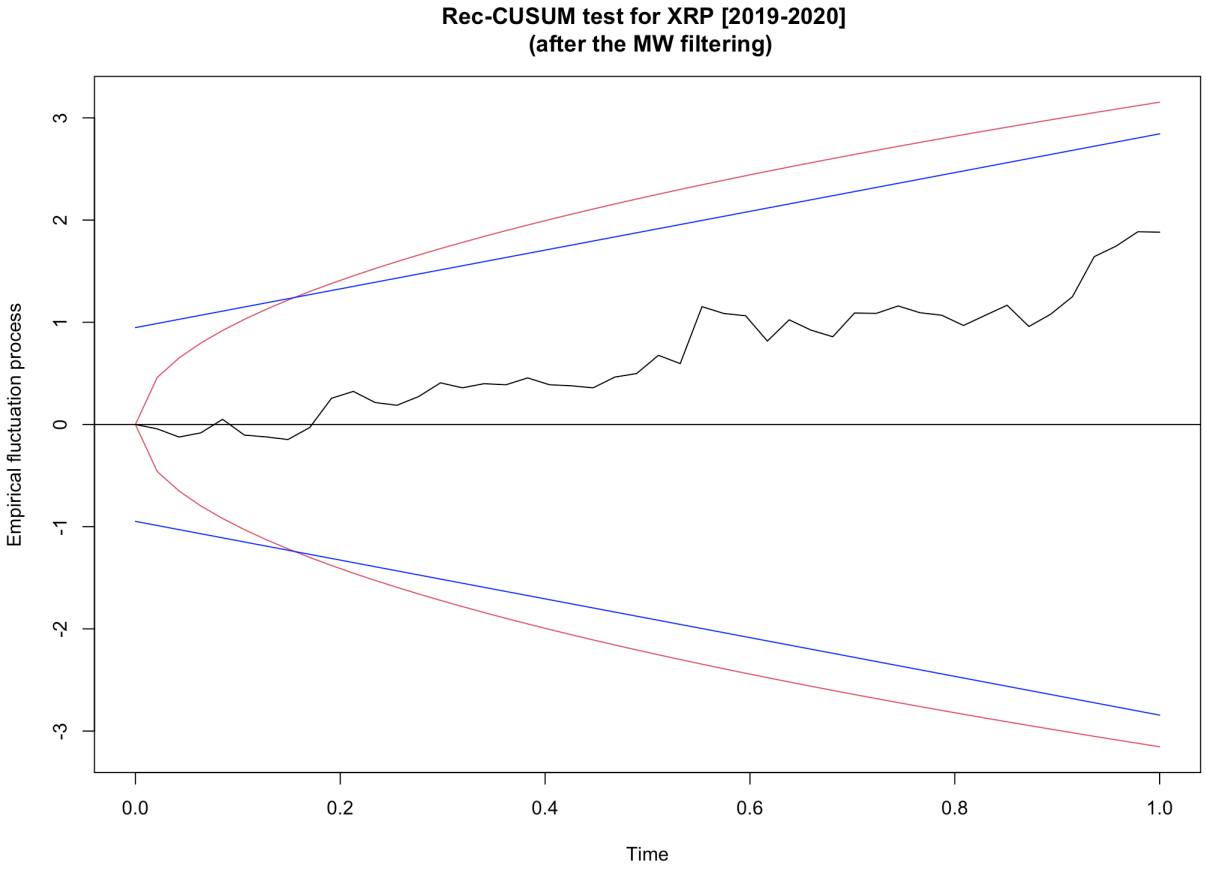

Figure 71: The Rec-CUSUM test of JPY [2016-2020] (after the Müller-Watson filtering)

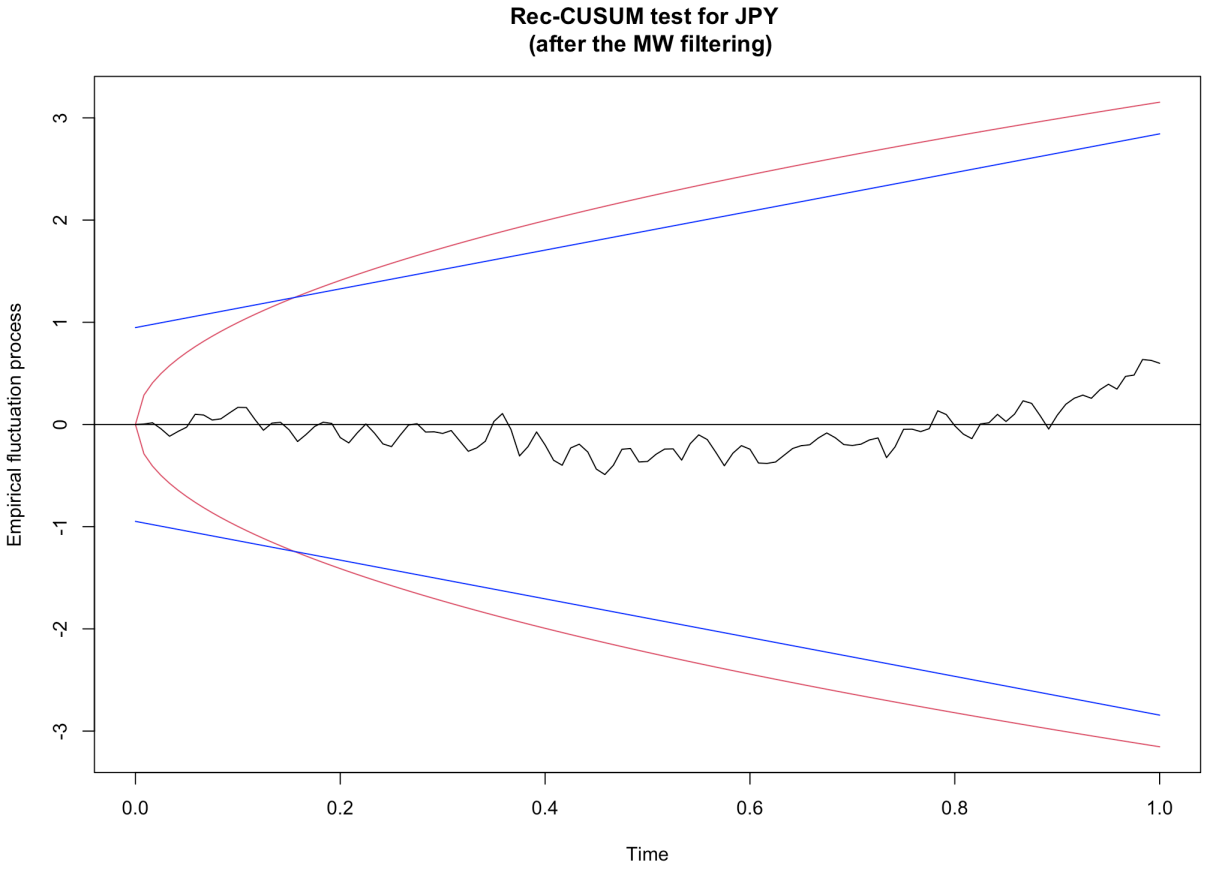

Figure 72: The Rec-CUSUM test of JPY [2017-2020] (after the Müller-Watson filtering)

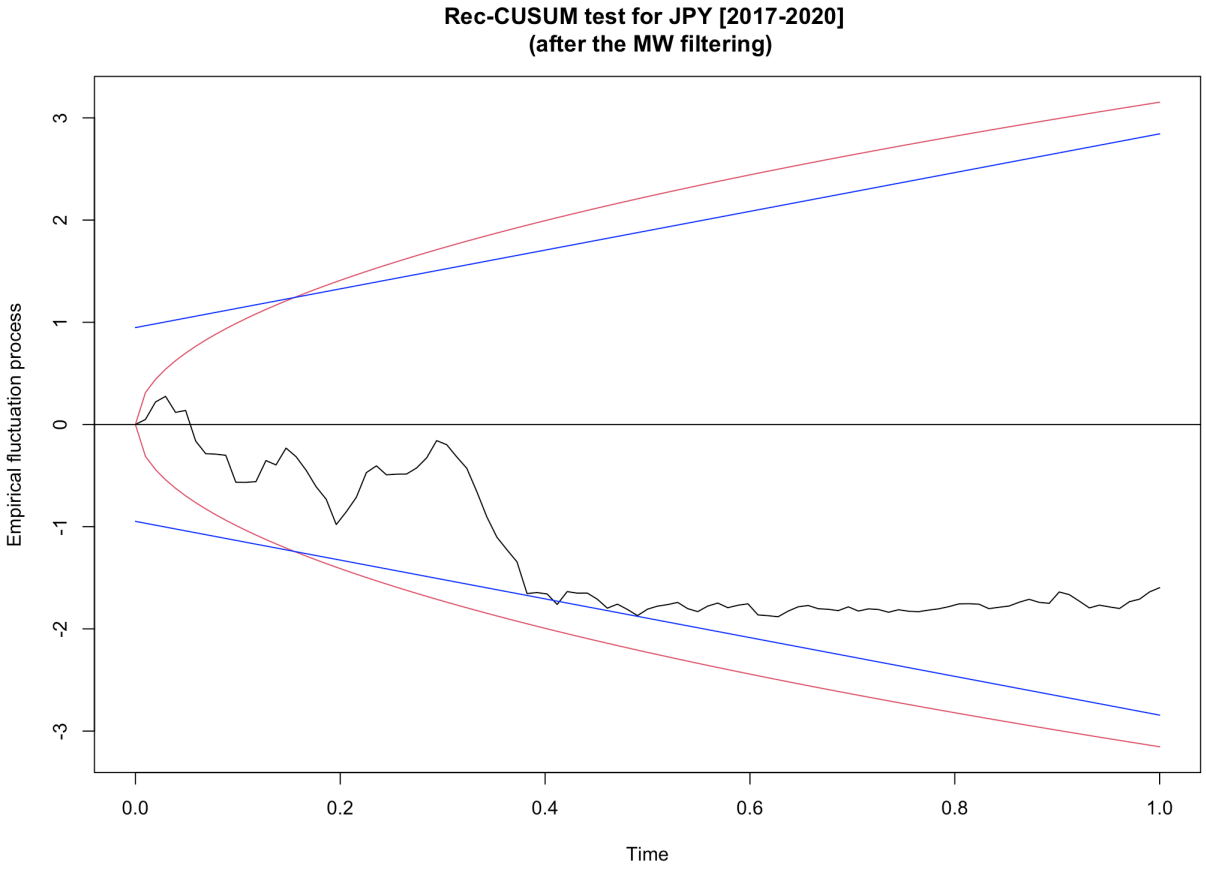

Figure 73: The Rec-CUSUM test of JPY [2018-2020] (after the Müller-Watson filtering)

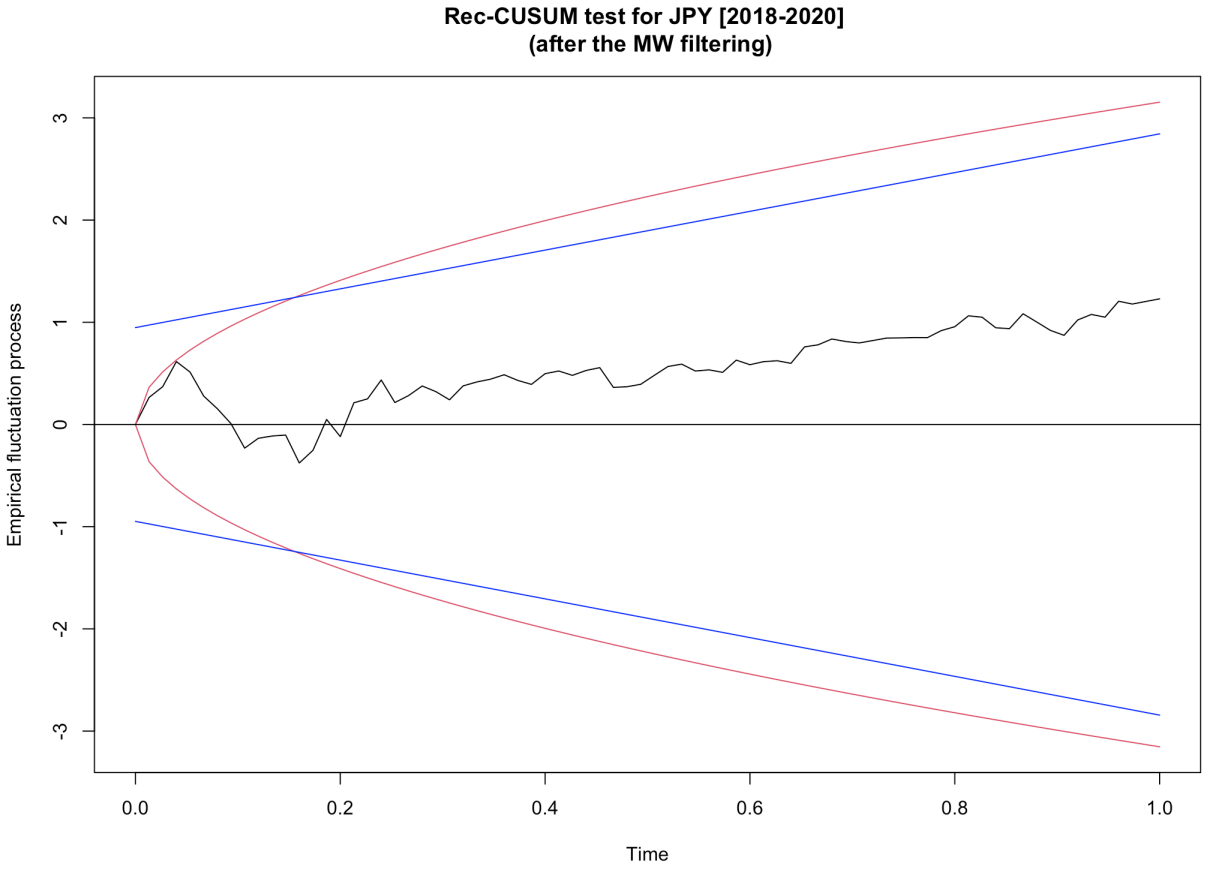

Figure 74: The Rec-CUSUM test of JPY [2019-2020] (after the Müller-Watson filtering)

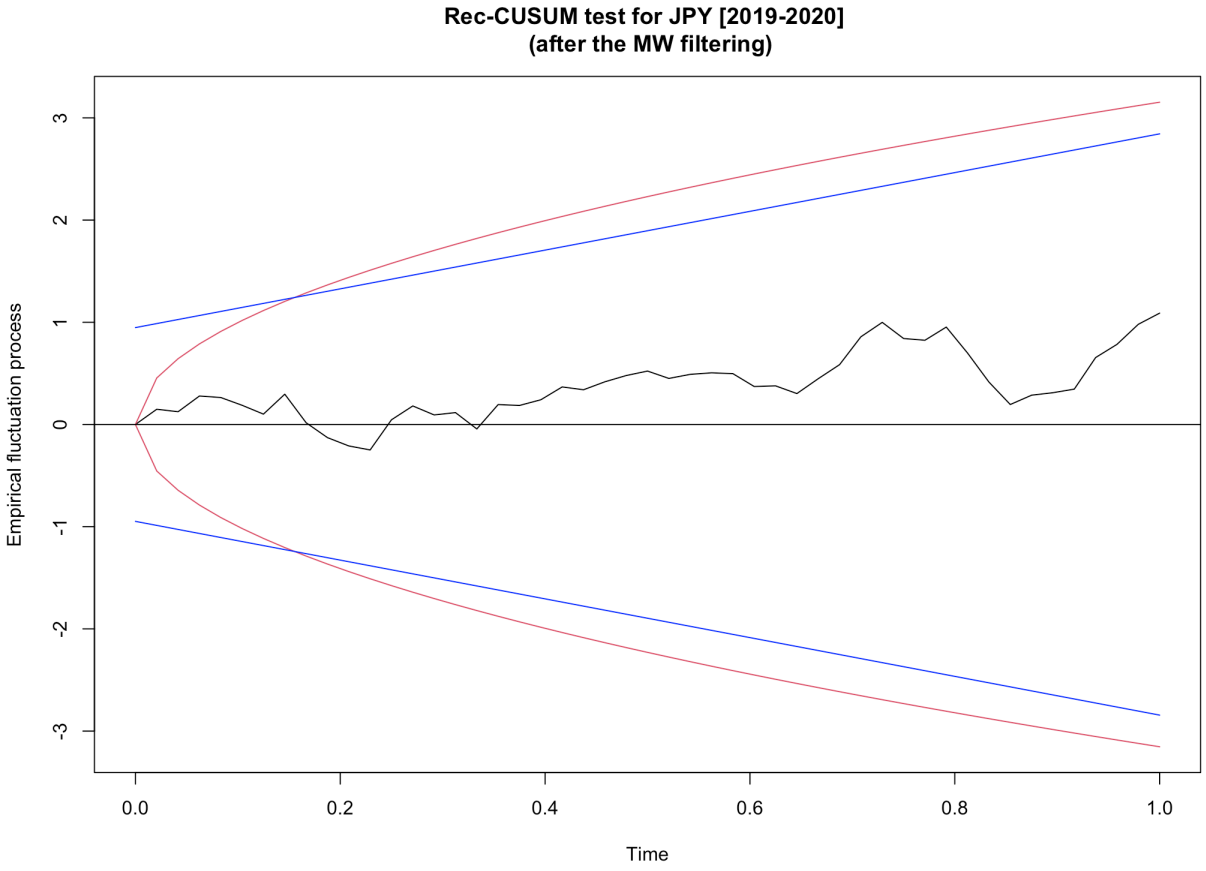

Figure 75: The Rec-CUSUM test of EUR [2016-2020] (after the Müller-Watson filtering)

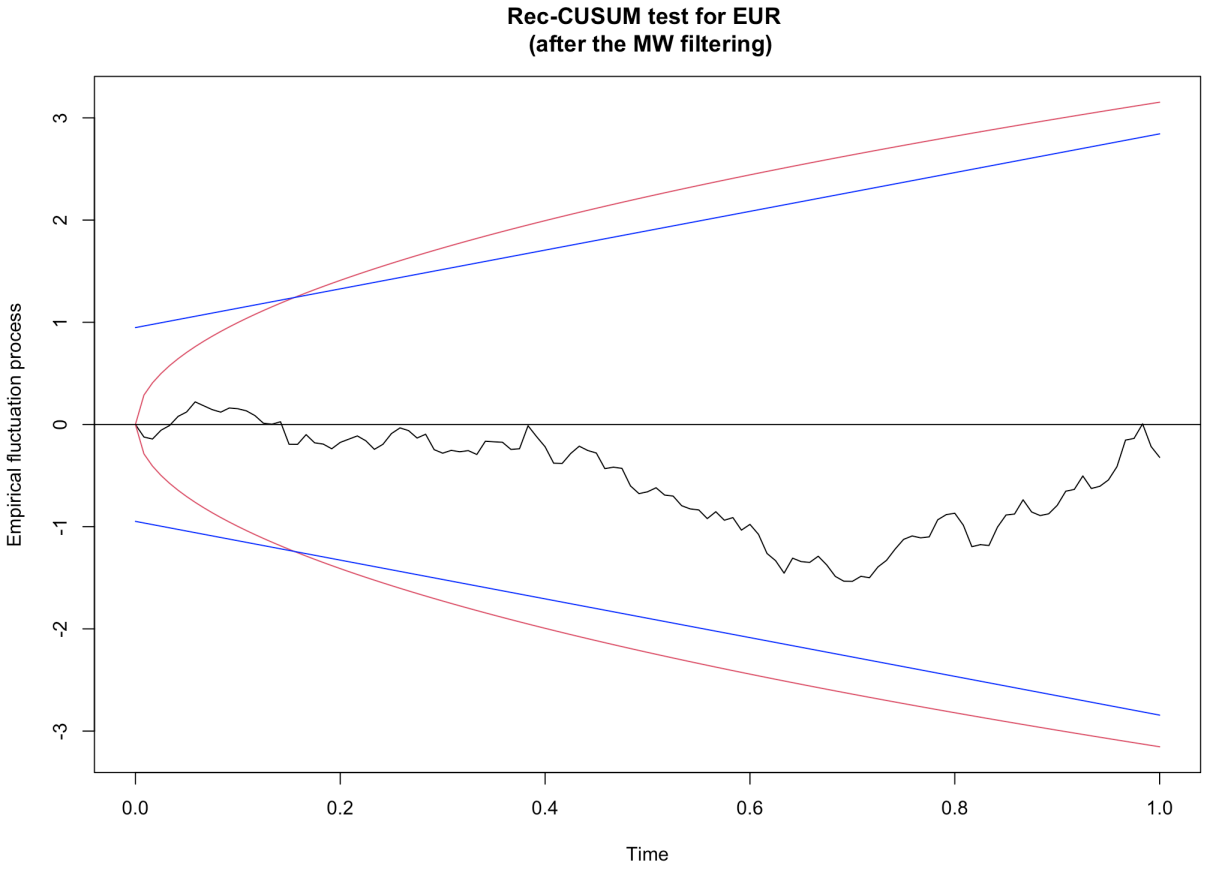

Figure 76: The Rec-CUSUM test of EUR [2017-2020] (after the Müller-Watson filtering)

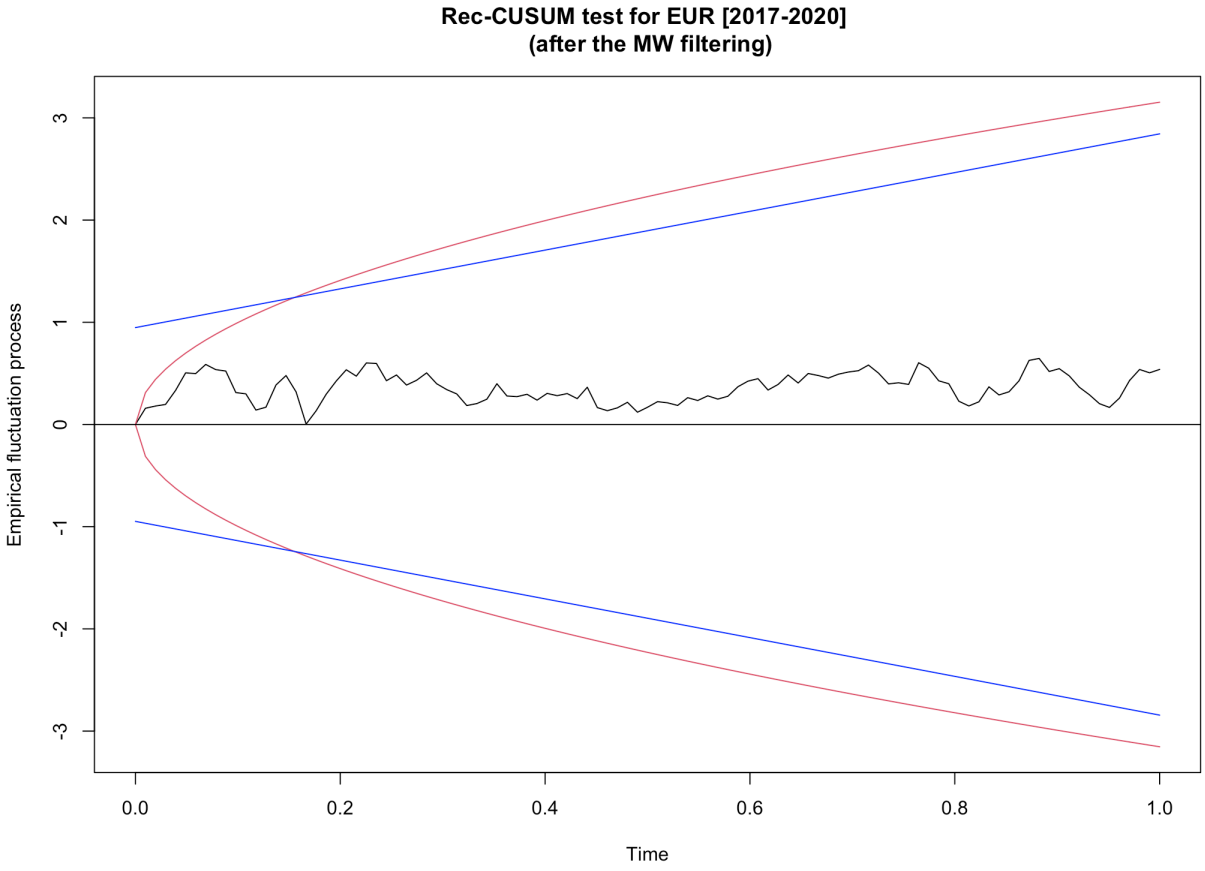

Figure 77: The Rec-CUSUM test of EUR [2018-2020] (after the Müller-Watson filtering)

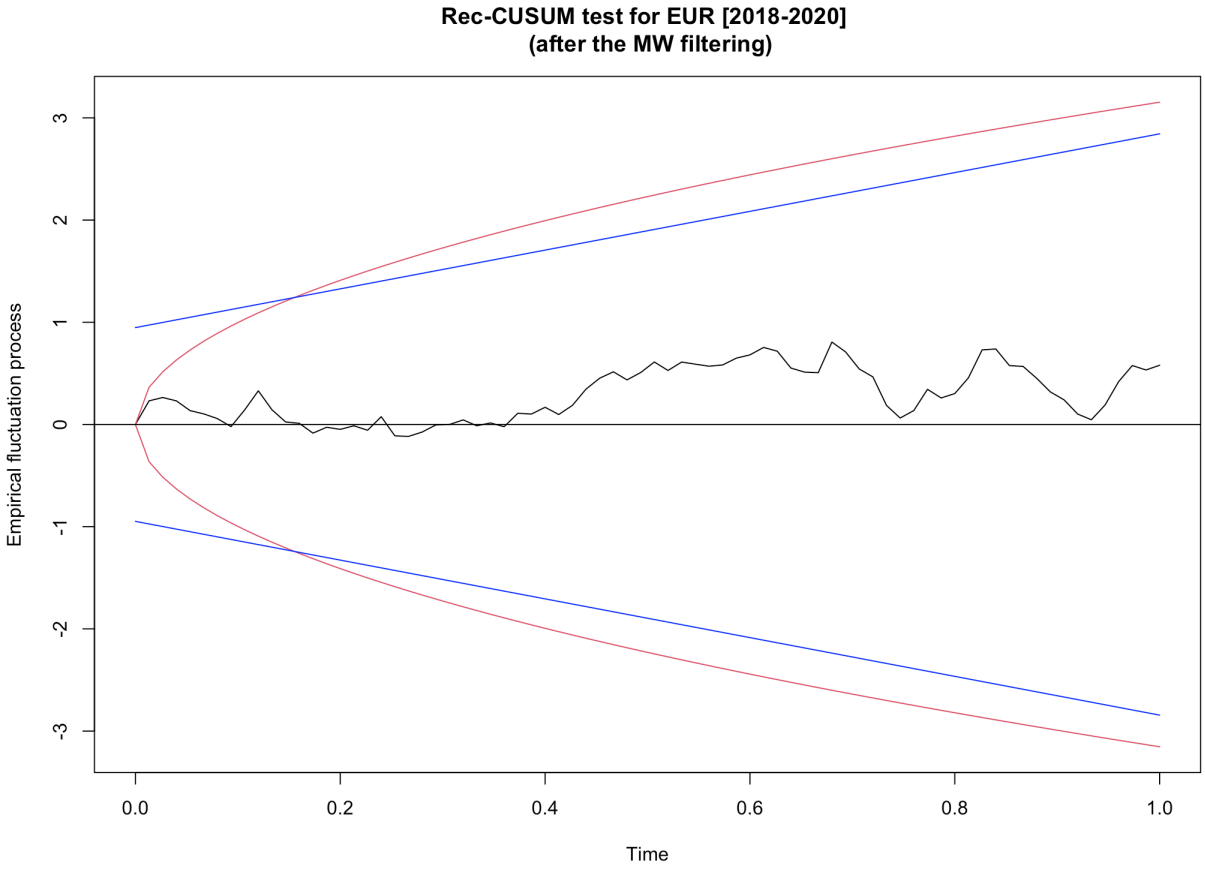

Figure 78: The Rec-CUSUM test of EUR [2019-2020] (after the Müller-Watson filtering)

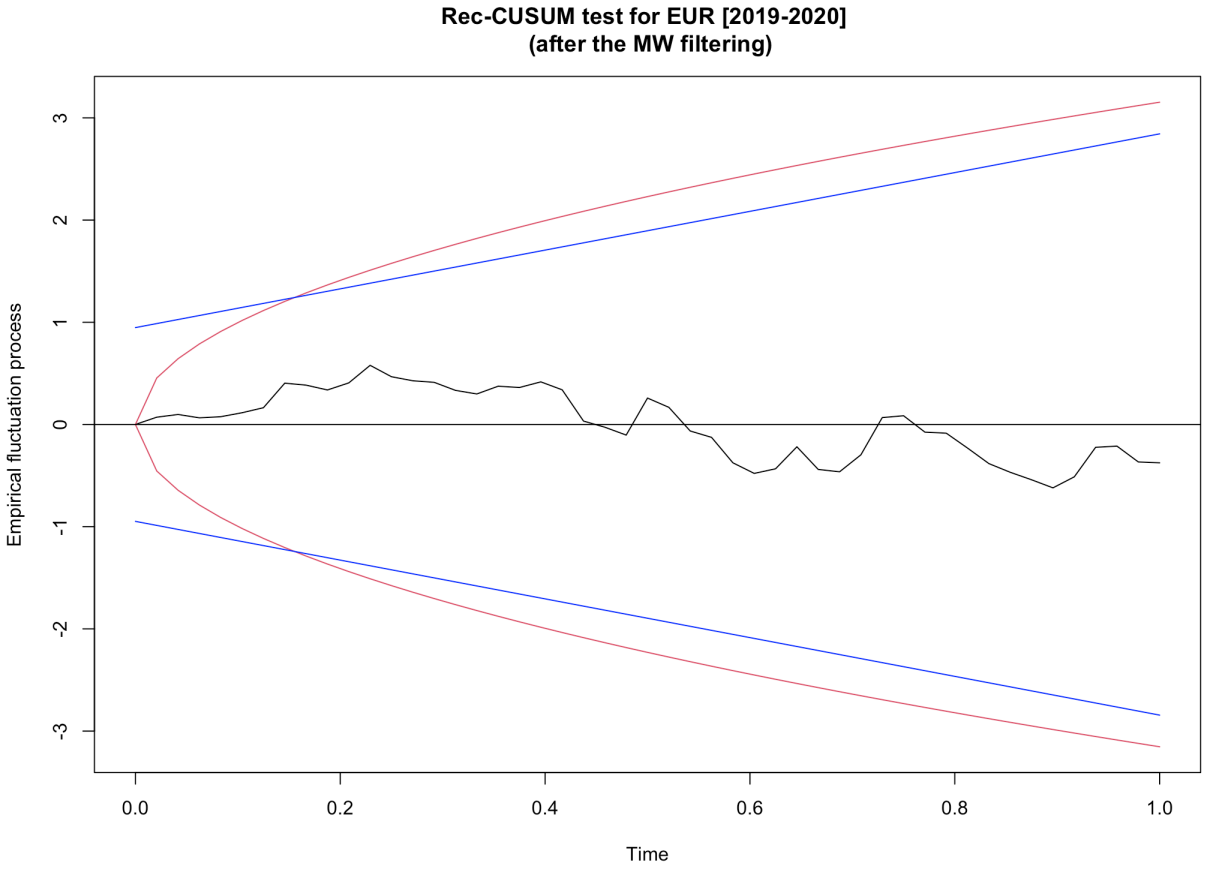

Figure 79: The Rec-CUSUM test of GOLD [2016-2020] (after the Müller-Watson filtering)

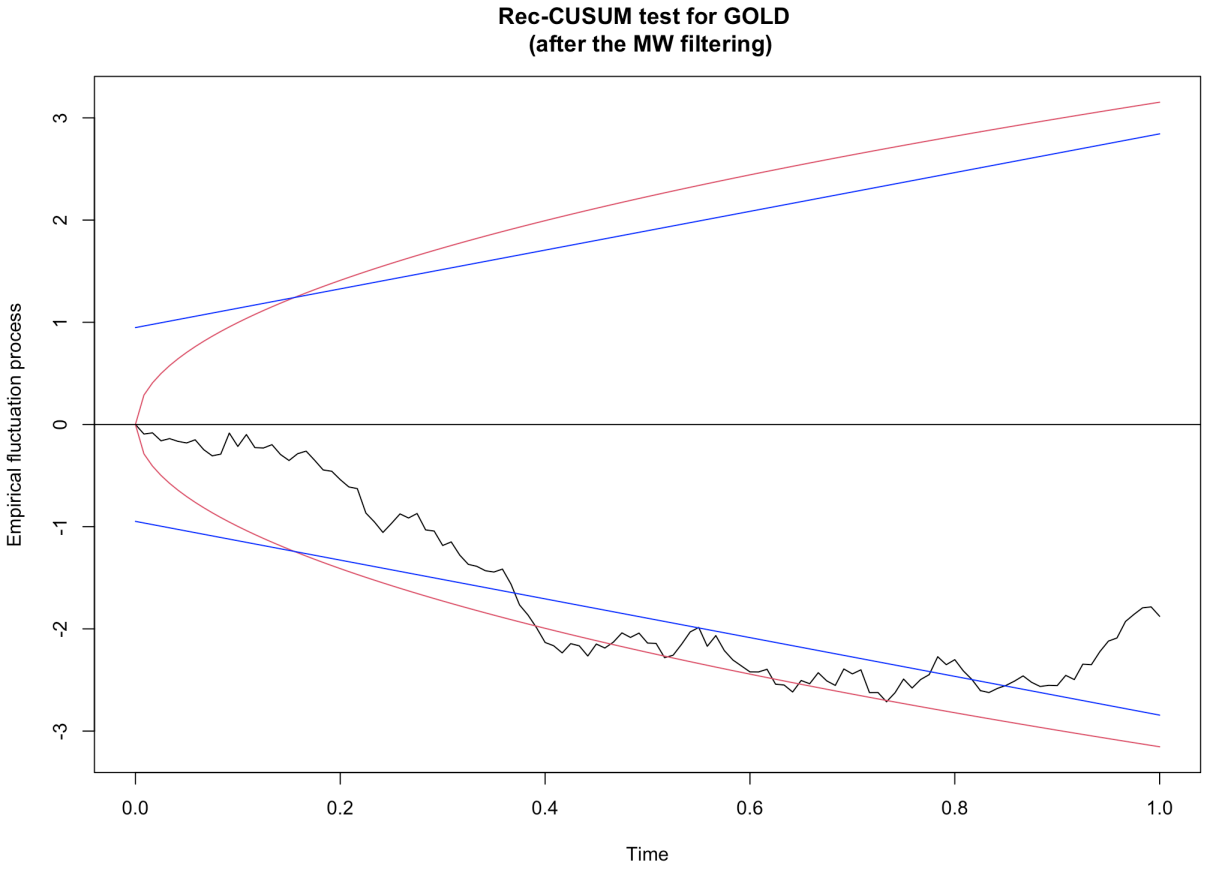

Figure 80: The Rec-CUSUM test of GOLD [2017-2020] (after the Müller-Watson filtering)

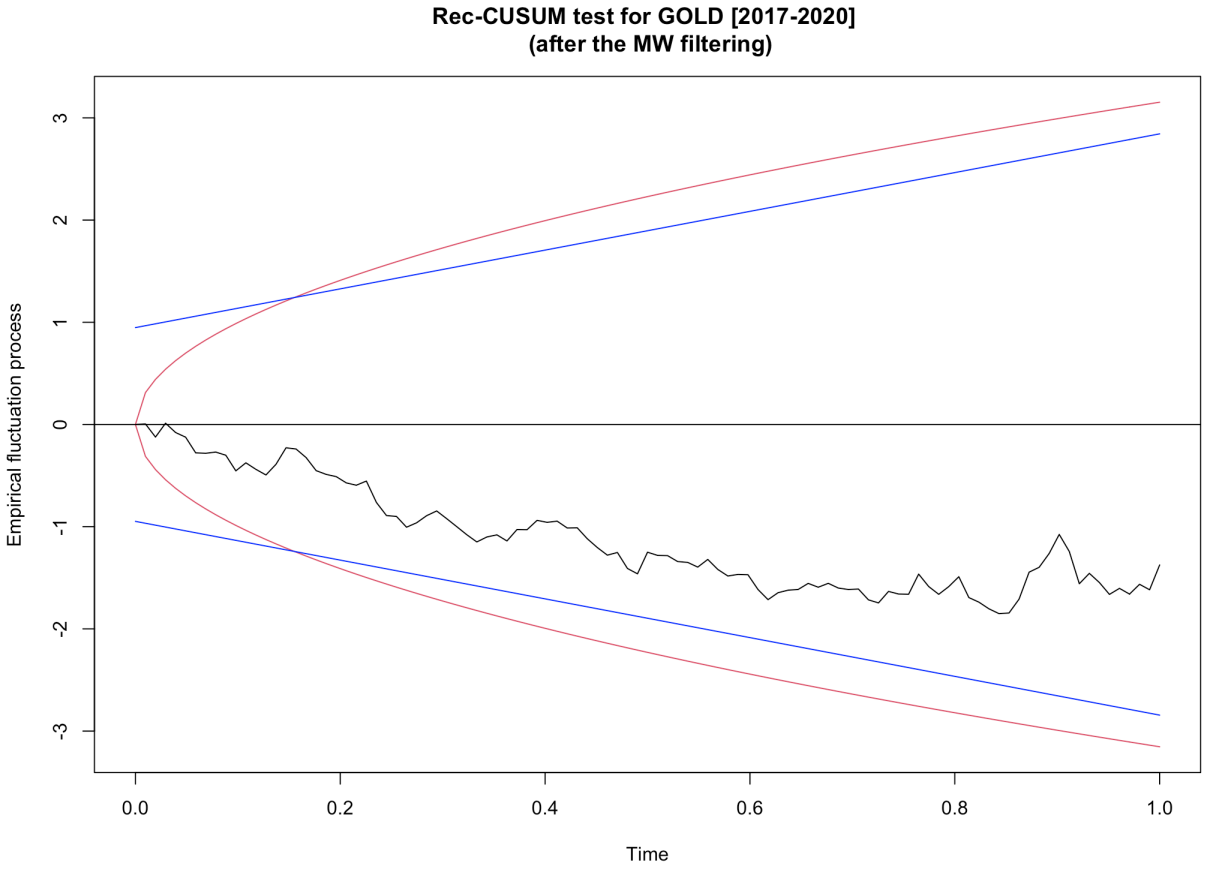

Figure 81: The Rec-CUSUM test of GOLD [2018-2020] (after the Müller-Watson filtering)

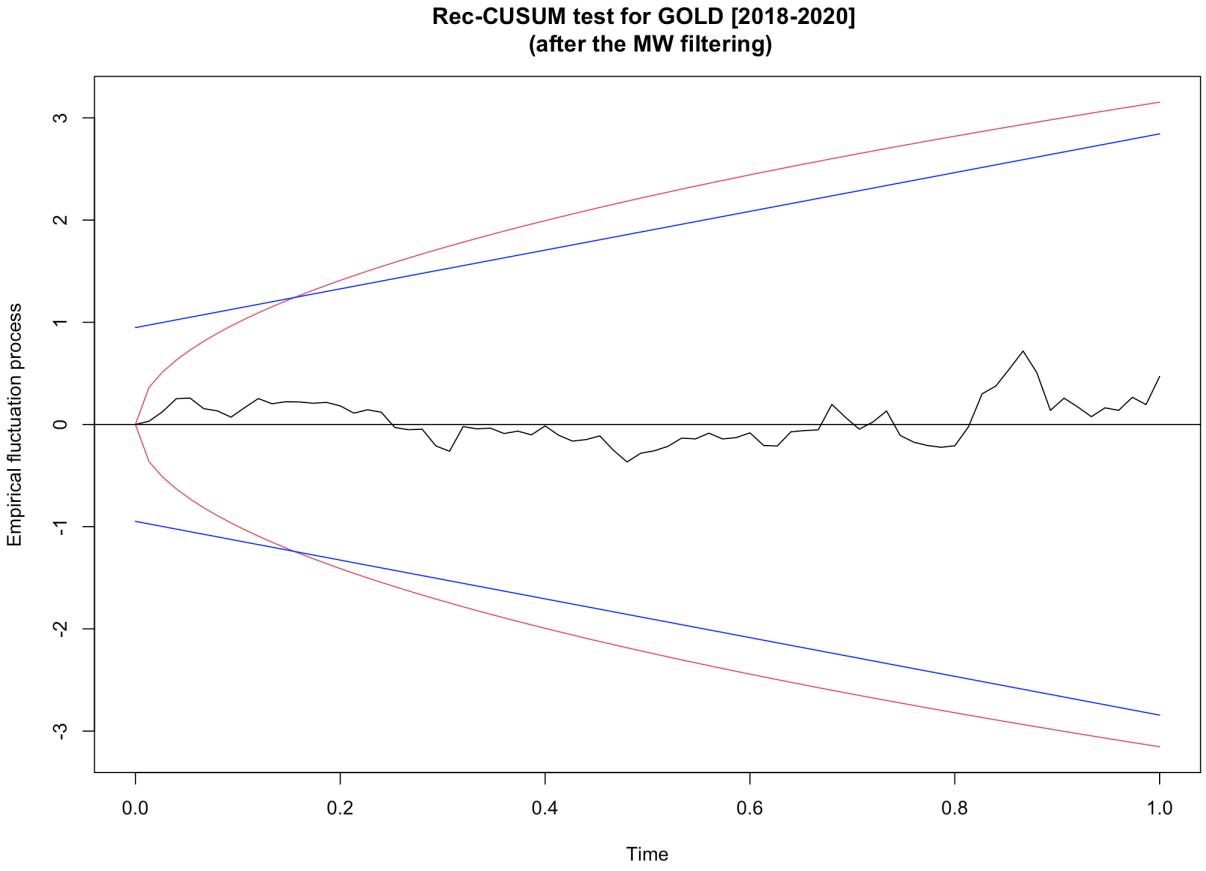

Figure 82: The Rec-CUSUM test of GOLD [2019-2020] (after the Müller-Watson filtering)

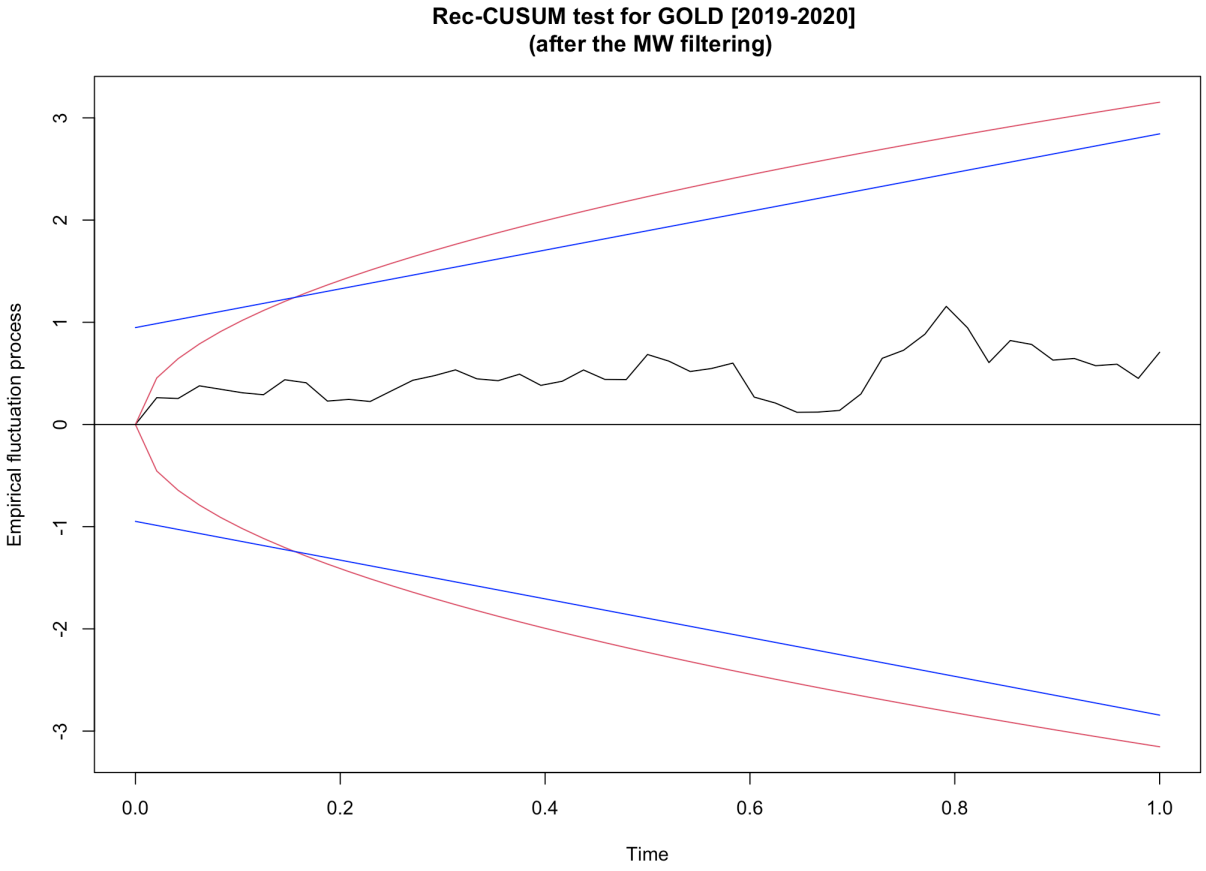

Figure 83: The Rec-CUSUM test of S&P500 [2016-2020] (after the Müller-Watson filtering)

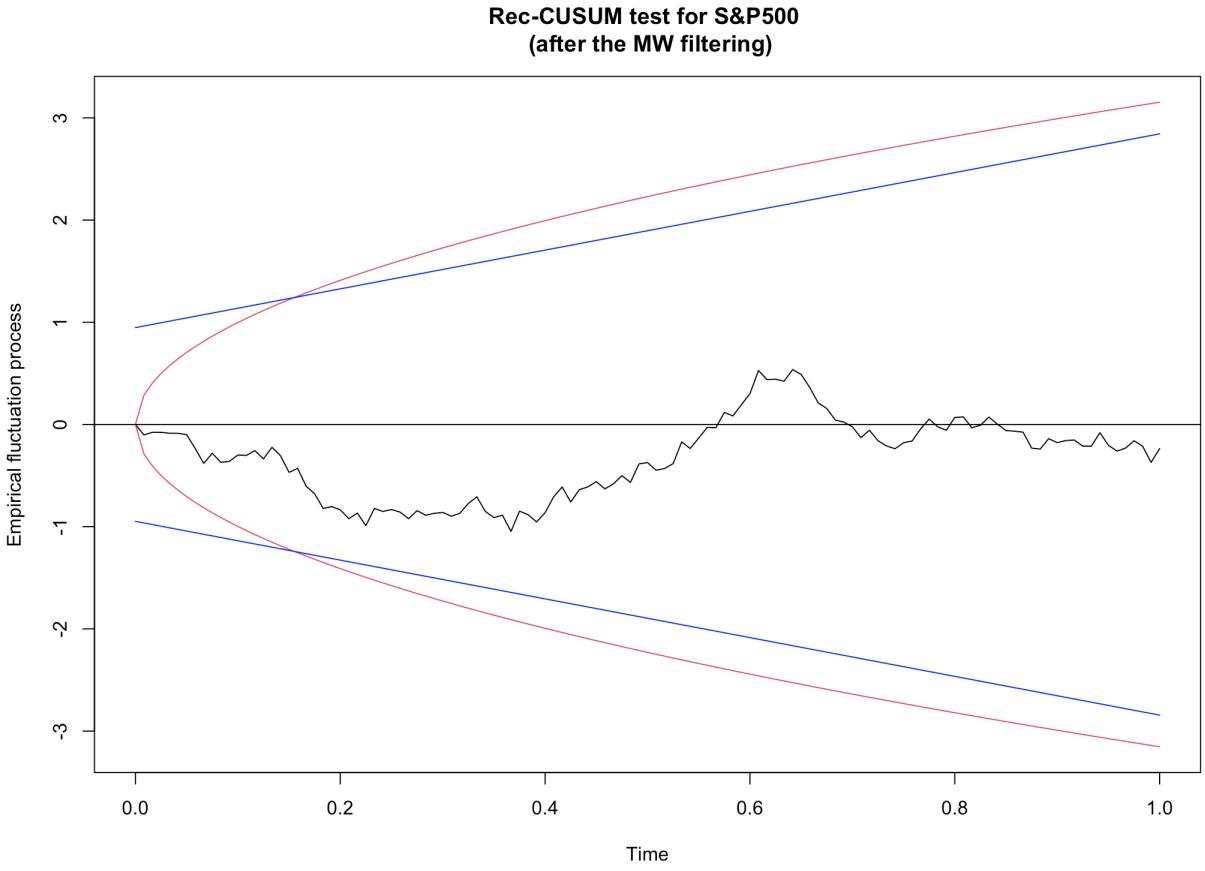

Figure 84: The Rec-CUSUM test of S&P500 [2017-2020] (after the Müller-Watson filtering)

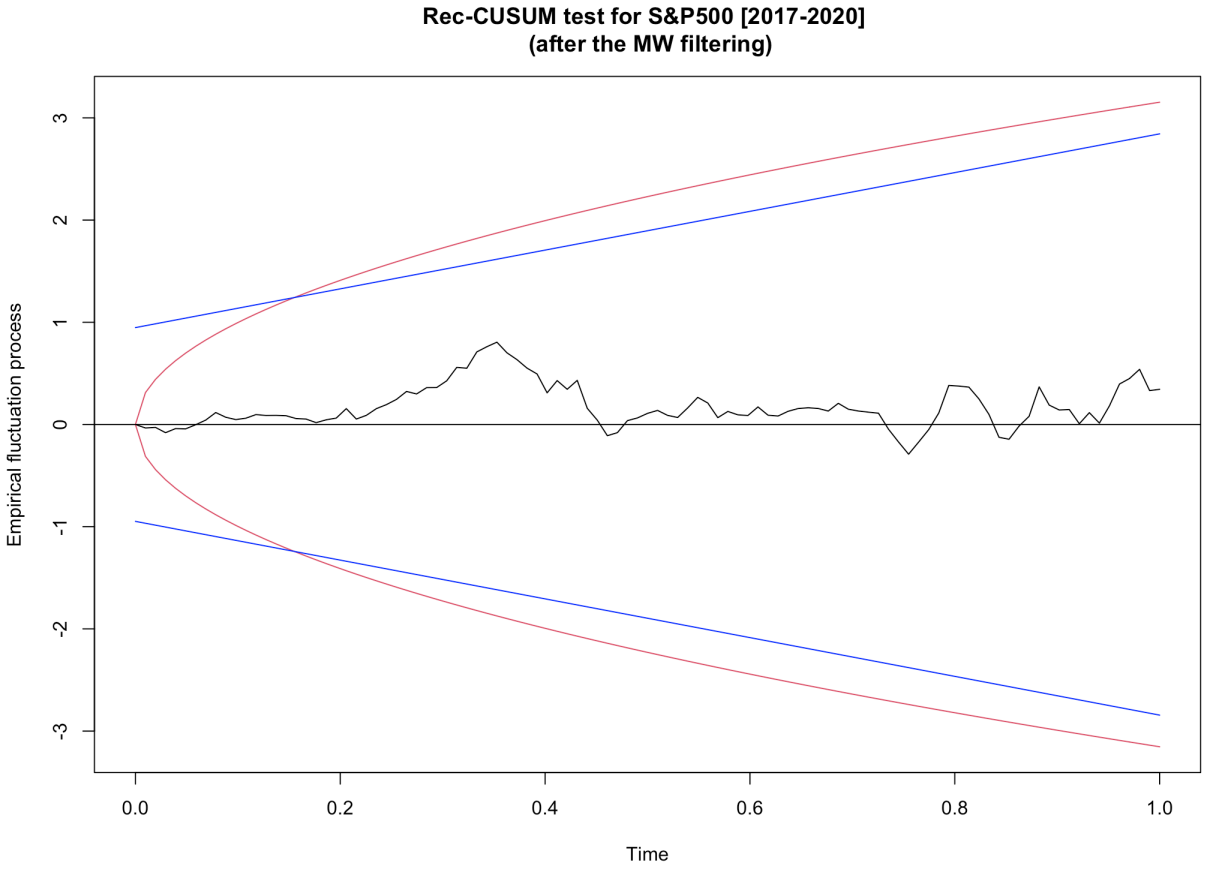

Figure 85: The Rec-CUSUM test of S&P500 [2018-2020] (after the Müller-Watson filtering)

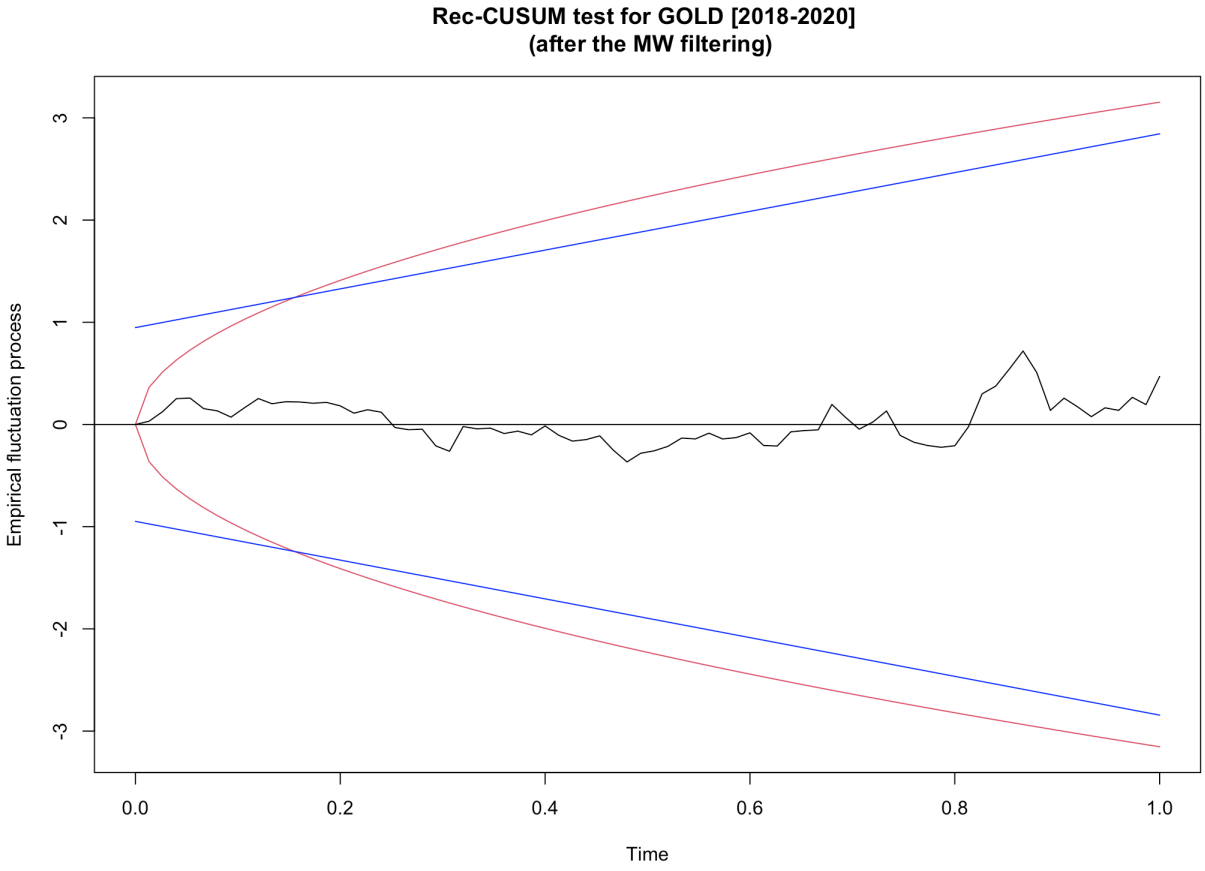

Figure 86: The Rec-CUSUM test of S&P500 [2019-2020] (after the Müller-Watson filtering)

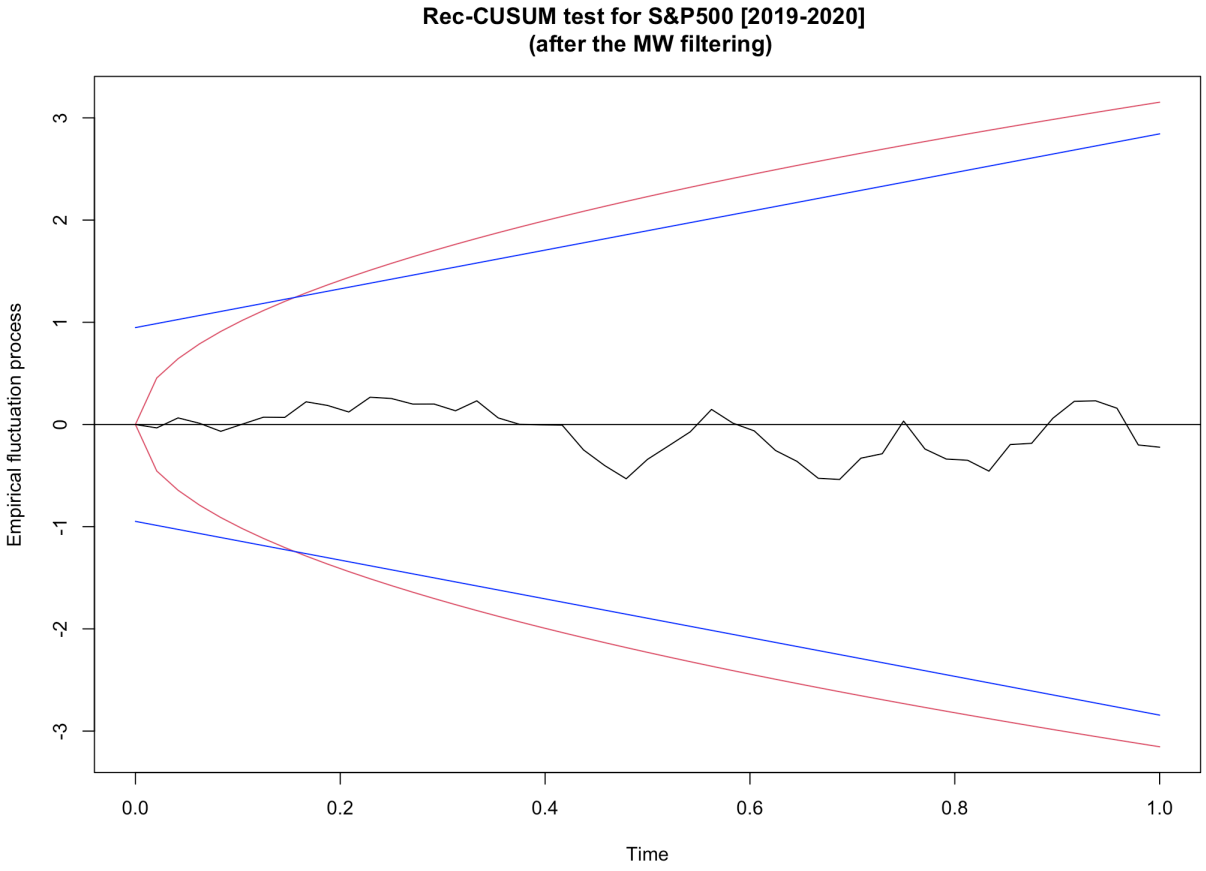

Figure 87: The Rec-CUSUM test of MSCI [2016-2020] (after the Müller-Watson filtering)

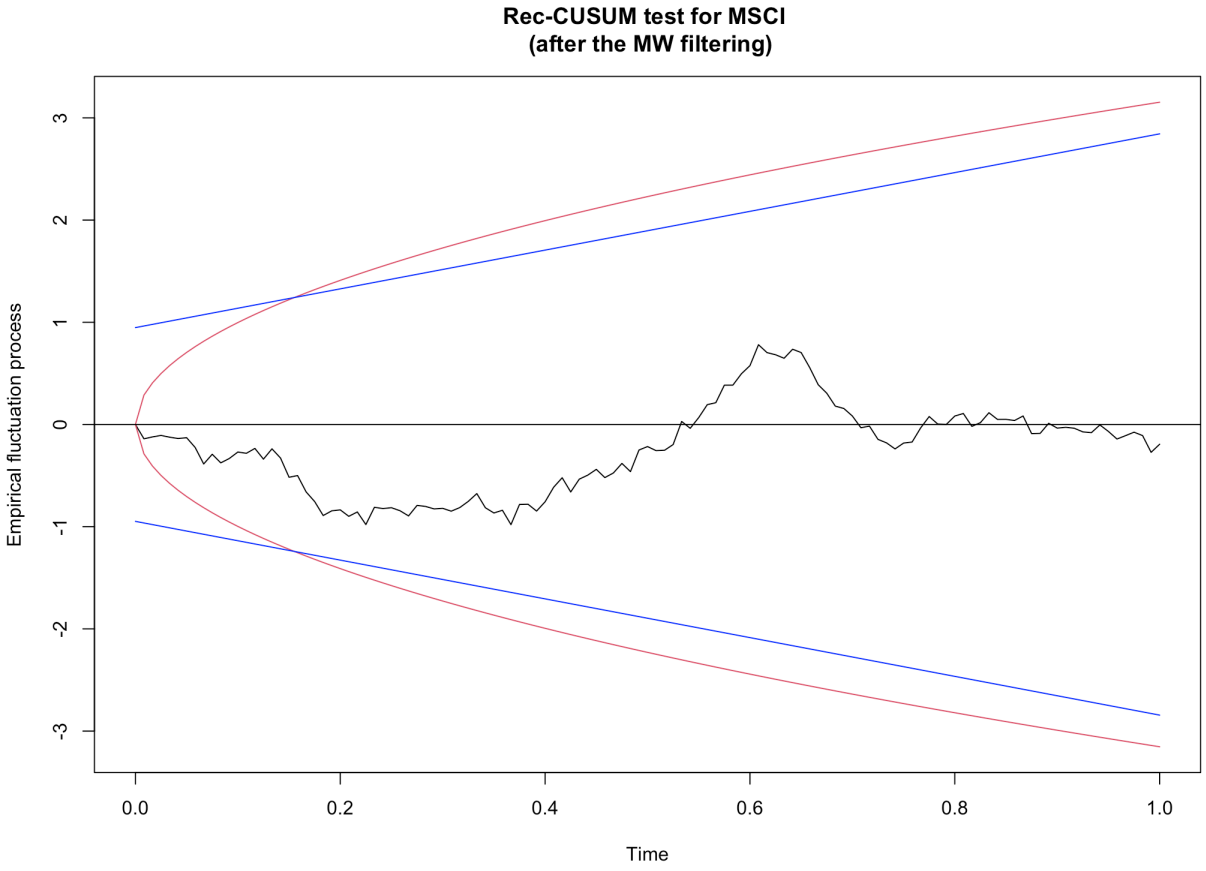

Figure 88: The Rec-CUSUM test of MSCI [2017-2020] (after the Müller-Watson filtering)

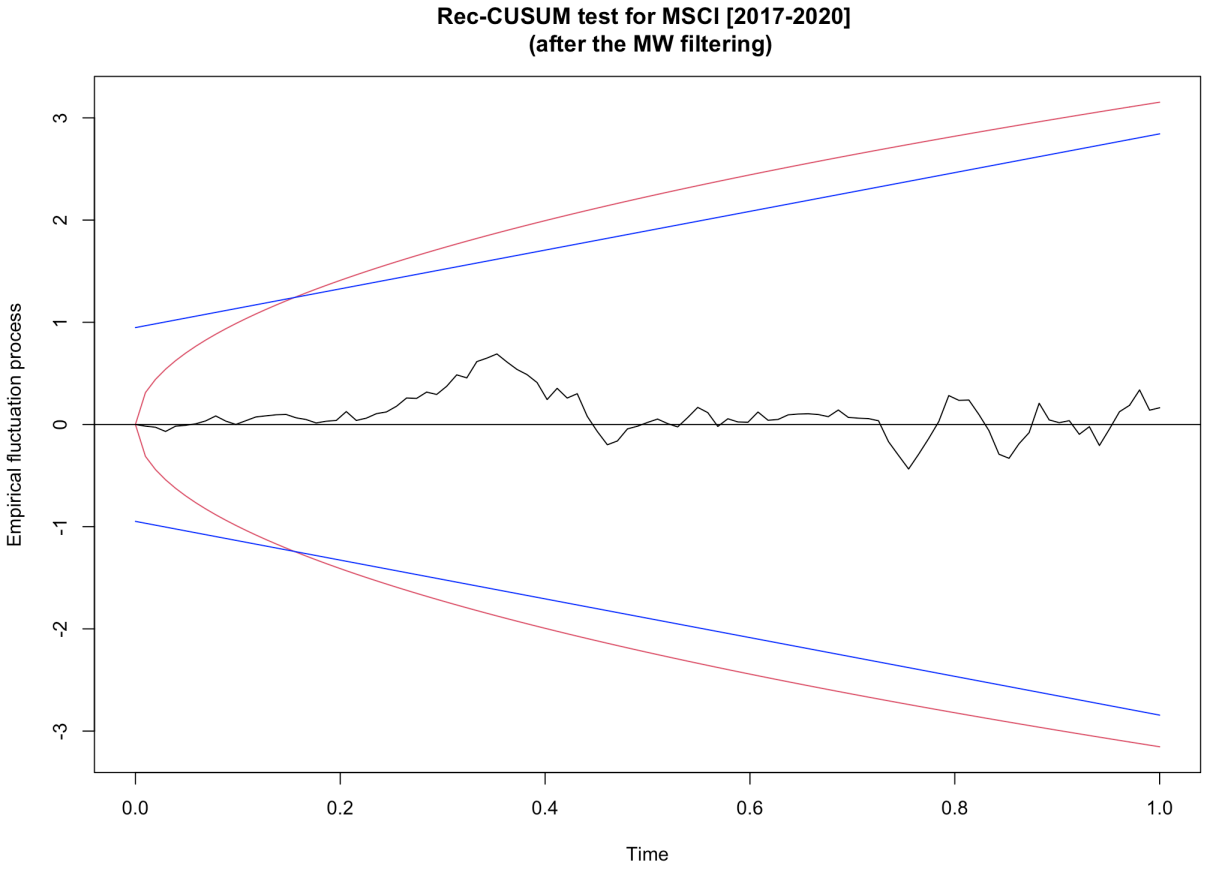

Figure 89: The Rec-CUSUM test of MSCI [2018-2020] (after the Müller-Watson filtering)

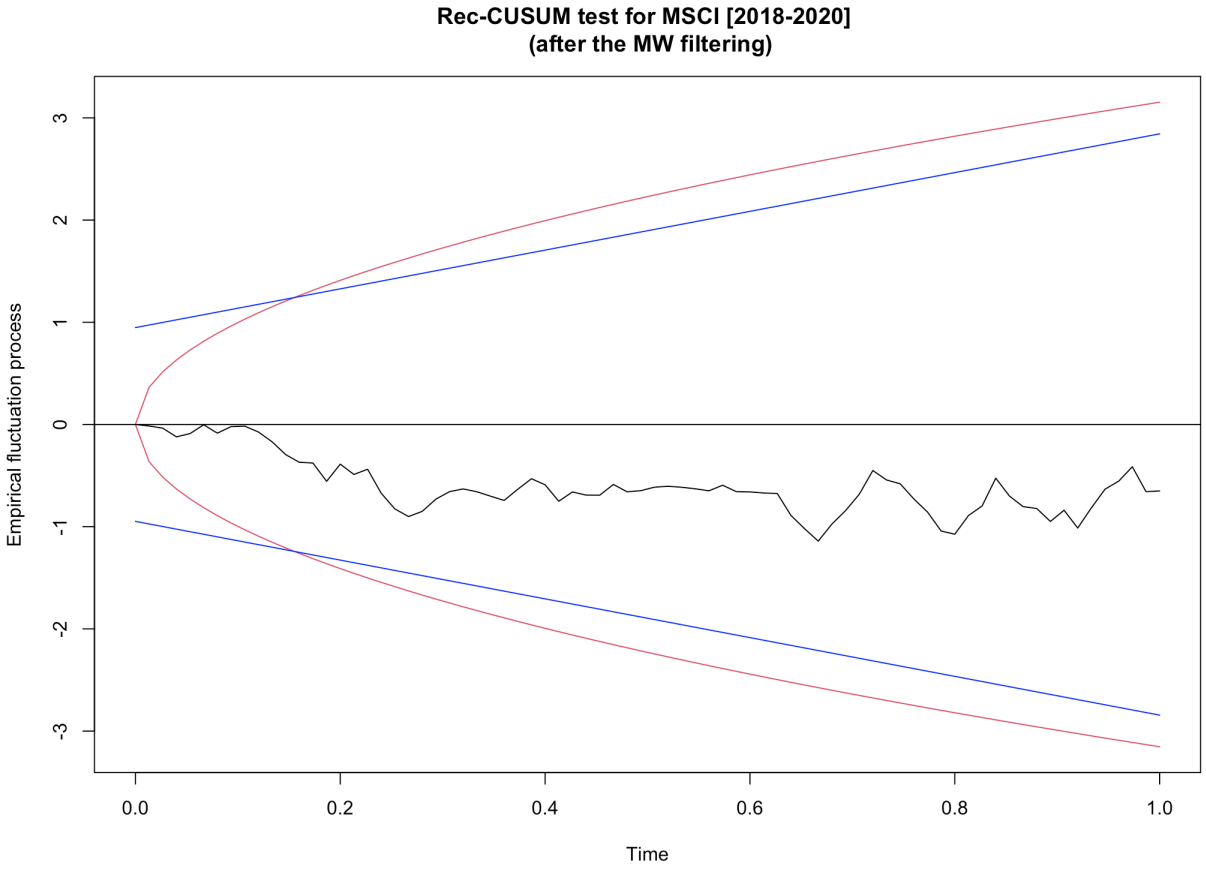

Figure 90: The Rec-CUSUM test of MSCI [2019-2020] (after the Müller-Watson filtering)

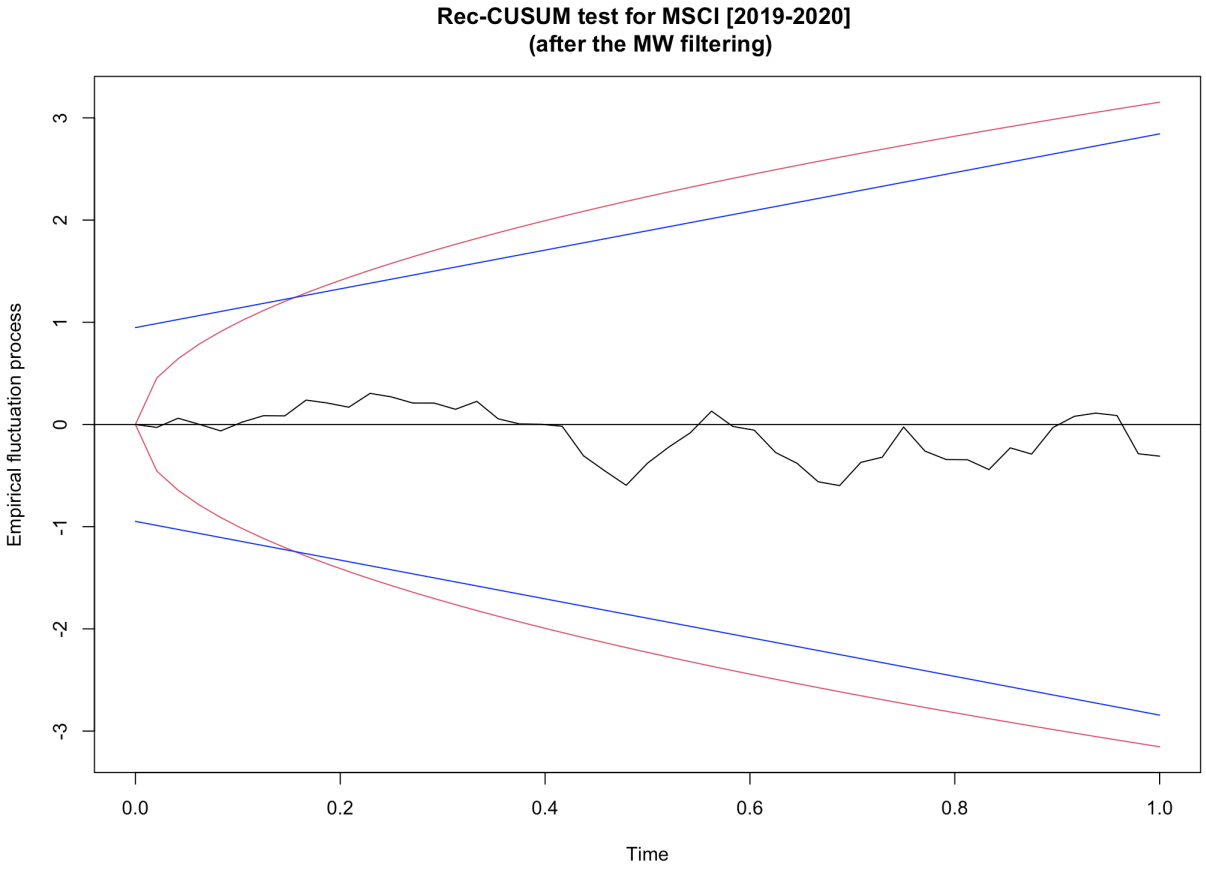

Table 1: Descriptive statistics of daily returns (annualized, %) for the whole sample period

Statistics	BTC	ETH	XRP	JPY	EUR	GOLD	S&P500	MSCI
N	1258	1258	1258	1249	1249	1249	1249	1258
Mean (%)	0.446	0.804	0.648	0.022	0.012	0.049	0.057	0.045
SD (%)	4.695	7.567	9.159	1.400	0.647	0.872	1.211	1.023
Min (%)	-38.118	-43.420	-43.069	-12.702	-4.160	-5.723	-11.984	-9.915
Max (%)	25.561	65.995	109.760	15.346	6.071	4.805	9.383	8.770
Skewness	-0.059	1.281	3.750	0.823	0.278	-0.200	-0.731	-1.234
Kurtosis	7.096	9.353	33.954	36.265	10.922	4.652	20.552	22.681

Table 2: Correlation matrix in 2016 (before the Müller-Watson filtering)

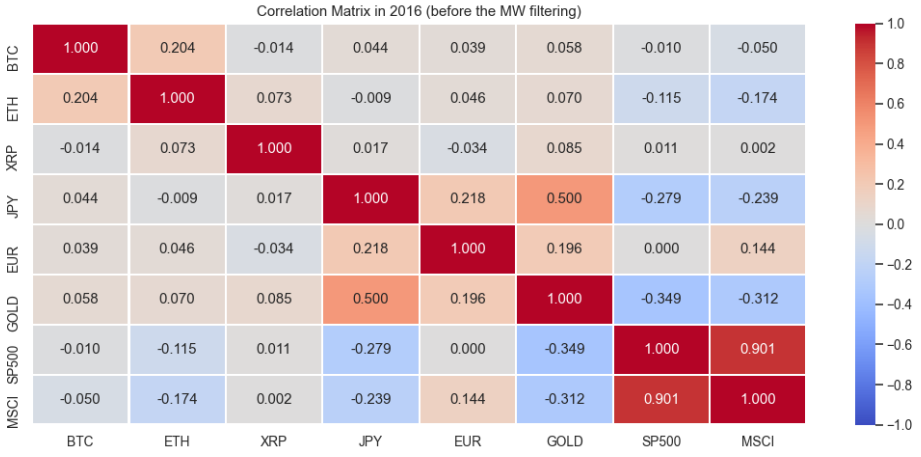

Table 3: Correlation matrix in 2017 (before the Müller-Watson filtering)

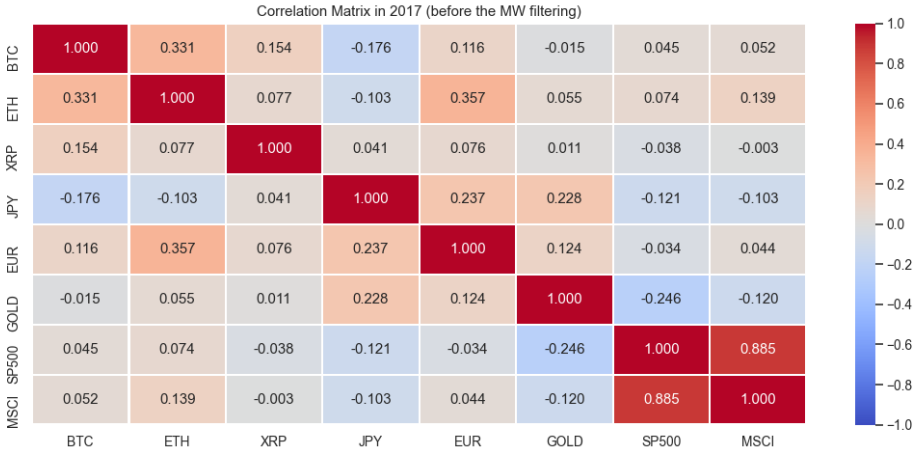

Table 4: Correlation matrix in 2018 (before the Müller-Watson filtering)

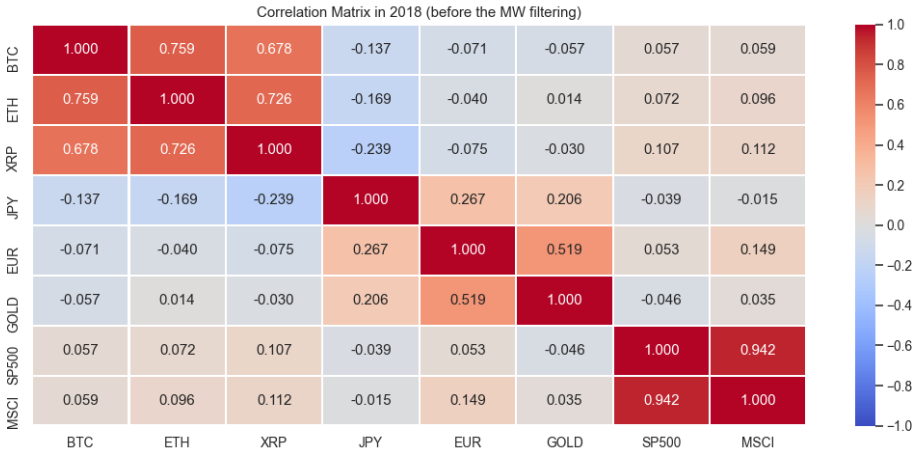

Table 5: Correlation matrix in 2019 (before the Müller-Watson filtering)

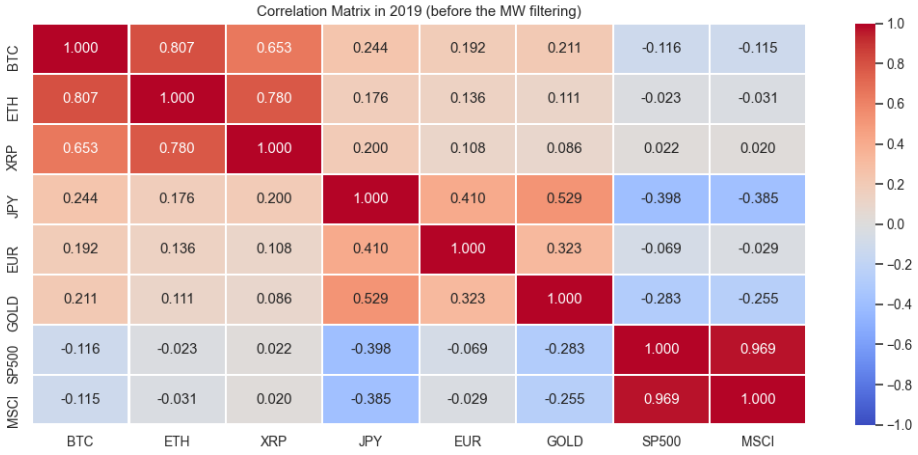

Table 6: Correlation matrix in 2020 (before the Müller-Watson filtering)

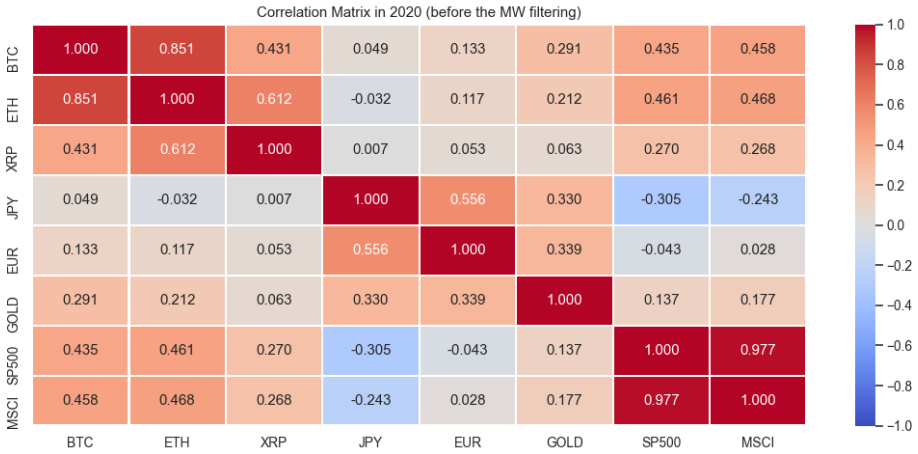

Table 7: Correlation matrix in 2016 (after the Müller-Watson filtering)

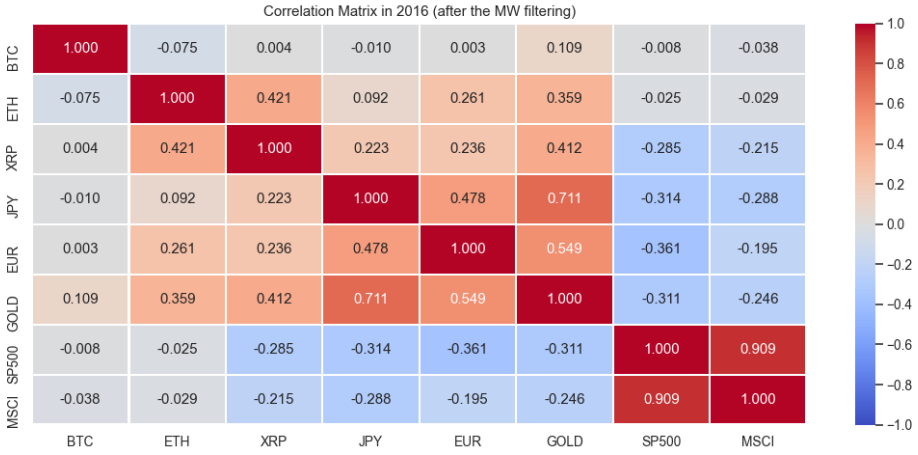

Table 8: Correlation matrix in 2017 (after the Müller-Watson filtering)

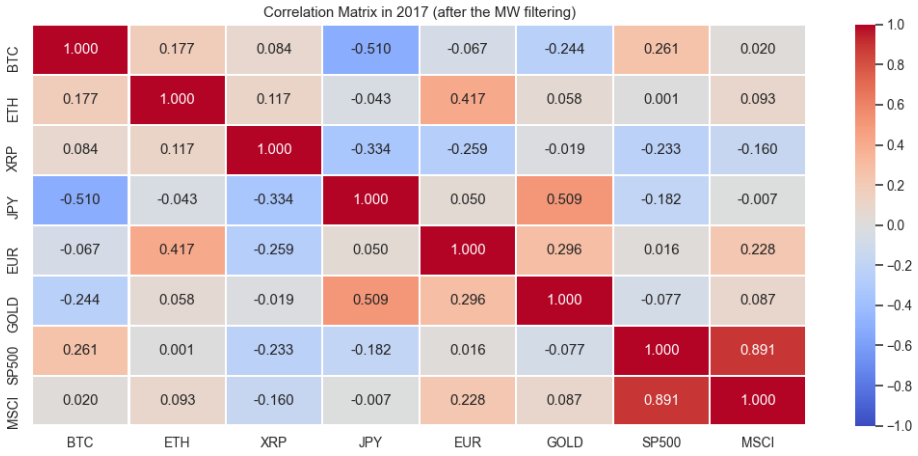

Table 9: Correlation matrix in 2018 (after the Müller-Watson filtering)

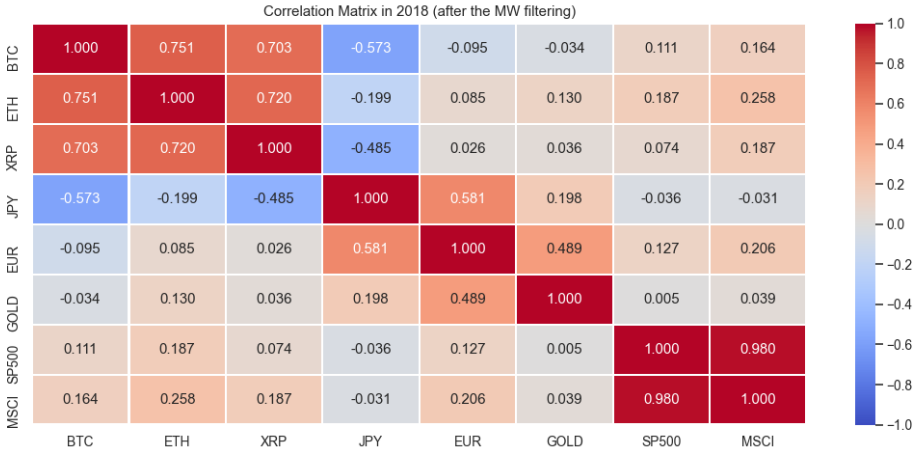

Table 10: Correlation matrix in 2019 (after the Müller-Watson filtering)

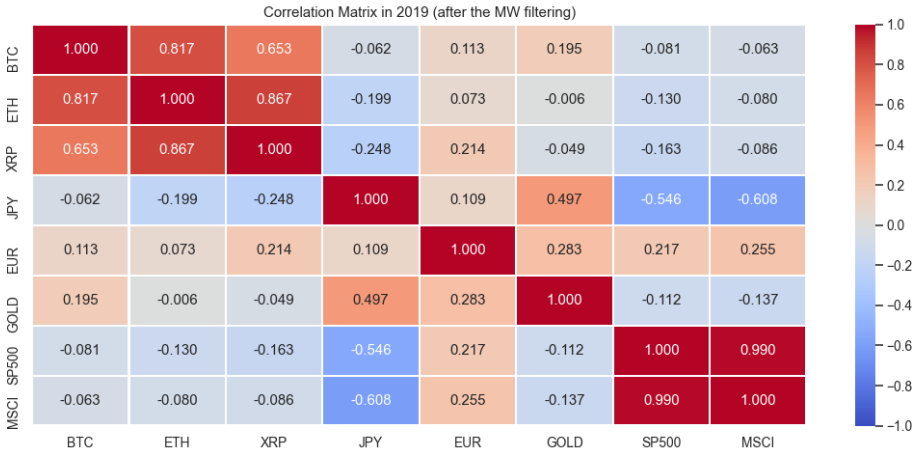

Table 11: Correlation matrix in 2020 (after the Müller-Watson filtering)

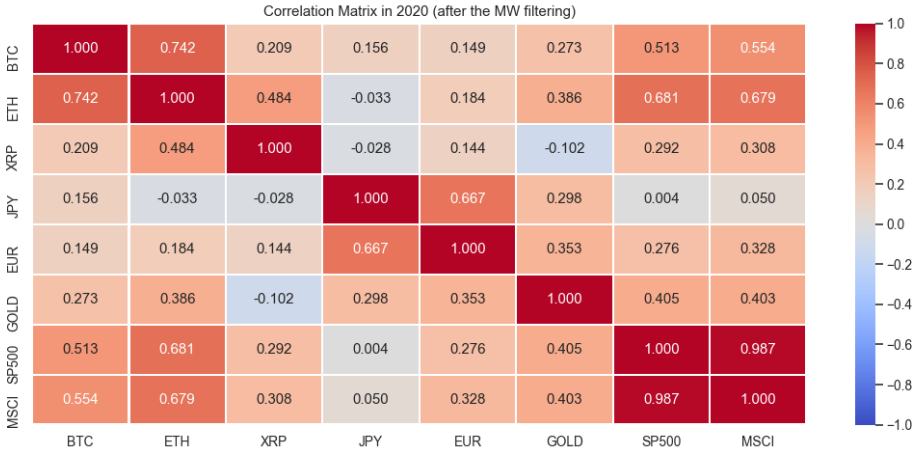

Table 12: DTW similarity matrix in 2016 (before the Müller-Watson filtering)

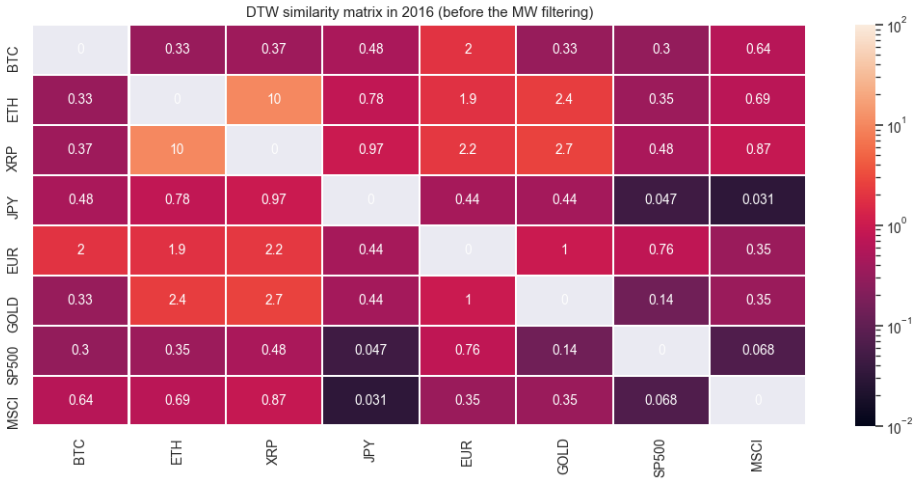

Table 13: DTW similarity matrix in 2017 (before the Müller-Watson filtering)

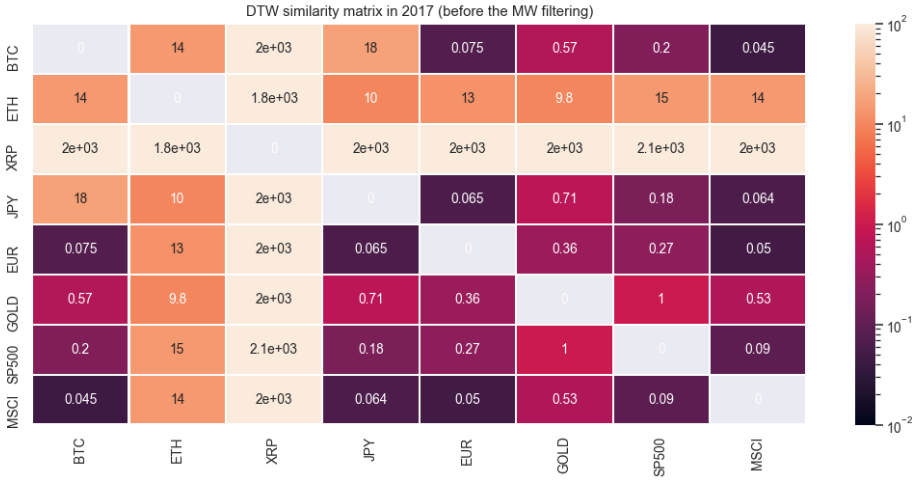

Table 14: DTW similarity matrix in 2018 (before the Müller-Watson filtering)

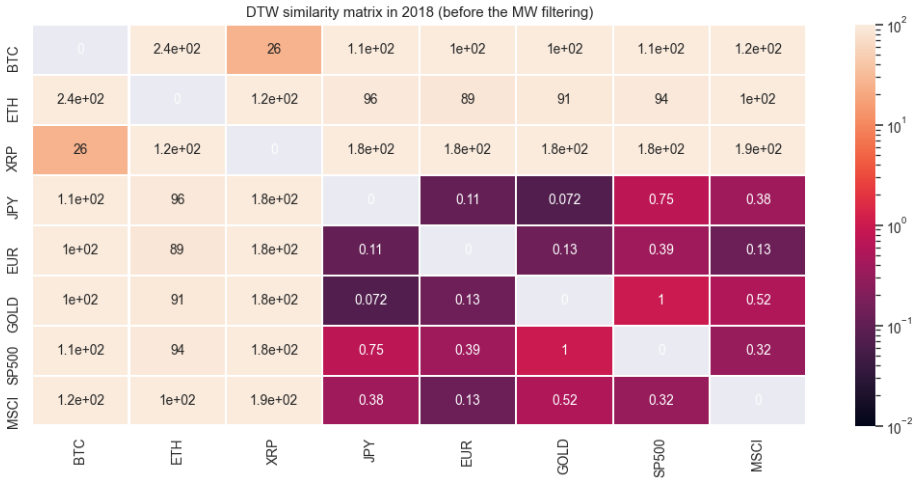

Table 15: DTW similarity matrix in 2019 (before the Müller-Watson filtering)

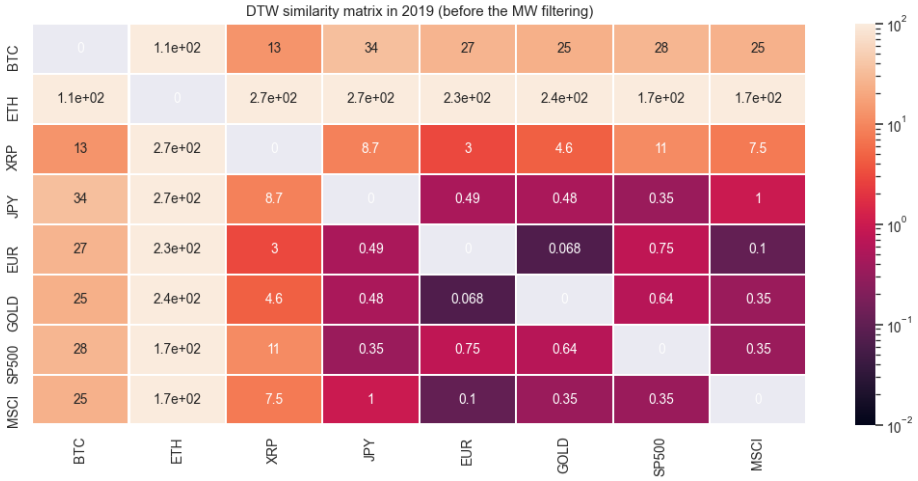

Table 16: DTW similarity matrix in 2020 (before the Müller-Watson filtering)

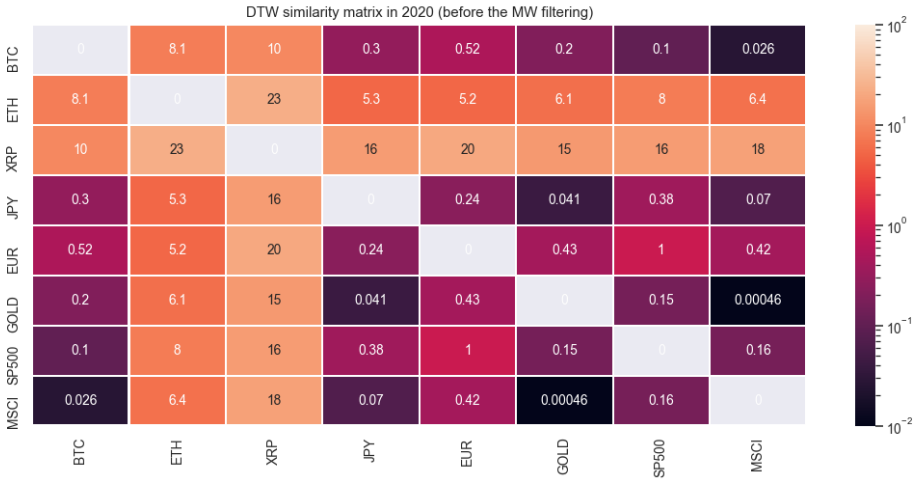

Table 17: DTW similarity matrix in 2016 (after the Müller-Watson filtering)

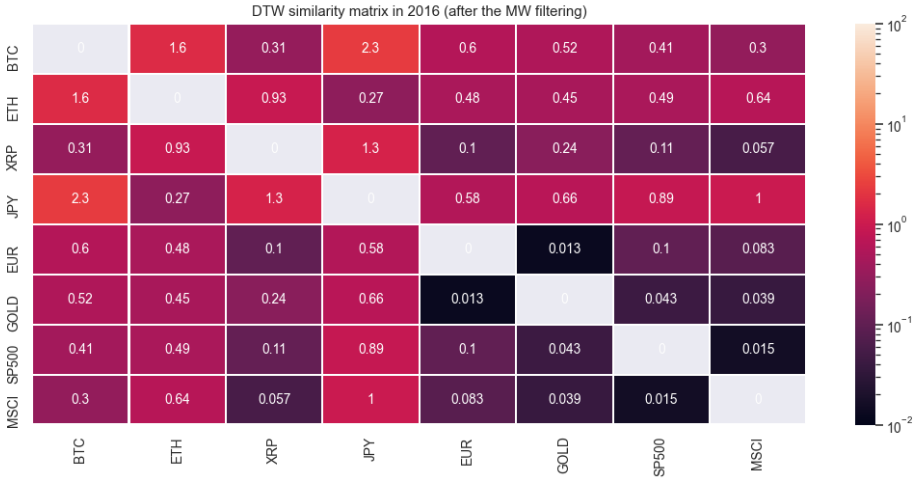

Table 18: DTW similarity matrix in 2017 (after the Müller-Watson filtering)

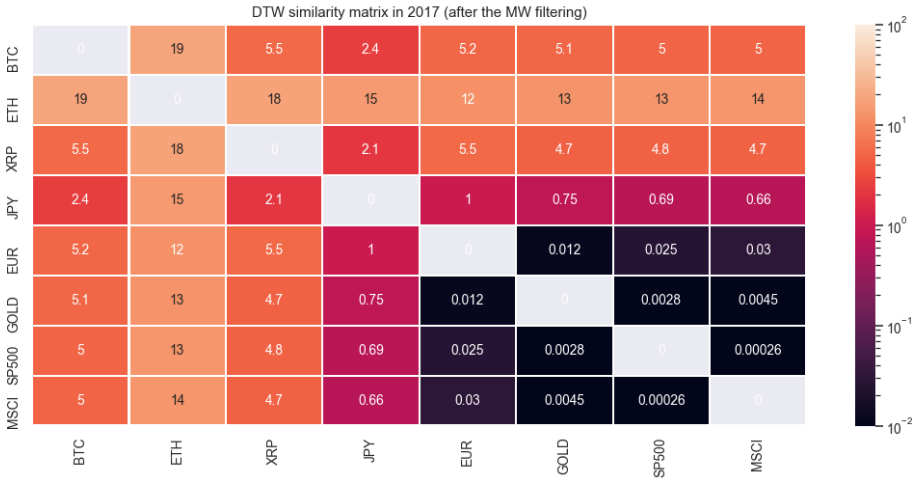

Table 19: DTW similarity matrix in 2018 (after the Müller-Watson filtering)

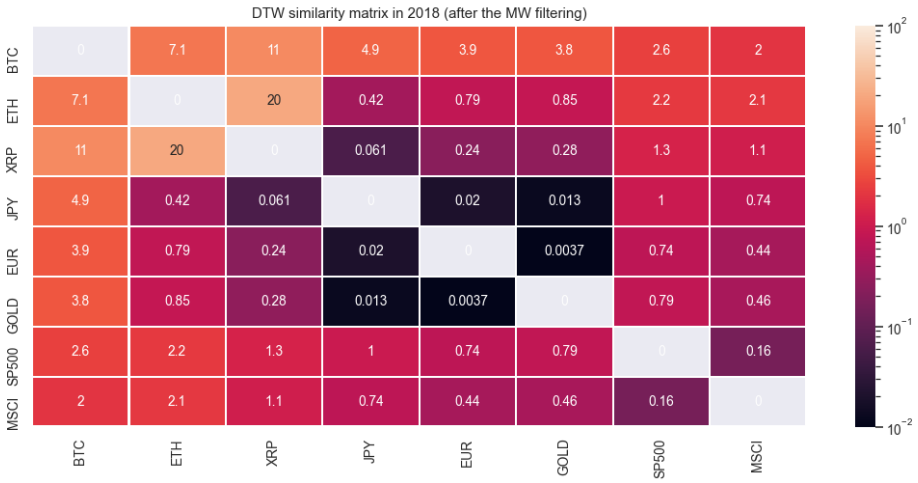

Table 20: DTW similarity matrix in 2019 (after the Müller-Watson filtering)

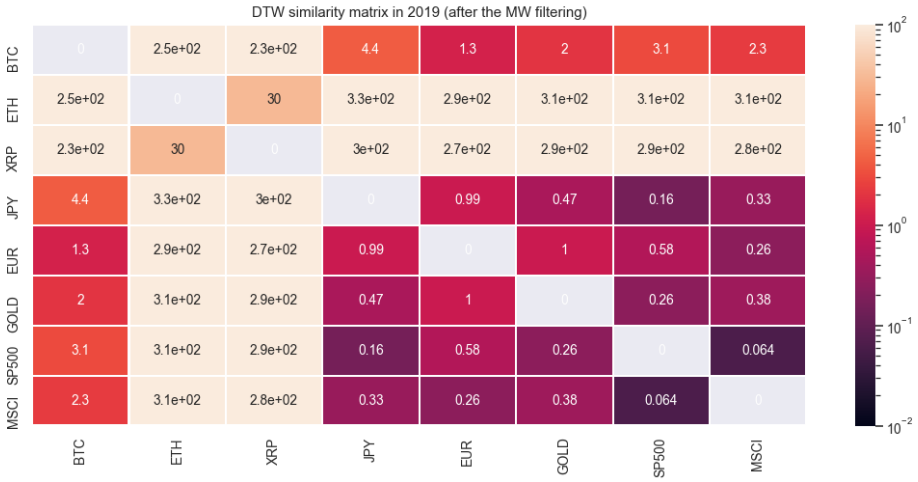

Table 21: DTW similarity matrix in 2020 (after the Müller-Watson filtering)